NONLINEAR IDENTIFICATION AND CONTROL OF BUILDING STRUCTURES EQUIPPED WITH MAGNETORHEOLOGICAL DAMPERS

A Dissertation

by

YEESOCK KIM

Submitted to the Office of Graduate Studies of
Texas A&M University
in partial fulfillment of the requirements for the degree of

DOCTOR OF PHILOSOPHY

December 2007

Major Subject: Civil Engineering

NONLINEAR IDENTIFICATION AND CONTROL OF BUILDING STRUCTURES EQUIPPED WITH MAGNETORHEOLOGICAL DAMPERS

A Dissertation

by

YEESOCK KIM

Submitted to the Office of Graduate Studies of
Texas A&M University
in partial fulfillment of the requirements for the degree of

DOCTOR OF PHILOSOPHY

Approved by:

Co-Chairs of Committee,	Stefan Hurlebaus
	Reza Langari
Committee Members,	Harry Jones
	Shankar Bhattacharyya
Head of Department,	David Rosowsky

December 2007

Major Subject: Civil Engineering

ABSTRACT

Nonlinear Identification and Control of Building Structures Equipped with Magnetorheological Dampers. (December 2007)

Yeesock Kim, B.E., Kwandong University; M.S., Yonsei University, Korea

Co-Chairs of Advisory Committee: Dr. Stefan Hurlebaus
Dr. Reza Langari

A new system identification algorithm, multiple autoregressive exogenous (ARX) inputs-based Takagi-Sugeno (TS) fuzzy model, is developed to identify nonlinear behavior of structure-magnetorheological (MR) damper systems. It integrates a set of ARX models, clustering algorithms, and weighted least squares algorithm with a TS fuzzy model. Based on a set of input-output data that is generated from building structures equipped with MR dampers, premise parameters of the ARX-TS fuzzy model are determined by clustering algorithms. Once the premise part is constructed, consequent parameters of the ARX-TS fuzzy model are optimized by the weighted least squares algorithm. To demonstrate the effectiveness of the proposed ARX-TS fuzzy model, it is applied to a three-, an eight-, a twenty-story building structures. It is demonstrated from the numerical simulation that the proposed ARX-TS fuzzy algorithm is effective to identify nonlinear behavior of seismically excited building structures equipped with MR dampers.

A new semiactive nonlinear fuzzy control (SNFC) algorithm is developed through integration of multiple Lyapunov-based state feedback gains, a Kalman filter,

and a converting algorithm with TS fuzzy interpolation method. First, the nonlinear ARX-TS fuzzy model is decomposed into a set of linear dynamic models that are operated in only a local linear operating region. Based on the decomposed models, multiple Lyapunov-based state feedback controllers are formulated in terms of linear matrix inequalities (LMIs) such that the structure-MR damper system is globally asymptotically stable and the performance on transient responses is guaranteed. Then, the state feedback controllers are integrated with a Kalman filter and a converting algorithm using a TS fuzzy interpolation method to construct semiactive output feedback controllers. To demonstrate the effectiveness of the proposed SNFC algorithm, it is applied to a three-, an eight-, and a twenty-story building structures. It is demonstrated from the numerical simulation that the proposed SNFC algorithm is effective to control responses of seismically excited building structures equipped with MR dampers. In addition, it is shown that the proposed SNFC system is better than a traditional optimal algorithm, H2/linear quadratic Gaussian-based semiactive control strategy.

ACKNOWLEDGEMENTS

I would like to express my deepest gratitude to my co-advisors Dr. Hurlebaus and Dr. Langari for excellent guidance, support, invaluable wisdom, and encouragement throughout the course of this research. The completion of this dissertation would not have been possible without their support.

I also extend my gratitude to Dr. Jones and Dr. Bhattacharyya for being on my committee. This dissertation has been improved by their comments and fruitful discussions.

I would like to extend my sincere appreciation to Dr. Roesset for his help and discussion throughout my study at Texas A&M University.

Last, I would especially like to thank my mother, aunt, and brother for their support and love all the time.

TABLE OF CONTENTS

Page

Page

LIST OF FIGURES

Page

Page

Page

Page

Page

Page

Page

LIST OF TABLES

1. INTRODUCTION

1.1 System Identification of Nonlinear Structure-damper Systems

One of the most difficult but important tasks in control system design for building structures subjected to natural hazards is the development of an accurate explicit mathematical model of the building system to be controlled because precise mathematical information related to the building structure is used for calculation of control forces. However, the development of a mathematical model for a nonlinear building system is still a challenging problem. One example of a nonlinear building structure occurs when highly nonlinear hysteretic actuators/dampers are applied to building systems for efficient energy dissipation. In this case, the building structure integrated with the nonlinear dampers behaves nonlinearly although the building structure itself is usually assumed to remain linear (Ramallo et al. 2004). The development of an appropriate nonlinear model of the integrated structure-damper system that includes the interaction effect between the structural system and the nonlinear damper plays a key role in control system design because the building structure integrated with a nonlinear damper is intrinsically nonlinear. In what follows it is demonstrated that a solution is available by means of nonlinear system identification based on fuzzy logic.

This dissertation follows the style of ASCE *Journal of Structural Engineering*.

Since Zadeh's paper (Zadeh 1965), fuzzy logic has been applied to many system identification problems (Langari 1999). In recent years, there have been a number of studies that use the Takagi-Sugeno (TS) fuzzy model, which provides an effective representation of nonlinear systems with the aid of fuzzy sets, fuzzy rules and a set of local linear models (Wang and Langari 1996). Research related to fuzzy logic-based system identification for large building structures first started from an ad-hoc approach based on the experience of individual investigators. However, this approach becomes unpractical when the number of design variables is large. To compensate for drawbacks of this ad-hoc approach, later research focused on using intelligent learning algorithms, e.g., genetic algorithms and neural networks. Jiang and Adeli (2005) developed a fuzzy wavelet neural network (FWNN) model for identification of high-rise building structures. In their work, the multi-input-single-output (MISO) FWNN was trained by a hybrid Levenberg-Marquardt least-squares algorithm. However, only a few papers have been published on nonlinear multi-input-multi-output (MIMO) fuzzy system identification algorithms for use with a building structure equipped with a nonlinear damper (Kim et al. 2006; Kim and Langari 2007).

1.2 Semiactive Nonlinear Fuzzy Control of Structures

Fuzzy logic has attracted great attention to control system design (Langari 1993; Langari 1999; Yen and Langari 1999; Lei and Langari 2000; Hong and Langari 2000). A number of design methodologies for fuzzy logic controllers have been successively

applied to a variety of large-scale civil engineering building structures. They include the following methods: trial-and-error-based methodologies (Abe 1996; Subramanian et al. 1996; Battaini et al. 1998; Symans and Kelly 1999; Loh et al. 2003; Battaini et al. 2004); a self-organizing approach (Al-Dawod et al. 2004; Samali et al. 2004); training using linear quadratic Gaussian (LQG) data (Al-Dawod et al. 2001); neural networks-based learning (Faravelli and Yao 1996; Tani et al. 1998; Faravelli and Rossi 2002; Schurter and Roschke 2001; Faravelli et al. 2002); adaptive fuzzy (Zhou et al. 2003); genetic algorithms-based training (Ahlawat and Ramaswany 2002a, 2002b, 2004; Yan and Zhou 2006; Kim and Roschke 2006); fuzzy sliding mode (Wang and Lee 2002; Kim et al. 2004; Alli and Yakut 2005); etc. However, no systematic framework has been conducted to design semiactive nonlinear fuzzy controller (SNFC) for a building structure equipped with a nonlinear semiactive device.

From a practical point of view, research related to a systematic semiactive control system design framework is still required for vibration control of large scale civil engineering structures subjected to destructive environmental forces, e.g., earthquakes or strong winds. Active nonlinear fuzzy control (ANFC) system design can be carried out in a systematic way via the so called parallel distributed compensation (PDC) approach, which employs multiple optimum linear controllers (Hong and Langari 2000; Joh et al. 1997). The linear controllers correspond to the local linear models with automatic scheduling performed through fuzzy rules. Tanaka and Sano (1994) proposed a theorem on the stability analysis of an ANFC system using the Lyapunov direct method. This theorem states sufficient conditions for an ANFC system to be globally asymptotically

stable by finding a common symmetric positive definite matrix such that a set of simultaneous Lyapunov inequalities are satisfied. However, no systematic design framework has been investigated to design SNFC systems for building structures equipped with nonlinear semiactive devices based on linear matrix inequalities (LMIs) for reduction of response to earthquakes and strong wind events.

1.3 Objectives and Outline of Dissertation

The first objective of this study is to propose a new system identification procedure for robust identification of large-scale building structures equipped with nonlinear magnetorheological (MR) dampers subjected to destructive environmental forces such as earthquakes and winds. The new identification algorithm, multiple autoregressive exogenous (ARX) input Takagi-Sugeno (TS) fuzzy model, integrates multiple MIMO ARX models with a TS fuzzy model. The premise part of the MIMO ARX-TS fuzzy model is determined through clustering algorithms and the consequent part is optimized using weighted least squares estimation. The goals are to achieve global system modeling under uncertain dynamic disturbances.

The second objective of this study is to develop a new semiactive nonlinear control algorithm for vibration control of large-scale building structures. First, multiple state feedback controllers in terms of LMIs are derived such that global asymptotical stability is guaranteed and the performance on the transient response is satisfied at the same time. Next, these state feedback gains are augmented with a Kalman observer to

construct output feedback control systems. Then, an active nonlinear fuzzy controller (ANFC) is developed through integration of the multiple output feedback controllers with fuzzy logic. Finally, the ANFC is integrated with a converting algorithm such as a clipped algorithm and an inverse MR damper model to develop a multi-input-single-output (MISO) semiactive nonlinear fuzzy controller (SNFC). To demonstrate the effectiveness of the proposed MISO SNFC algorithm, a three story shear type building structure that has been used as a benchmark building example by a number of other researchers is investigated.

The third objective of this study is to generalize or extend capacities of the MISO semiactive nonlinear control system into MIMO semiactive nonlinear control one. Practical point of view, it might difficult to apply for a centralized control system that a single control unit operates all the actuators and sensors to large-scale building structures due to high cost of installation and maintenance as well as vulnerability to small damage of structural systems. In such cases, a solution can be found in decentralized control techniques. In this research, a MIMO semiactive nonlinear control system is proposed that combines multiple MISO semiactive nonlinear controllers with decentralized control strategies such as a fully decentralized and a supervisory control. To demonstrate the effectiveness of the proposed approaches, these decentralized semiactive nonlinear control system design methodologies are applied to an eight story building structure and a full scale Los Angeles 20 story building structure that many investigators have used as benchmark building structures.

In Section 2, a variety of analytical models for a MR damper are introduced. They include a Bingham, a polynomial, a Bouc-Wen, and a modified Bouc-Wen model. In addition to the forward MR damper models, the corresponding inverse MR damper models are addressed. The associated equations of motion are described in detail.

In Section 3, the equations of motion of building structures equipped with MR dampers are derived to be used for the performance evaluation of the proposed identification and control methodologies. Furthermore, excitation inputs and output time history responses are provided.

In Section 4, a nonlinear multiple ARX-TS fuzzy model, which integrates multiple ARX models with TS fuzzy logic, is introduced. The method is applied to a three and an eight story building structure to demonstrate its effectiveness.

In Section 5, based on the nonlinear multiple ARX-TS fuzzy models, multiple optimum linear controllers are formulated in terms of linear matrix inequalities (LMIs) such that global asymptotical stability is guaranteed and the performance on transient response is also satisfied. The stability issue is formulated via the Lyapunov direct method and the transient response performance is achieved by the pole-assignment algorithm. Then, such multiple state feedback controllers are integrated with a Kalman estimator to construct multiple output feedback controllers. Finally, a semiactive nonlinear control system is developed though integration of the output feedback controllers with converting algorithms and MR dampers.

In Section 6, a MIMO semiactive nonlinear control system is proposed that combines multiple MISO semiactive nonlinear controllers using decentralized control strategies. They include a fully decentralized control and a supervisory control.

In Section 7, the proposed design framework of the nonlinear multiple ARX-TS fuzzy identification and the SNFC system is further investigated for nonlinear identification and control of response of a Los Angeles 20 story benchmark building structure employing MR dampers. The effectiveness and robustness of the proposed identification and control approaches for the benchmark building structure under various seismic excitations are evaluated.

Finally, concluding remarks and recommendation on future works are given in Section 8.

2. MAGNETORHEOLOGICAL DAMPER

2.1 Introduction

In recent years, smart structures have been adopted from many engineering fields because the performance of structural systems can be improved without either significantly increasing the structure mass or requiring high cost of control power. They may be called intelligent structures, adaptive structures, active structures, adaptronics, structronics, etc. These terminologies refer to a smart structure which is an integration of actuators, sensors, control units, and signal processing units with a structural system. The materials that are usually used to make a smart structure are: piezoelectrics, shape memory alloys, electrostrictive/magnetostrictive materials, polymer gels, and magnetorheological/electrorheological fluids (Hurlebaus and Gaul 2006).

Semiactive devices have been applied to large scale civil engineering structures. Semiactive control strategies combine favorable features of both active and passive control systems. Semiactive control systems include devices such as variable-orifice dampers, variable-stiffness devices, variable-friction dampers, controllable-fluid dampers, shape memory alloy actuators, and piezoelectrics (Hurlebaus and Gaul 2006). In particular, one of the controllable-fluid dampers, magnetorheological (MR) damper developed by Lord Corporation has attracted attention in recent years because it has many attractive characteristics.

In general, a MR damper consists of a hydraulic cylinder, magnetic coils, and MR fluids that consist of micron-sized magnetically polarizable particles floating within oil-type fluids as shown in Fig. 2.1. The MR damper is operated as a passive damper; however, when a magnetic field is applied to the MR fluids, the MR fluids are changed into a semi-active device in a few milliseconds. Its characteristics are summarized: 1) a MR damper is operated with low power sources, e.g., SD-1000 MR damper can generate a force up to 3000 N using a small battery with capacity less than 10 W; 2) it has high yield strength level, e.g., its maximum yield strength is beyond 80 kPa; 3) the performance is stable in a broad temperature range, e.g., MR fluids operates at the temperature between -40 ^{o}C and 150 ^{o}C; 4) the response time is a few milliseconds; 5) the performance is not sensitive to contamination during manufacturing the MR damper. Moreover, the operating point of the MR damper, which is a current-controlled device, can be changed by a permanent magnet.

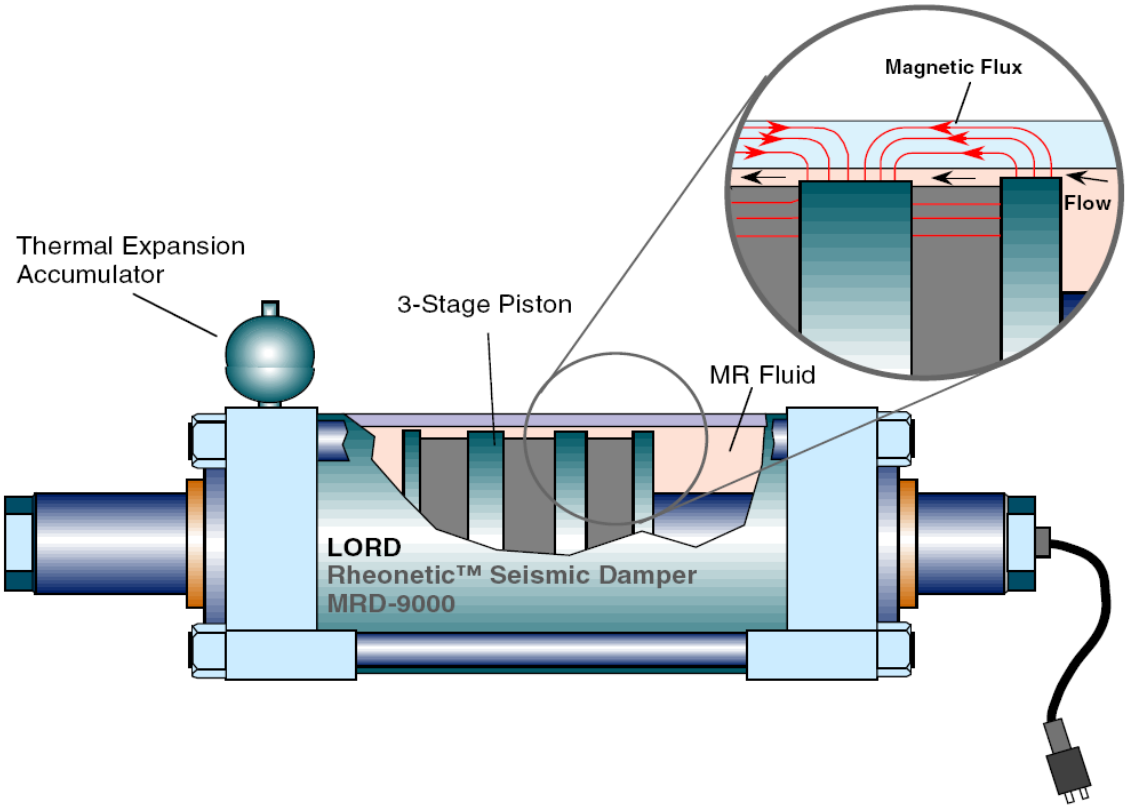

Fig. 2.1. A schematic of the prototype 20-ton large-scale MR damper (Yang 2002)

To fully use the best features of the MR damper, a mathematical model that portrays nonlinear behavior of the MR damper has to be developed first. However, this is challenging because the MR damper is a highly nonlinear hysteretic device. Therefore, research related to response control of building structures using MR dampers first started from development of a model that can describe the behavior of MR damper (Spencer et al. 1997). In this section, several models for the MR damper are introduced.

In Section 2.2, several forward models for a MR damper are introduced. It includes a Bingham, a polynomial, a Bouc-Wen, and a modified Bouc-Wen model. The

associated inverse models are provided in Section 2.3. Finally, in Section 2.4, concluding remarks are made.

2.2 Forward Models of a MR Damper

Ideally, a forward model of a MR damper has three inputs and a single output. The inputs include the piston displacement, the piston velocity, and the voltage applied to magnetic field of the MR damper; while the associated output is a control force signal. Many investigators have suggested several types of models that can effectively describe the relationship between the inputs and the output signals of the MR damper. In what follows, four different models that are widely recognized are introduced. They include a Bingham, a polynomial, a Bouc-Wen and a modified Bouc-Wen model.

2.2.1 Bingham Model

In general, the simplest model for a damper would be a viscous dashpot model

$$f = c\dot{x}, \tag{2.1}$$

where the damper force f is linearly related to the applied velocity $\dot{x}$. However, this can not be used for the MR damper modeling because the relationship between MR

damper forces and piston velocities is highly nonlinear. Furthermore, a MR damper has two more design parameters: the piston displacement and the applied voltage.

Stanway et al. (1985, 1987) suggested a viscoplastic model, which is called Bingham model, by adding a Coulomb friction element into the viscous damper model for the highly nonlinear hysteretic behavior of an electrorheological (ER) damper as shown in Fig. 2.2 which is a schematic of Bingham model of a controllable fluid device. Such a Bingham model can be also applied to a MR damper (Spencer et al. 1997)

$$f_{\mathrm{MR}} \triangleq F = f_{\mathrm{C}} \operatorname{sgn}(\dot{x}) v + c\dot{x} + f_0, \tag{2.2}$$

where f_{C} is a Coulomb friction coefficient, $\dot{x}$ is the piston velocity, v is the applied voltage, c is the damping coefficient, and f_0 is an offset value to adjust a nonzero force value due to an accumulator. When a MR damper is designed, an accumulator can be incorporated into the MR damper in order to adjust expansion or contraction of MR fluids due to changed temperature.

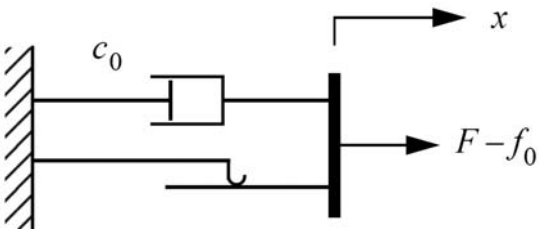

Fig. 2.2. Bingham model of an ER/MR damper
(Stanway et al. 1985, 1987)

The reason that the Bingham model can be used to describe the behavior of a MR damper is that a MR damper has approximately two operation stages, i.e., pre-yielding and post-yielding regions. Note that it is simple and easy for this Bingham model to be incorporated with a control system for analysis and design purpose; however, the piston displacement is not considered in this model, i.e., the effects of stiffness of the MR damper is ignored. In addition, the performance is degraded when the magnitude of the piston velocity is small. The problem that the performance of the Bingham model is degraded at low velocity range can be solved by a polynomial model.

2.2.2 Polynomial Model

Choi et al. (2001) developed a polynomial model such that it portrays the nonlinear behavior of a MR damper. In this model, the hysteretic loop of the MR damper is divided into two parts, i.e., the upper loop and the lower loop. Fig. 2.3 shows a schematic of the polynomial model after the hysteretic loop is started: the solid line represents the upper hysteresis loop and the dotted line is the lower hysteresis loop.

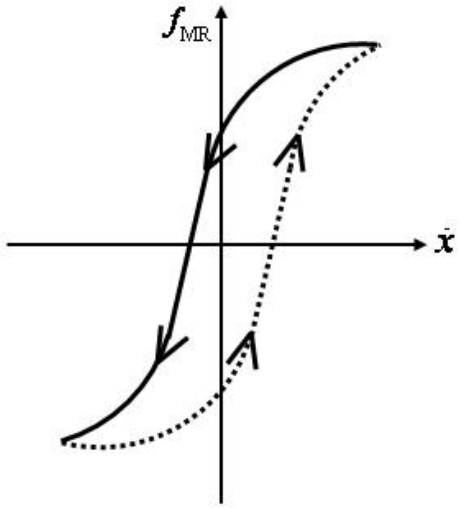

Fig. 2.3. A schematic of a polynomial model for a MR damper

The upper and lower parts of the hysteresis loop can be modeled via polynomials with the power of the piston velocity

$$f_{\mathrm{MR}}^{\mathrm{Upper}} = \sum_{i=0}^{n} a_i^{\mathrm{Upper}} \dot{x}^i \quad \text{for the upper hysteresis loop,} \tag{2.3}$$

$$f_{\mathrm{MR}}^{\mathrm{Lower}} = \sum_{i=0}^{n} a_i^{\mathrm{Lower}} \dot{x}^i \quad \text{for the lower hysteresis loop,} \tag{2.4}$$

where $f_{\mathrm{MR}}^{\mathrm{Upper}}$ and $f_{\mathrm{MR}}^{\mathrm{Lower}}$ are the level of the MR damper force that is represented by the upper part of the hysteresis loop and the lower hysteresis part, respectively; a_i^{Upper} and a_i^{Lower} are determined such that they match with experimental data; $\dot{x}$ is the piston

velocity; and n is the order of the polynomial that is selected based on trial and error approach.

Since the coefficients a_i^{Upper} and a_i^{Lower} depend on input current I, they need to be expressed in terms of the input current. Although the relationship between the current and the coefficients is nonlinear, they can be related linearly without loss of the performance

$$a_i^{\text{Upper}} = b_i^{\text{Upper}} + c_i^{\text{Upper}} I, \quad i = 0,1,...,n, \tag{2.5}$$

$$a_i^{\text{Lower}} = b_i^{\text{Lower}} + c_i^{\text{Lower}} I, \quad i = 0,1,...,n. \tag{2.6}$$

Substitution of Eq. (2.5) and Eq. (2.6) into Eq. (2.3) and Eq. (2.4) yields

$$f_{\text{MR}}^{\text{Upper}} = \sum_{i=0}^{n} \left(b_i^{\text{Upper}} + c_i^{\text{Upper}} I \right) \dot{x}^i, \tag{2.7}$$

$$f_{\text{MR}}^{\text{Lower}} = \sum_{i=0}^{n} \left(b_i^{\text{Lower}} + c_i^{\text{Lower}} I \right) \dot{x}^i. \tag{2.8}$$

This polynomial model is as simple as the Bingham model. Moreover, it is easy to derive an inverse model to implement a semiactive control system as well. Furthermore, the performance at low velocity range is improved comparing with the Bingham model. However, the effect of the piston displacement is sill not considered in this polynomial

model, i.e., the impact of stiffness of a MR damper is ignored. However, the displacement parameter can be incorporated into the MR damper model by introducing a Bouc-Wen model.

2.2.3 Bouc-Wen Model

One of the most popular mathematical models for modeling a MR damper is the Bouc-Wen model (Wen 1976) depicted in Fig. 2.4.

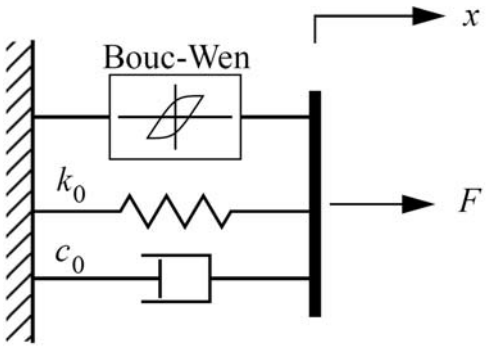

Fig. 2.4. Bouc-Wen model of the MR Damper
(Spencer et al., 1997)

The hysteretic behavior of the Bouc-Wen model for a MR damper is governed by the following equations (Spencer et al. 1997; Tse and Chang 2004)

$$f_{\mathrm{MR}} \triangleq F = c_0\dot{x} + k_0\left(x - x_0\right) + \alpha z_{\mathrm{BW}}, \tag{2.9}$$

$$\dot{z}_{\mathrm{BW}} = -\gamma \left|\dot{x}\right| z_{\mathrm{BW}} \left|z_{\mathrm{BW}}\right|^{n-1} - \beta \dot{x} \left|z_{\mathrm{BW}}\right|^{n} + A\dot{x}, \tag{2.10}$$

$$\alpha = \alpha_{\mathrm{a}} + \alpha_{\mathrm{b}} u + \alpha_{\mathrm{c}} u^{2}, \tag{2.11}$$

$$c_0 = c_{0\mathrm{a}} + c_{0\mathrm{b}} u, \tag{2.12}$$

$$\dot{u} = -\eta(u - v), \tag{2.13}$$

where z_{BW} and α, called evolutionary variables, describe the hysteretic behavior of the MR damper; c_0 is the viscous damping; k_0 is the stiffness; x_0 is the initial displacement, which is caused by an accumulator, of the spring that is corresponding to the stiffness k_0; γ, β and A are adjustable shape parameters of the hysteresis loops; and v and u are input and output voltages of a first-order filter, respectively.

Although this model describes the hysteretic behavior of the MR damper, it is still difficult for the Bouc-Wen model to capture the response behavior at the small piston velocities (Spencer et al. 1997). Such a problem can be solved by introducing additional stiffness and damping elements into the Bouc-Wen model, which is named a modified Bouc-Wen model.

2.2.4 Modified Bouc-Wen Model

To improve the performance at small magnitude of velocities, Spencer et al. (1997) proposed a modified version of the Bouc-Wen model, as shown in Fig. 2.5. The

MR damper force $f_{\mathrm{MR}}(t)$ predicted by the modified Bouc-Wen model is governed by the following differential equations according to Spencer et al. (1997)

$$f_{\mathrm{MR}} \triangleq F = c_1\dot{y} + k(x - x_0), \tag{2.14}$$

$$\dot{z}_{\mathrm{BW}} = -\gamma\left|\dot{x} - \dot{y}\right| z_{\mathrm{BW}} \left|z_{\mathrm{BW}}\right|^{n-1} - \beta(\dot{x} - \dot{y})\left|z_{\mathrm{BW}}\right|^{n} + A(\dot{x} - \dot{y}), \tag{2.15}$$

$$\dot{y} = \frac{1}{(c_0 + c_1)}\left\{\alpha z_{\mathrm{BW}} + c_0\dot{x} + k_0(x - y)\right\}, \tag{2.16}$$

$$\alpha = \alpha_{\mathrm{a}} + \alpha_{\mathrm{b}}u, \tag{2.17}$$

$$c_1 = c_{1\mathrm{a}} + c_{1\mathrm{b}}u, \tag{2.18}$$

$$c_0 = c_{0\mathrm{a}} + c_{0\mathrm{b}}u, \tag{2.19}$$

$$\dot{u} = -\eta(u - v), \tag{2.20}$$

where z_{BW} and α, called evolutionary variables, describe the hysteretic behavior of the MR damper; c_0 and c_1 are viscous damping at high and low velocities, respectively; k_0 and k_1 control the stiffness at large velocities and the accumulator stiffness, respectively; the x_0 is the initial displacement of spring with stiffness k_1; γ, β and A are adjustable shape parameters of the hysteresis loops; and v and u are input and output voltages of a first-order filter, respectively. Note that the modified Bouc-Wen model is one of the

most effective models to describe the behavior of a MR damper; however, it is not easy to derive the inverse model for control system design purpose. In the following sections, the corresponding inverse models are introduced.

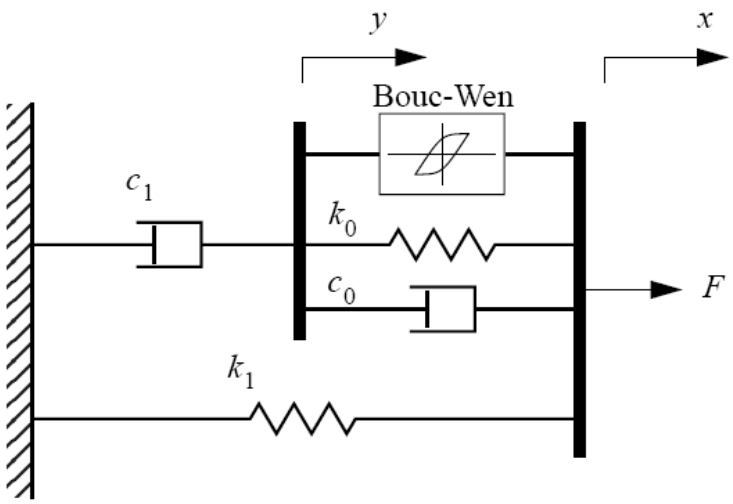

Fig. 2.5. Modified Bouc-Wen model of the MR damper (Spencer et al. 1997)

2.3 Inverse Models of a MR Damper

A MR damper force cannot be directly controlled, but applied voltage only can be directly controlled, i.e., control force signals that are provided by a control algorithm should be converted into voltage or current signals to operate the MR damper. For the signal transformation, there might exist two ways: 1) use of an inverse model of the MR damper 2) use of an algorithm to be able to convert control forces into voltage or current signals. In this section, several types of inverse models for a MR damper are introduced. They include a Bingham, a polynomial, a Bouc-Wen, and a modified Bouc-Wen model.

2.3.1 Inverse Bingham Model

An inverse Bingham model for a MR damper can be easily derived from Eq. (2.2) by solving for the voltage v

$$v = \frac{f_{\mathrm{MR}} - c\dot{x} + f_0}{f_c \operatorname{sgn}(\dot{x})}. \tag{2.21}$$

2.3.2 Inverse Polynomial Model

As one of the simplest ways of converting the control force level into a current signal, the inverse polynomial model is determined from Eq. (2.7) and Eq. (2.8) by solving for the current I (Choi et al. 2001)

$$I = \begin{cases} \dfrac{f_{\mathrm{SNC}} - \sum_{i=0}^{n} b_i^{\mathrm{Upper}} \dot{x}^i}{\sum_{i=0}^{n} c_i^{\mathrm{Upper}} \dot{x}^i} & \text{for the upper hysteresis loop,} \\ \dfrac{f_{\mathrm{SNC}} - \sum_{i=0}^{n} b_i^{\mathrm{Lower}} \dot{x}^i}{\sum_{i=0}^{n} c_i^{\mathrm{Lower}} \dot{x}^i} & \text{for the lower hysteresis loop,} \end{cases} \tag{2.22}$$

where f_{SNC} is a desirable control force that is generated by a semiactive nonlinear controller (SNC) in this research although it can be any type of control force.

2.3.3 Inverse Bouc-Wen Model

Tse and Chang (2004) have derived an inverse Bouc-Wen model for a MR damper assuming that the evolutionary variable z_{BW} can be approximated as its ultimate hysteretic strength and the MR damper is always operated in the postyielding region.

The differential equations of the inverse Bouc-Wen model are given by

$$f_{\mathrm{MR}} \cong (c_{0\mathrm{a}} + c_{0\mathrm{a}}u)\dot{x} + k_0 x + (\alpha_{\mathrm{a}} + \alpha_{\mathrm{b}}u + \alpha_{\mathrm{c}}u^2)z_u, \tag{2.23}$$

$$z \cong z_u = \mathrm{sgn}(\dot{x})\left(\frac{A}{\gamma+\beta}\right)^{1/n}, \tag{2.24}$$

$$\left(\alpha_{\mathrm{c}}z_u\right)u^2 + (\alpha_{\mathrm{b}}z_u + c_{0\mathrm{b}}\dot{x})u + (\alpha_{\mathrm{a}}z_u + c_{0\mathrm{a}}\dot{x} + k_0 x - f_{\mathrm{MR}}) = 0, \tag{2.25}$$

$$v = u + \frac{\dot{u}}{\eta}. \tag{2.26}$$

2.3.4 Inverse Modified Bouc-Wen Model

Tsang et al. (2006) derived an inverse dynamics of a modified Bouc-Wen model for a MR damper to synthesis a control system, assuming that the evolutionary variable z_{BW} can be approximated as its ultimate hysteretic strength; a MR damper is operated within post-yielding region (Spencer 1986); and stiffness of the MR damper can be

neglected. The differential equation for the inverse modified Bouc-Wen model is given by

$$I(t) = -\frac{1}{p_2}\ln\left[\frac{|f_{\mathrm{MR}}| - |f_{\mathrm{SNC}}|}{p_1} + \mathrm{e}^{-p_2 I(t-\Delta t)}\right], \tag{2.27}$$

where p_1 and p_2 are related to the MR fluid stress; they are found by ad-hoc approach using experimental results. More detailed description is given in Tsang et al. (2006).

2.4 Concluding Remarks

In this section, four forward and the associated inverse models for a MR damper are presented. They include a Bingham, a polynomial, a Bouc-Wen, and a modified Bouc-Wen model.

The Bingham model can be quickly and easily applied to control system of building structures; however, it is difficult to accurately capture the hysteretic loop of the MR damper, in particular, in the range of low velocities.

Derivation of the polynomial model-based forward and inverse MR damper models can be easily carried out; however, the piston displacement is not considered as an input parameter, which is the same as the Bingham model, in the polynomial models; it means that the effects of the stiffness of the MR fluid are ignored. However, the impact of the MR damper stiffness can be incorporated with a Bouc-Wen model.

Highly nonlinear hysteretic loop of a MR damper can be described with the Bouc-Wen model; however, it is still not effective to capture the behavior of the MR damper at low velocities. Such a drawback of the Bouc-Wen model can be overcome by modifying the Bouc-Wen model, i.e., the modified Bouc-Wen model has good performance at both high velocity and low velocity ranges. However, it is difficult to derive the inverse dynamics for the Bouc-Wen and the modified Bouc-Wen models for the purpose of control system design.

3. BUILDING STRUCTURES EQUIPPED WITH MR DAMPERS

3.1 Introduction

In this section, two building structures which include a three and an eight story shear type building structures employing magnetorheological (MR) dampers are presented. The goal is to create integrated building-MR damper system models that are used for the performance evaluation of nonlinear system identification procedure and semiactive nonlinear fuzzy control (SNFC) system design framework for building structures equipped with MR dampers.

In Section 3.2, the equations of motion of a three story building structure are derived first. Then, differential equations of a MR damper are integrated with the equations of motion of the three story building structure. In Section 3.3, the equations of motion of an eight story building-MR damper are presented. Excitation inputs and output time history responses are provided in Section 3.4. Finally, in Section 3.5, concluding remarks are made.

3.2 A Three Story Building Structure Equipped with a MR Damper

In this section, the equations of motion of a three story building structure employing a MR damper are derived in terms of state space equations for use with the performance evaluation of a multi-input-single-output (MISO) SNFC system.

3.2.1 A Three Story Shear Type Building Structure

Consider a deflected three story building frame shown in Fig. 3.1. The building structure is modeled as a lumped mass-spring system, i.e., the mass of each floor is lumped; the stiffness and the damping of columns are modeled as a spring and a dashpot element, respectively. In this model, each floor is assumed to be axially rigid and the vertical deformation and rotation of each column are assumed to be negligible.

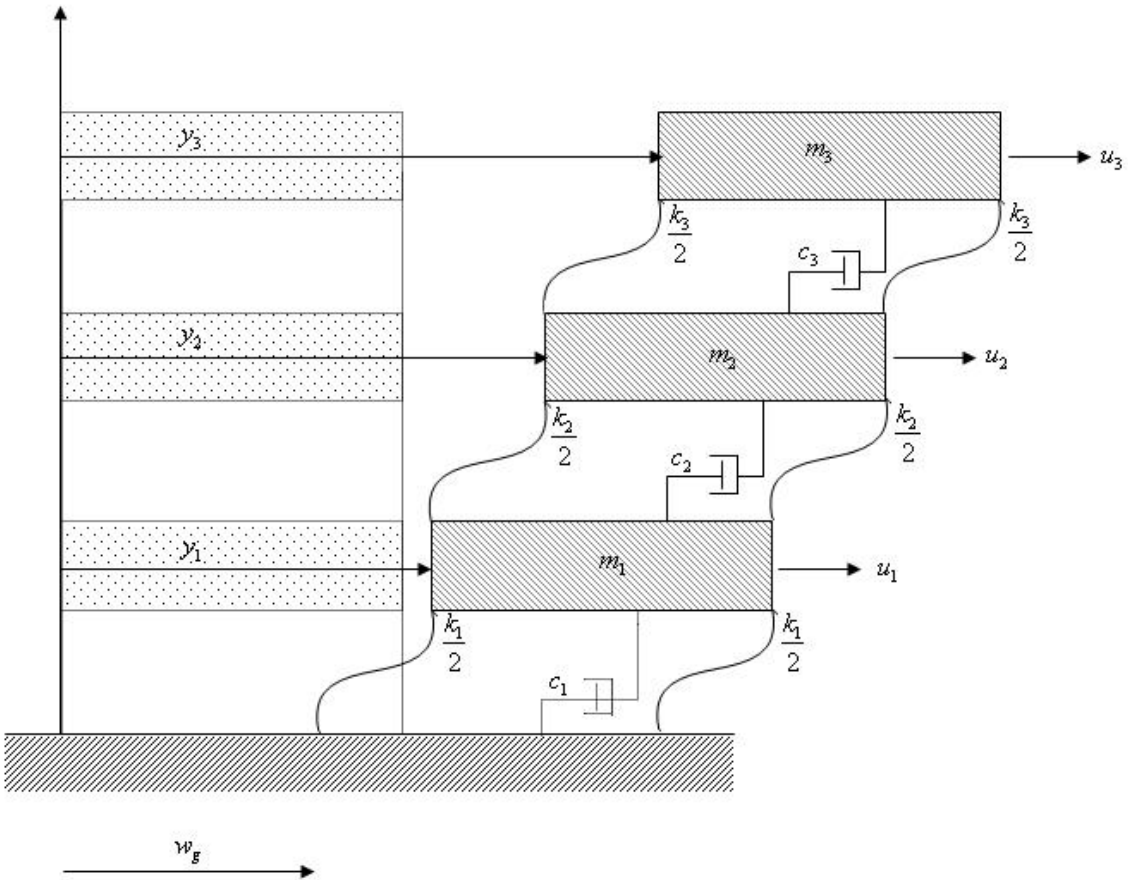

Fig. 3.1. Deflected three story building structure

In Fig. 3.1, w_g denotes the displacement of the ground that is induced by earthquake-type ground accelerations; y_i are absolute displacements; m_i are the mass of the i^{th} floor; k_i are the stiffness of the i^{th} floor columns; c_i are the damping of the i^{th} floor columns; and u_i are control forces acting each floor.

To derive the associated differential equations of motion, an isolated free body diagram (FBD) is depicted in Fig. 3.2 and then Newton's second law is applied to each mass.

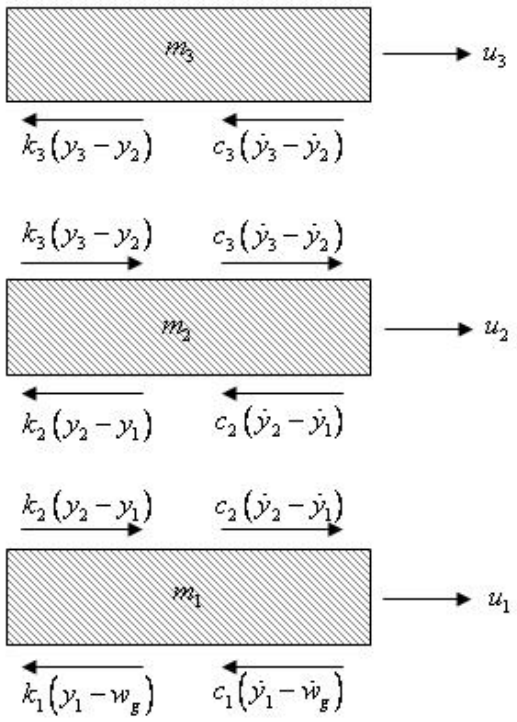

Fig. 3.2. An isolated FBD of a three story building structure

Summation of all the forces acting on each mass to the horizontal direction leads to

$$\sum F = m_1\ddot{y}_1 = -k_1\left(y_1 - w_g\right) + k_2\left(y_2 - y_1\right) - c_1\left(\dot{y}_1 - \dot{w}_g\right) + c_2\left(\dot{y}_2 - \dot{y}_1\right) + u_1, \tag{3.1}$$

$$\sum F = m_2\ddot{y}_2 = -k_2\left(y_2 - y_1\right) + k_3\left(y_3 - y_2\right) - c_2\left(\dot{y}_2 - \dot{y}_1\right) + c_3\left(\dot{y}_3 - \dot{y}_2\right) + u_2, \tag{3.2}$$

$$\sum F = m_3\ddot{y}_3 = -k_3\left(y_3 - y_2\right) - c_3\left(\dot{y}_3 - \dot{y}_2\right) + u_3. \tag{3.3}$$

With the definition of the relative displacements between the ground and each mass

$$x_1 = y_1 - w_g, \tag{3.4}$$

$$x_2 = y_2 - w_g, \tag{3.5}$$

$$x_3 = y_3 - w_g, \tag{3.6}$$

and substituting Eq. (3.4) to Eq. (3.6) into Eq. (3.1) to Eq. (3.3), the equations of motion become

$$m_1\ddot{x}_1 + \left(c_1 + c_2\right)\dot{x}_1 - c_2\dot{x}_2 + \left(k_1 + k_2\right)x_1 - k_2x_2 = u_1 - m_1\ddot{w}_g, \tag{3.7}$$

$$m_2\ddot{x}_2 - c_2\dot{x}_1 + \left(c_2 + c_3\right)\dot{x}_2 - c_3\dot{x}_3 - k_2x_1 + \left(k_2 + k_3\right)x_2 - k_3x_3 = u_2 - m_2\ddot{w}_g, \tag{3.8}$$

$$m_3\ddot{x}_3 - c_3\dot{x}_2 + c_3\dot{x}_3 - k_3x_2 - k_3x_3 = u_3 - m_3\ddot{w}_g. \tag{3.9}$$

Eq. (3.7) to Eq. (3.9) can be expressed in more compact form by defining new matrix variables

$$\mathbf{M}\ddot{\mathbf{x}} + \mathbf{C}\dot{\mathbf{x}} + \mathbf{K}\mathbf{x} = \mathbf{\Gamma}\mathbf{U} - \mathbf{M}\mathbf{\Lambda}\ddot{w}_g, \tag{3.10}$$

where the system matrices are given by

$$\mathbf{M} = \begin{bmatrix} m_1 & 0 & 0 \\ 0 & m_2 & 0 \\ 0 & 0 & m_3 \end{bmatrix} \tag{3.11}$$

is the mass matrix,

$$\mathbf{C} = \begin{bmatrix} c_1 + c_2 & -c_2 & 0 \\ -c_2 & c_2 + c_3 & -c_3 \\ 0 & -c_3 & c_3 \end{bmatrix} \tag{3.12}$$

is the damping matrix,

$$\mathbf{K} = \begin{bmatrix} k_1 + k_2 & -k_2 & 0 \\ -k_2 & k_2 + k_3 & -k_3 \\ 0 & -k_3 & k_3 \end{bmatrix} \tag{3.13}$$

is the stiffness matrix,

$$\mathbf{U} = \begin{bmatrix} u_1 \\ u_2 \\ u_3 \end{bmatrix} \tag{3.14}$$

is the control input vector,

$$\mathbf{\Gamma} = \begin{bmatrix} 1 & 0 & 0 \\ 0 & 1 & 0 \\ 0 & 0 & 1 \end{bmatrix} \tag{3.15}$$

is the control input location matrix,

$$\mathbf{\Lambda} = \begin{bmatrix} 1 \\ 1 \\ 1 \end{bmatrix} \tag{3.16}$$

is the disturbance signal location matrix, the vector $\mathbf{x}$ is the displacement relative to the ground, and $\ddot{w}_g$ is the disturbance acceleration, i.e., earthquake.

Properties of the three story building structure are taken from a scaled model (Dyke et al. 1996) of a prototype building structure that was developed by Chung et al.

(1989). The mass of each floor $m_1 = m_2 = m_3 = 98.3$ kg; the stiffness of each story $k_1 =$ 516,000 N/m, $k_2 = 684000$ N/m, and $k_3 = 684{,}000$ N/m; and the damping coefficients of each floor $c_1 = 125$ Ns/m, $c_2 = 50$ Ns/m and $c_3 = 50$ Ns/m.

It is advantageous to convert the second order differential Eq. (3.10) into the 1st order differential equation such that it is expressed in state space equations with the state space vector $\mathbf{z} = \begin{bmatrix} \mathbf{x} & \dot{\mathbf{x}} \end{bmatrix}^{\mathrm{T}}$. Eq. (3.10) can be expressed in the following form

$$\begin{aligned} \dot{\mathbf{z}} &= \mathbf{A}\mathbf{z} + \mathbf{B}\mathbf{u} - \mathbf{E}\ddot{w}_g \\ \mathbf{y} &= \mathbf{C}\mathbf{z} + \mathbf{D}\mathbf{u} + \mathbf{n}, \end{aligned} \tag{3.17}$$

where the system matrices are given by

$$\mathbf{A} = \begin{bmatrix} \mathbf{0} & \mathbf{I} \\ -\mathbf{M}^{-1}\mathbf{K} & -\mathbf{M}^{-1}\mathbf{C} \end{bmatrix} \tag{3.18}$$

is the state matrix,

$$\mathbf{B} = \begin{bmatrix} \mathbf{0} \\ \mathbf{M}^{-1}\mathbf{F} \end{bmatrix} \tag{3.19}$$

is the input matrix,

$$\mathbf{C} = \begin{bmatrix} \mathbf{I} & \mathbf{0} \\ \mathbf{0} & \mathbf{I} \\ -\mathbf{M}^{-1}\mathbf{K} & -\mathbf{M}^{-1}\mathbf{C} \end{bmatrix} \tag{3.20}$$

is the output matrix,

$$\mathbf{D} = \begin{bmatrix} \mathbf{0} \\ \mathbf{0} \\ \mathbf{M}^{-1}\mathbf{F} \end{bmatrix} \tag{3.21}$$

is the feedthrough matrix,

$$\mathbf{E} = \begin{bmatrix} \mathbf{0} \\ \mathbf{F} \end{bmatrix} \tag{3.22}$$

is the disturbance location matrix,

$$\mathbf{u} = \begin{bmatrix} u_1 & u_2 & u_3 \end{bmatrix}^T \tag{3.23}$$

is the control vector, and

$$\mathbf{F} = \begin{bmatrix} -1 & 1 & 0 \\ 0 & -1 & 1 \\ 0 & 0 & -1 \end{bmatrix} \tag{3.24}$$

is the location matrix that a Chevron brace is located within a building structure. The vector **n** represents noise that is generated by a zero-mean Gaussian white noise generator. A Chevron brace is used to connect a MR damper into the three story building structure; the control force and disturbance are not acting only on each floor. Thus, the control force and disturbance matrices are transformed (Hart and Wong 2000) using a matrix **F** that represents control and disturbance locations that is derived from configuration of a Chevron brace. In the following section, this building structure is integrated with a MR damper.

3.2.2 An Integrated Three Story Building-MR Damper System

An integrated building-MR damper system is presented through integration of a MR damper with a building structure. Then, the integrated system is not linear anymore although it is assumed that the structural system itself is linear. Fig. 3.3 and Fig. 3.4 show a configuration on how a MR damper is integrated with a building structure.

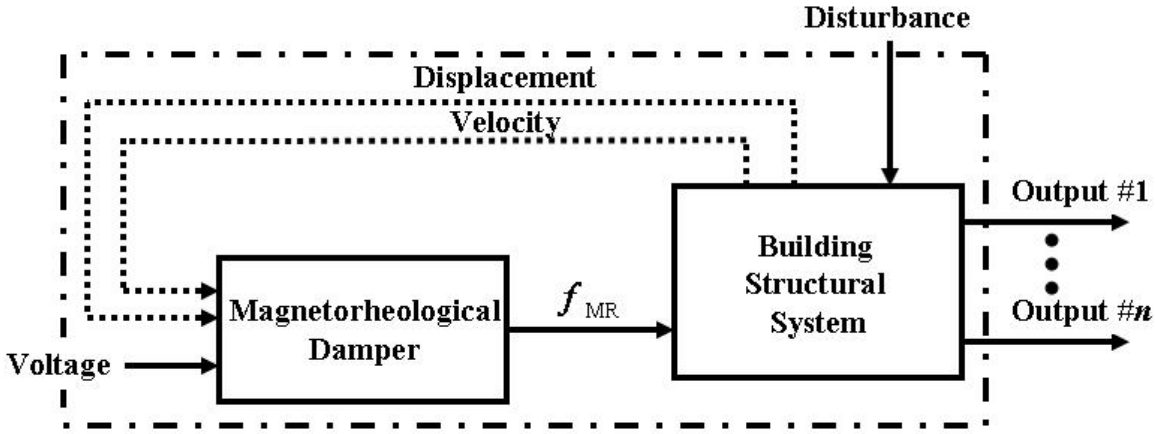

Fig. 3.3. Integrated building structure-MR damper system

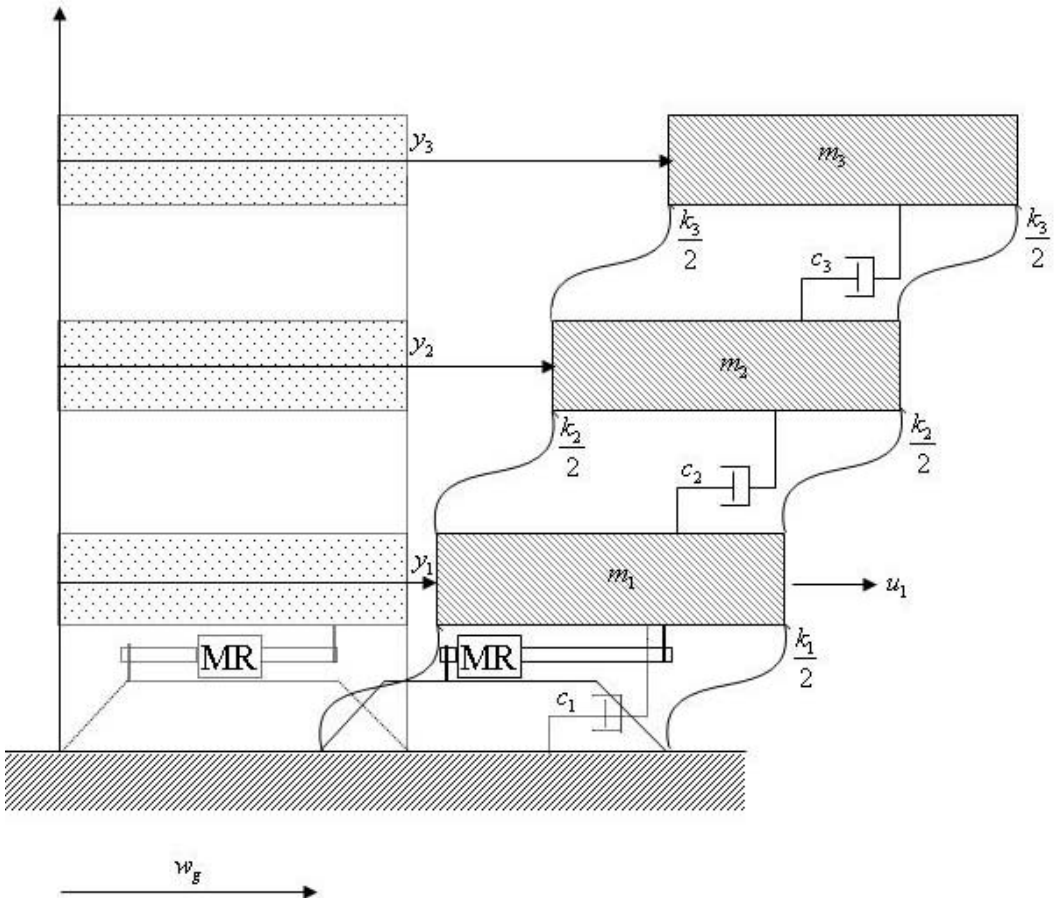

Fig. 3.4. A schematic of a building-MR damper system

The associated equation of motion is given by

$$\mathbf{M}^*\ddot{\mathbf{x}} + \mathbf{C}^*\dot{\mathbf{x}} + \mathbf{K}^*\mathbf{x} = \mathbf{\Gamma}\mathbf{f}_{\mathbf{MR}}\left(t, x_1, \dot{x}_1, v_1\right) - \mathbf{M}^*\mathbf{\Lambda}\ddot{w}_g, \tag{3.25}$$

where the system matrices are given by

$$\mathbf{M}^{*}=\begin{bmatrix} m_1+m_1^{*} & 0 & 0 \\ 0 & m_2 & 0 \\ 0 & 0 & m_3 \end{bmatrix} \tag{3.26}$$

is the mass matrix of the building equipped with a MR damper,

$$\mathbf{C}^{*}=\begin{bmatrix} c_1+c_1^{*}\left(t,x_1,x_2,v\right)+c_2 & -c_2 & 0 \\ -c_2 & c_2+c_3 & -c_3 \\ 0 & -c_3 & c_3 \end{bmatrix} \tag{3.27}$$

is the damping matrix of the building equipped with a MR damper,

$$\mathbf{K}^{*}=\begin{bmatrix} k_1+k_1^{*}\left(t,x_1,x_2,v\right)+k_2 & -k_2 & 0 \\ -k_2 & k_2+k_3 & -k_3 \\ 0 & -k_3 & k_3 \end{bmatrix} \tag{3.28}$$

is the stiffness matrix of the building equipped with a MR damper,

$$\mathbf{f}_{\mathbf{MR}}\left(t,x_1,\dot{x}_1,v_1\right)=\begin{bmatrix} f_{\mathrm{MR}}\left(t,x_1,\dot{x}_1,v_1\right) \\ 0 \\ 0 \end{bmatrix} \tag{3.29}$$

is the MR damper force matrix, m_1^* is the mass of the applied MR damper, c_1^* is the damping value that is produced by the MR damper, k_1^* is the stiffness that is caused by the MR damper, x_1 and $\dot{x}_1$ are the displacement and the velocity at the 1st floor level relative to the ground of the three story building structure, respectively, and v is the voltage level to be applied. Note that it might not be reasonable to identify $\mathbf{M}^*$, $\mathbf{C}^*$, and $\mathbf{K}^*$ through linear time invariant (LTI) model framework because m_1^*, c_1^*, and k_1^* are nonlinear time-varying values. However, a solution can be found in nonlinear system identification using a set of input and output data. This second order differential equations can be converted into state space

$$\begin{aligned}\dot{\mathbf{z}} &= \mathbf{A}^*\mathbf{z} + \mathbf{B}^*\mathbf{f}_{\mathbf{MR}}\left(t, z_1, z_4, v\right) - \mathbf{E}\ddot{w}_g \\ \mathbf{y} &= \mathbf{C}^*\mathbf{z} + \mathbf{D}^*\mathbf{f}_{\mathbf{MR}}\left(t, z_1, z_4, v\right) + \mathbf{n},\end{aligned} \tag{3.30}$$

where

$$\mathbf{A}^* = \begin{bmatrix} \mathbf{0} & \mathbf{I} \\ -\mathbf{M}^{*-1}\mathbf{K}^* & -\mathbf{M}^{*-1}\mathbf{C}^* \end{bmatrix} \tag{3.31}$$

is the state matrix,

$$\mathbf{B}^* = \begin{bmatrix} \mathbf{0} \\ \mathbf{M}^{*-1}\mathbf{F} \end{bmatrix} \tag{3.32}$$

is the input matrix,

$$\mathbf{C}^* = \begin{bmatrix} \mathbf{I} & \mathbf{0} \\ \mathbf{0} & \mathbf{I} \\ -\mathbf{M}^{*-1}\mathbf{K}^* & -\mathbf{M}^{*-1}\mathbf{C}^* \end{bmatrix} \tag{3.33}$$

is the output matrix,

$$\mathbf{D}^* = \begin{bmatrix} \mathbf{0} \\ \mathbf{0} \\ \mathbf{M}^{*-1}\mathbf{F} \end{bmatrix} \tag{3.34}$$

is the feedthrough matrix,

$$\mathbf{E} = \begin{bmatrix} \mathbf{0} \\ \mathbf{F} \end{bmatrix} \tag{3.35}$$

is the disturbance location matrix, and z_1 and z_4 are the displacement and the velocity at the 1st floor level of the three story building structure, respectively. In this building

structure, a SD-1000 MR damper (Spencer et al. 1997) has been applied whose parameters are given in Appendix A.

To evaluate the effectiveness of the SNFC strategy with the larger scale building structure, an eight story building structure is investigated in the following section.

3.3 An Eight Story Building Structure Equipped with MR Dampers

In order to demonstrate the effectiveness of the MIMO SNFC system with a larger scale example, an eight story shear type building structure is investigated here. The reason to choose this example is that it has been used as a benchmark problem by a number of researchers (Yang 1982; Yang et al. 1987; Soong 1990; Spencer et al. 1994). Note that the equations of motion of the eight story building model are not derived here because its derivation can be easily extended from the equations of motion of the three story building model. The equation of motion of the eight story building structure is

$$\mathbf{M}\ddot{\mathbf{x}} + \mathbf{C}\dot{\mathbf{x}} + \mathbf{K}\mathbf{x} = \mathbf{\Gamma}\mathbf{U} - \mathbf{M}\mathbf{\Lambda}\ddot{w}_g, \tag{3.36}$$

where the system matrices are given by

$$\mathbf{M} = \begin{bmatrix} m_1 & 0 & 0 & 0 & 0 & 0 & 0 & 0 \\ 0 & m_2 & 0 & 0 & 0 & 0 & 0 & 0 \\ 0 & 0 & m_3 & 0 & 0 & 0 & 0 & 0 \\ 0 & 0 & 0 & m_4 & 0 & 0 & 0 & 0 \\ 0 & 0 & 0 & 0 & m_5 & 0 & 0 & 0 \\ 0 & 0 & 0 & 0 & 0 & m_6 & 0 & 0 \\ 0 & 0 & 0 & 0 & 0 & 0 & m_7 & 0 \\ 0 & 0 & 0 & 0 & 0 & 0 & 0 & m_8 \end{bmatrix} \tag{3.37}$$

is the mass matrix,

$$\mathbf{C} = \begin{bmatrix} c_1 + c_2 & -c_2 & 0 & 0 & 0 & 0 & 0 & 0 \\ -c_2 & c_2 + c_3 & -c_3 & 0 & 0 & 0 & 0 & 0 \\ 0 & -c_3 & c_3 + c_4 & -c_4 & 0 & 0 & 0 & 0 \\ 0 & 0 & -c_4 & c_4 + c_5 & -c_5 & 0 & 0 & 0 \\ 0 & 0 & 0 & -c_5 & c_5 + c_6 & -c_6 & 0 & 0 \\ 0 & 0 & 0 & 0 & -c_6 & c_6 + c_7 & -c_7 & 0 \\ 0 & 0 & 0 & 0 & 0 & -c_7 & c_7 + c_8 & -c_8 \\ 0 & 0 & 0 & 0 & 0 & 0 & -c_8 & c_8 \end{bmatrix} \tag{3.38}$$

is the damping matrix,

$$\mathbf{K} = \begin{bmatrix} k_1 + k_2 & -k_2 & 0 & 0 & 0 & 0 & 0 & 0 \\ -k_2 & k_2 + k_3 & -k_3 & 0 & 0 & 0 & 0 & 0 \\ 0 & -k_3 & k_3 + k_4 & -k_4 & 0 & 0 & 0 & 0 \\ 0 & 0 & -k_4 & k_4 + k_5 & -k_5 & 0 & 0 & 0 \\ 0 & 0 & 0 & -k_5 & k_5 + k_6 & -k_6 & 0 & 0 \\ 0 & 0 & 0 & 0 & -k_6 & k_6 + k_7 & -k_7 & 0 \\ 0 & 0 & 0 & 0 & 0 & -k_7 & k_7 + k_8 & -k_8 \\ 0 & 0 & 0 & 0 & 0 & 0 & -k_8 & k_8 \end{bmatrix} \tag{3.39}$$

is the stiffness matrix,

$$\mathbf{U} = \begin{bmatrix} u_1 & u_2 & u_3 & u_4 & u_5 & u_6 & u_7 & u_8 \end{bmatrix}^{\mathrm{T}} \tag{3.40}$$

is the control input vector,

$$\mathbf{\Gamma} = \begin{bmatrix} 1 & 0 & 0 & 0 & 0 & 0 & 0 & 0 \\ 0 & 1 & 0 & 0 & 0 & 0 & 0 & 0 \\ 0 & 0 & 1 & 0 & 0 & 0 & 0 & 0 \\ 0 & 0 & 0 & 1 & 0 & 0 & 0 & 0 \\ 0 & 0 & 0 & 0 & 1 & 0 & 0 & 0 \\ 0 & 0 & 0 & 0 & 0 & 1 & 0 & 0 \\ 0 & 0 & 0 & 0 & 0 & 0 & 1 & 0 \\ 0 & 0 & 0 & 0 & 0 & 0 & 0 & 1 \end{bmatrix} \tag{3.41}$$

is the control input location matrix, and

$$\mathbf{\Lambda} = \begin{bmatrix} 1 & 1 & 1 & 1 & 1 & 1 & 1 & 1 \end{bmatrix}^{\mathrm{T}} \tag{3.42}$$

is the disturbance location matrix. The mass of each floor $m_1 = m_2 = m_3 = m_4 = m_5 = m_6 = m_7 = m_8 = 345{,}600$ kg; the stiffness of each story $k_1 = k_2 = k_3 = k_4 = k_5 = k_6 = k_7 = k_8 = 340{,}400$ kN/m; and the damping coefficient of each floor $c_1 = c_2 = c_3 = c_4 = c_5 = c_6 = c_7 = c_8 = 2{,}937{,}000$ Ns/m (Yang 1982). The second order differential equation can be converted into state space

$$\begin{aligned} \dot{\mathbf{z}} &= \mathbf{A}\mathbf{z} + \mathbf{B}\mathbf{u} - \mathbf{E}\ddot{w}_g \\ \mathbf{y} &= \mathbf{C}\mathbf{z} + \mathbf{D}\mathbf{u} + \mathbf{n}, \end{aligned} \tag{3.43}$$

where the system matrices are given by

$$\mathbf{A} = \begin{bmatrix} \mathbf{0} & \mathbf{I} \\ -\mathbf{M}^{-1}\mathbf{K} & -\mathbf{M}^{-1}\mathbf{C} \end{bmatrix} \tag{3.44}$$

is the state matrix,

$$\mathbf{B} = \begin{bmatrix} \mathbf{0} \\ \mathbf{M}^{-1}\mathbf{F} \end{bmatrix} \tag{3.45}$$

is the input matrix,

$$\mathbf{C} = \begin{bmatrix} \mathbf{I} & \mathbf{0} \\ \mathbf{0} & \mathbf{I} \\ -\mathbf{M}^{-1}\mathbf{K} & -\mathbf{M}^{-1}\mathbf{C} \end{bmatrix} \tag{3.46}$$

is the output matrix,

$$\mathbf{D} = \begin{bmatrix} \mathbf{0} \\ \mathbf{0} \\ \mathbf{M}^{-1}\mathbf{F} \end{bmatrix} \tag{3.47}$$

is the feedthrough matrix,

$$\mathbf{E} = \begin{bmatrix} \mathbf{0} \\ \mathbf{F} \end{bmatrix} \tag{3.48}$$

is the disturbance location matrix, and

$$\mathbf{F} = \begin{bmatrix} 1 & -1 & 0 & 0 & 0 & 0 & 0 & 0 \\ 0 & 1 & -1 & 0 & 0 & 0 & 0 & 0 \\ 0 & 0 & 1 & -1 & 0 & 0 & 0 & 0 \\ 0 & 0 & 0 & 1 & -1 & 0 & 0 & 0 \\ 0 & 0 & 0 & 0 & 1 & -1 & 0 & 0 \\ 0 & 0 & 0 & 0 & 0 & 1 & -1 & 0 \\ 0 & 0 & 0 & 0 & 0 & 0 & 1 & -1 \\ 0 & 0 & 0 & 0 & 0 & 0 & 0 & -1 \end{bmatrix} \tag{3.49}$$

is the location matrix that Chevron braces are located within a building structure.

In this eight story building structure, two MR dampers are installed into the 5th and 8th floor levels using Chevron braces. Fig. 3.5 shows a configuration on how the MR dampers are integrated with a building structure.

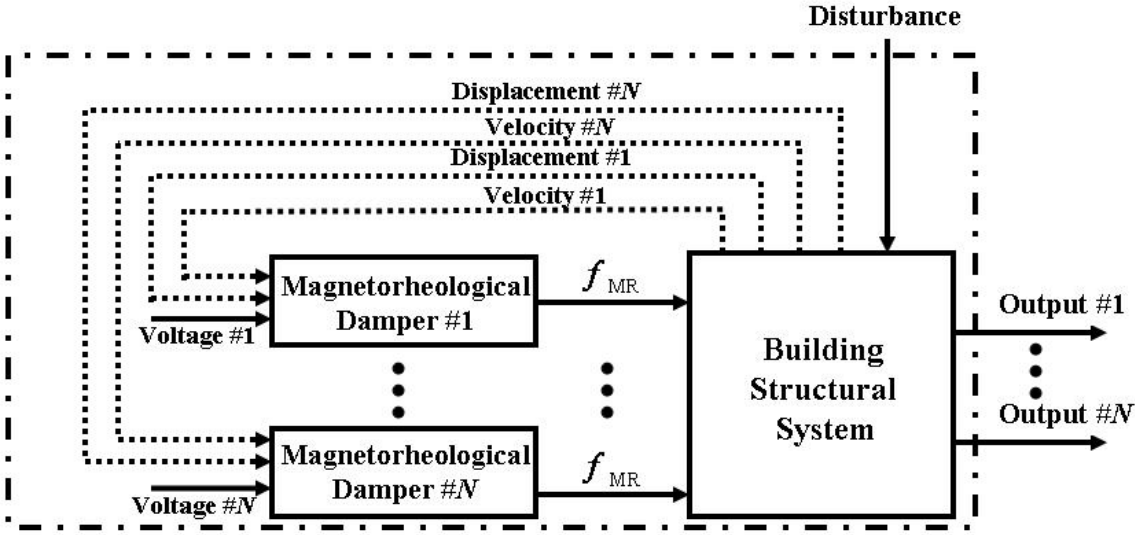

Fig. 3.5. A building structure equipped with multiple MR dampers

The equation of motion of the integrated building-MR damper system is given by

$$\mathbf{M}^*\ddot{\mathbf{x}} + \mathbf{C}^*\dot{\mathbf{x}} + \mathbf{K}^*\mathbf{x} = \mathbf{\Gamma}\mathbf{f}_{\mathrm{MR}}\left(t, x_5, \dot{x}_5, v_1, x_8, \dot{x}_8, v_2\right) - \mathbf{M}^*\mathbf{\Lambda}\ddot{w}_g, \tag{3.50}$$

where the system matrices are given by

$$\mathbf{M}^* = \begin{bmatrix} m_1 & 0 & 0 & 0 & 0 & 0 & 0 & 0 \\ 0 & m_2 & 0 & 0 & 0 & 0 & 0 & 0 \\ 0 & 0 & m_3 & 0 & 0 & 0 & 0 & 0 \\ 0 & 0 & 0 & m_4 & 0 & 0 & 0 & 0 \\ 0 & 0 & 0 & 0 & m_5 + m_5^* & 0 & 0 & 0 \\ 0 & 0 & 0 & 0 & 0 & m_6 & 0 & 0 \\ 0 & 0 & 0 & 0 & 0 & 0 & m_7 & 0 \\ 0 & 0 & 0 & 0 & 0 & 0 & 0 & m_8 + m_8^* \end{bmatrix} \tag{3.51}$$

is the mass matrix of the building equipped with MR dampers,

$$\mathbf{C}^{*}=\begin{bmatrix} c_1+c_2 & -c_2 & 0 & 0 \\ -c_2 & c_2+c_3 & -c_3 & 0 \\ 0 & -c_3 & c_3+c_4 & -c_4 \\ 0 & 0 & -c_4 & c_4+c_5+c_5^{*}\left(t,x_5,\dot{x}_5,v\right) \\ 0 & 0 & 0 & -c_5+c_5^{*}\left(t,x_5,\dot{x}_5,v\right) \\ 0 & 0 & 0 & 0 \\ 0 & 0 & 0 & 0 \\ 0 & 0 & 0 & 0 \end{bmatrix} \tag{3.52}$$

$$\begin{bmatrix} 0 & 0 & 0 & 0 \\ 0 & 0 & 0 & 0 \\ 0 & 0 & 0 & 0 \\ -c_5+c_5^{*}\left(t,x_5,\dot{x}_5,v\right) & 0 & 0 & 0 \\ c_5+c_5^{*}\left(t,x_5,\dot{x}_5,v\right)+c_6 & -c_6 & 0 & 0 \\ -c_6 & c_6+c_7 & -c_7 & 0 \\ 0 & -c_7 & c_7+c_8+c_8^{*}\left(t,x_8,\dot{x}_8,v\right) & -c_8+c_8^{*}\left(t,x_8,\dot{x}_8,v\right) \\ 0 & 0 & -c_8+c_8^{*}\left(t,x_8,\dot{x}_8,v\right) & c_8+c_8^{*}\left(t,x_8,\dot{x}_8,v\right) \end{bmatrix}$$

is the damping matrix of the building equipped with MR dampers,

$$\mathbf{K}^* = \begin{bmatrix} k_1+k_2 & -k_2 & 0 & 0 \\ -k_2 & k_2+k_3 & -k_3 & 0 \\ 0 & -k_3 & k_3+k_4 & -k_4 \\ 0 & 0 & -k_4 & k_4+k_5+k_5^*\left(t,x_5,\dot{x}_5,v\right) \\ 0 & 0 & 0 & -k_5+k_5^*\left(t,x_5,\dot{x}_5,v\right) \\ 0 & 0 & 0 & 0 \\ 0 & 0 & 0 & 0 \\ 0 & 0 & 0 & 0 \end{bmatrix}$$

$$\begin{bmatrix} 0 & 0 & 0 & 0 \\ 0 & 0 & 0 & 0 \\ 0 & 0 & 0 & 0 \\ -k_5+k_5^*\left(t,x_5,\dot{x}_5,v\right) & 0 & 0 & 0 \\ k_5+k_5^*\left(t,x_5,\dot{x}_5,v\right)+k_6 & -k_6 & 0 & 0 \\ -k_6 & k_6+k_7 & -k_7 & 0 \\ 0 & -k_7 & k_7+k_8+k_8^*\left(t,x_8,\dot{x}_8,v\right) & -k_8+k_8^*\left(t,x_8,\dot{x}_8,v\right) \\ 0 & 0 & -k_8+k_8^*\left(t,x_8,\dot{x}_8,v\right) & k_8+k_8^*\left(t,x_8,\dot{x}_8,v\right) \end{bmatrix} \tag{3.53}$$

is the stiffness matrix of the building equipped with MR dampers; m_i^* is the mass of the MR damper on the i^{th} floor; c_i^* and k_i^* are the damping and stiffness values that are produced by the MR damper on the i^{th} floor; x_5 and $\dot{x}_5$ are the displacement and the velocity at the 5th floor level relative to the 4th floor level of the eight story building structure, respectively; x_8 and $\dot{x}_8$ are the displacement and the velocity at the 8th floor level relative to the 7th floor level, respectively; v_1 and v_2 are the voltage levels to be applied to the MR damper installed on the 5th and the 8th floors of the structure, respectively; and **n** is noise. Note again, it might not be reasonable to identify $\mathbf{M}^*$, $\mathbf{C}^*$, and $\mathbf{K}^*$ through LTI model framework because m_1^*, c_1^*, and k_1^* are nonlinear time-

varying values. However, a solution can be found in nonlinear system identification. The second order differential equations can be converted into state space

$$\begin{aligned}\dot{\mathbf{z}} &= \mathbf{A}^*\mathbf{z} + \mathbf{B}^*\mathbf{f}_{\mathrm{MR}}\left(t, z_5, z_{13}, v_1, z_8, z_{16}, v_2\right) - \mathbf{E}\ddot{w}_g \\ \mathbf{y} &= \mathbf{C}^*\mathbf{z} + \mathbf{D}^*\mathbf{f}_{\mathrm{MR}}\left(t, z_5, z_{13}, v_1, z_8, z_{16}, v_2\right) + \mathbf{n},\end{aligned} \tag{3.54}$$

where

$$\mathbf{A}^* = \begin{bmatrix} \mathbf{0} & \mathbf{I} \\ -\mathbf{M}^{*-1}\mathbf{K}^* & -\mathbf{M}^{*-1}\mathbf{C}^* \end{bmatrix} \tag{3.55}$$

is the state matrix,

$$\mathbf{B}^* = \begin{bmatrix} \mathbf{0} \\ \mathbf{M}^{*-1}\mathbf{F} \end{bmatrix} \tag{3.56}$$

is the input matrix,

$$\mathbf{C}^* = \begin{bmatrix} \mathbf{I} & \mathbf{0} \\ \mathbf{0} & \mathbf{I} \\ -\mathbf{M}^{*-1}\mathbf{K}^* & -\mathbf{M}^{*-1}\mathbf{C}^* \end{bmatrix} \tag{3.57}$$

is the output matrix,

$$\mathbf{D}^* = \begin{bmatrix} \mathbf{0} \\ \mathbf{0} \\ \mathbf{M}^{*-1}\mathbf{F} \end{bmatrix} \tag{3.58}$$

is the feedthrough matrix,

$$\mathbf{E}^* = \begin{bmatrix} \mathbf{0} \\ \mathbf{F} \end{bmatrix} \tag{3.59}$$

is the disturbance location matrix, z_5 and z_{13} are the displacement and the velocity at the 5^{th} floor level relative to the 4^{th} floor level of the eight story building structure, respectively, and z_8 and z_{16} are the displacement and the velocity at the 8^{th} floor level relative to the 7^{th} floor, respectively.

Once the integrated building-MR damper system is constructed, a set of input-output data for nonlinear system identification can be generated; the integrated systems are also used for the performance evaluation of SNFC systems as nonlinear dynamic models. However, since the eight story building structure is much larger than the three story building structure, MR dampers with much larger capacity are needed. In the eight story building structure, two 1000 kN MR dampers are used whose optimum parameters are given in Appendix A.

3.4 Excitation Sources and Time History Responses

Three different random signals are employed here as disturbance input signals: a pseudo random binary signal (PRBS); artificial earthquake (AEQ) ground acceleration; and the 1940 El Centro earthquake ground record. The PRBS is used for system identification of the three story building-MR damper system as an input signal, the AEQ acceleration is used for exciting the eight story building-MR damper system, and the 1940 El Centro earthquake record is used to demonstrate the effectiveness of the SNFC systems for the three and eight story building-MR damper systems. In addition, MR damper forces are used for control input signals.

3.4.1 Input and Output Signals for Identification of the Three Story Building

In this research, two input signals, which are the disturbance and control signals, are applied to the three story building structure to generate two output data. The PRBS is used as a disturbance input signal for the purpose of system identification of the three story building structure equipped with a MR damper. The reason to choose the PRBS as an input signal is that an input spectrum, not the waveform of the input, mainly influences the asymptotic characteristics of a given estimation problem, i.e., bias and covariance. Furthermore, computational cost can be significantly saved (Åström and Eykhoff 1971). As a PRBS is with only two values, it is generated via a random process first. Then, it is filtered to improve the smoothness of numerical simulation shown in

Fig. 3.6. However, note that the filtered PRBS spectrum has to include characteristics of real recorded ground acceleration spectrum. The MR damper force is used as the 2nd input signal as shown in Fig. 3.7.

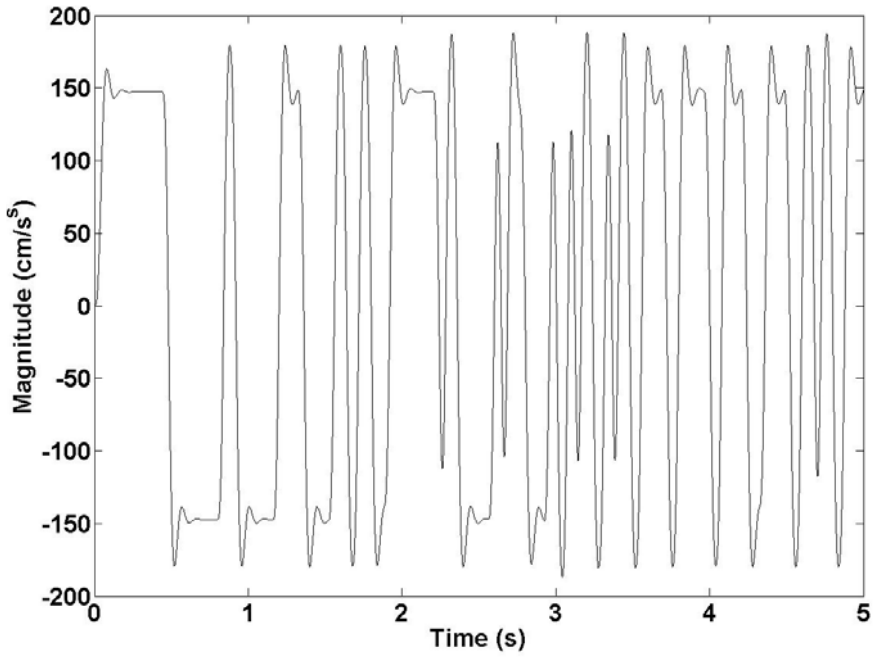

Fig. 3.6. The filtered PRBS for earthquake-type ground accelerations

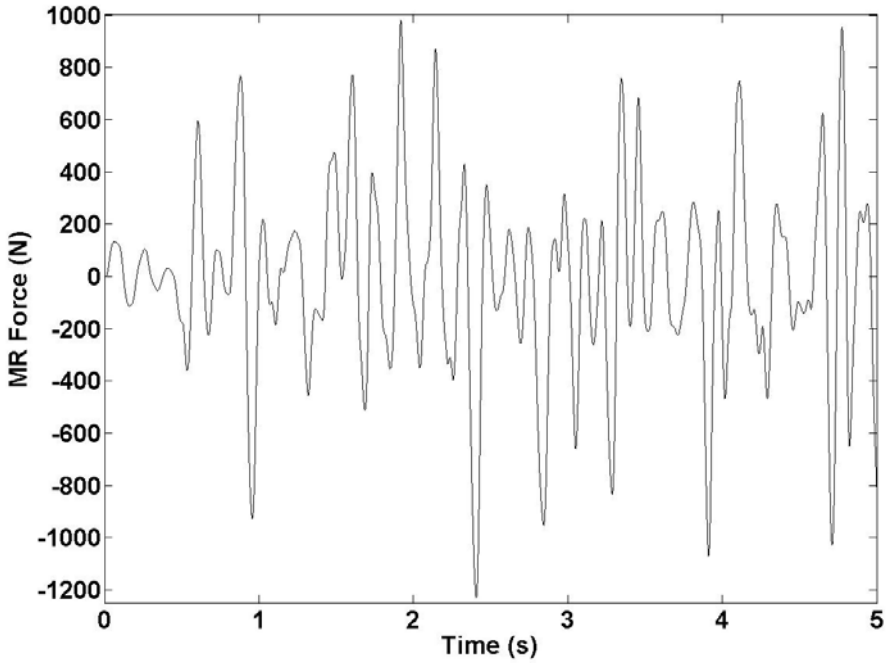

Fig. 3.7. Magnetorheological damper force

3.4.2 Input and Output Signals for Identification of the Eight Story Building

Although a PRBS disturbance signal is effective to excite a building-MR damper system for the system identification purpose, it may have strict limitations in real world application because the PRBS-type disturbance that has only minimum and maximum values, i.e., the bang-bang type signal may cause a building structure to be damaged during operation due to more nonlinearities. Therefore, an AEQ ground acceleration whose spectrum and waveform are close to real-recorded earthquake signals is applied to the eight story building employing two MR dampers for the system identification

purpose. The generation of the AEQ ground accelerations is carried out by the following steps.

Step 1: Generate a zero-mean Gaussian white noise (GWN).

Step 2: Filter the generated GWN by an appropriate designed filter such that the spectrum of the AEQ ground accelerations is to be close to real recorded ground accelerations. The Kanai-Tajimi filter (Soong and Grigoriu 1993; Ramallo et al. 1999) is used here because its effectiveness has been demonstrated by many other researchers. The filter is given by

$$F_{\mathrm{KT}}(s)=\frac{2\xi_g\omega_g s+\omega_g^2}{s^2+2\xi_g\omega_g s+\omega_g^2}, \tag{3.60}$$

where $\omega_g=17\,\mathrm{rads/s}$ and $\xi_g=0.3$.

Step 3: Apply for a time-envelope function to the filtered GWN to specify the shape and duration of earthquake records. The following envelope function, $\phi(t)$, is used.

$$\phi(t)=\begin{cases}(t/t_1)^2 & 0\le t\le t_1\\ 1 & \text{for } t_1\le t\le t_2\\ \exp\left[-\alpha(t-t_2)\right] & t>t_2,\end{cases} \tag{3.61}$$

where $t_1 = 7\,\mathrm{s}$, $t_2 = 12\,\mathrm{s}$, and $\alpha = 0.3\,\mathrm{s}^{-1}$. The AEQ signal shown in Fig. 3.8 is used to generate time history responses of the eight story shear type building structure for the system identification purpose. Fig. 3.9 shows a MR damper force signal to be applied.

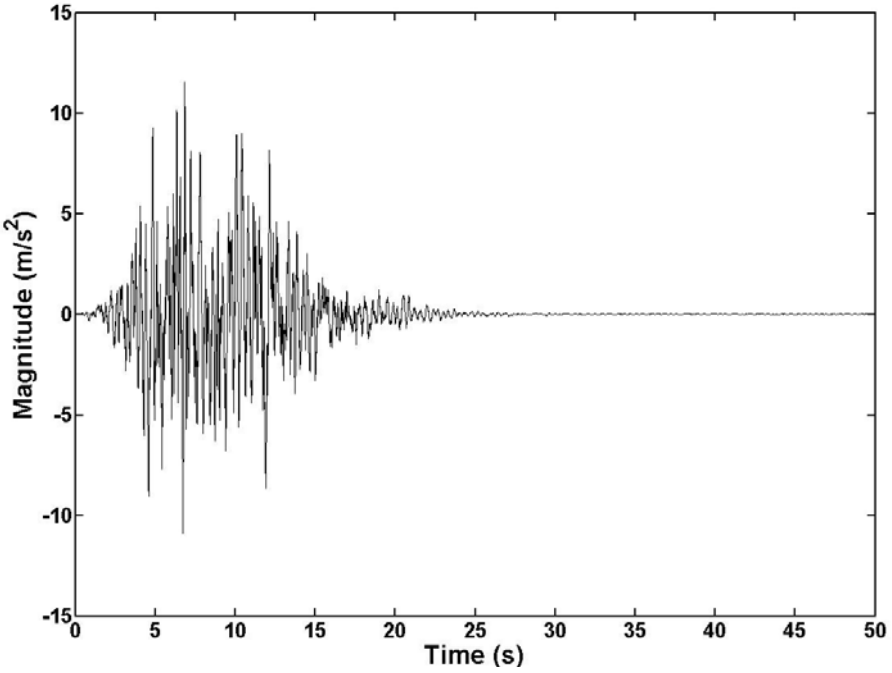

Fig. 3.8. Artificial earthquake signal

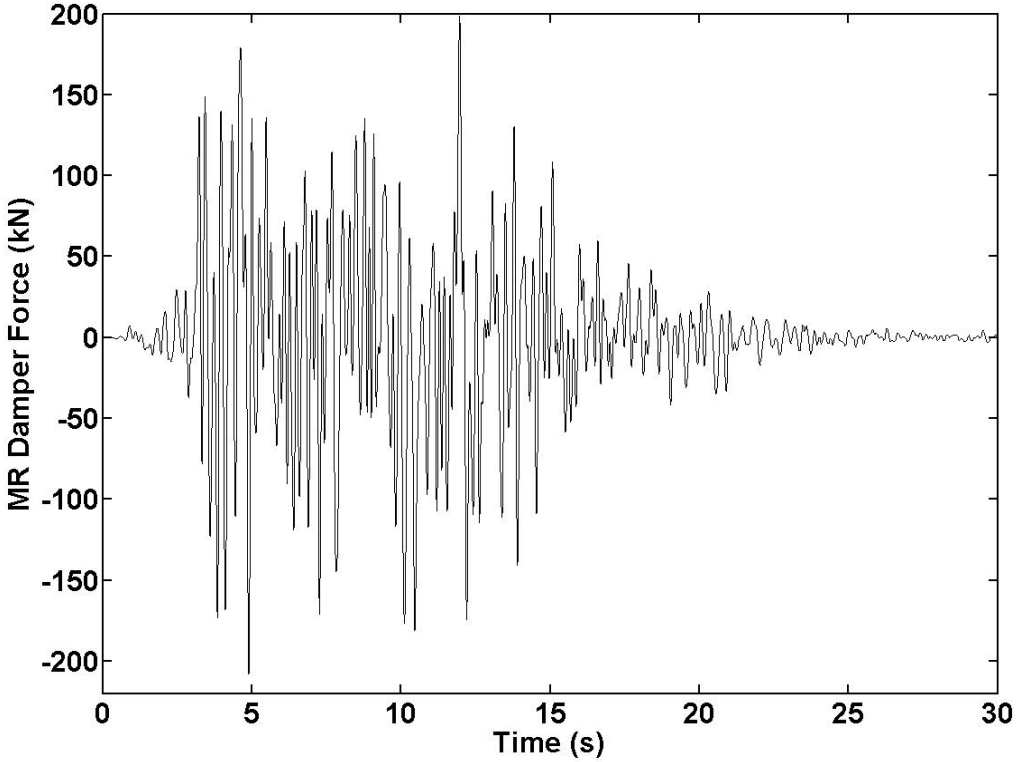

Fig. 3.9. Magnetorheological damper force

Once the structure-damper systems are identified based on the set of input-output signals, the identified models are used to design SNFC systems. Then, the effectiveness of those SNFC systems are demonstrated by applying for real-recorded earthquake ground acceleration.

3.4.3 Real-recorded Earthquake Signal

To demonstrate the performance of the SNFC system, the 1940 El Centro earthquake ground record is used shown in Fig. 3.10.

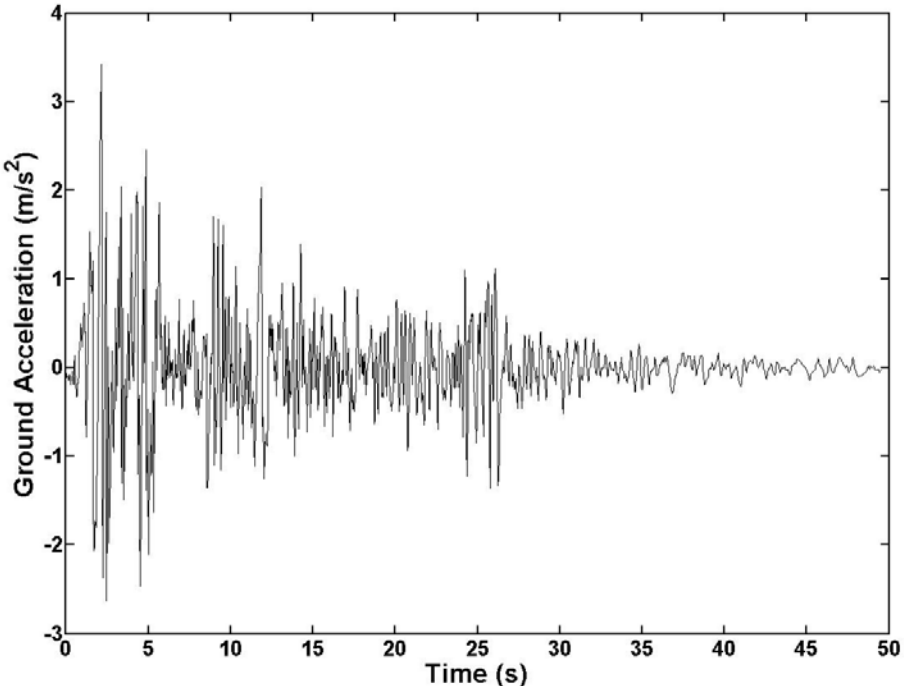

Fig. 3.10. The 1940 El Centro earthquake record

The intensity or time of the El Centro earthquake ground acceleration record can be scaled up or down such that it is appropriate to given problems, e.g., the time rate is scaled down five times the real recorded rate for the three story building structure because the scale factor of the three story building model is 0.2; an intensity of 0.25 is

applied to the eight story building structure because the maximum magnitude of the ground acceleration used by previous researchers is less than $0.8\ \mathrm{m/s^2}$.

3.5 Concluding Remarks

In this section, the equations of motion of two shear type building structures subjected to earthquake-induced motion, which include a three and an eight story building structures, have been derived as state space equations. Then, MR dampers have been added into the building structures using Chevron braces. The associated equations of motion of the integrated building-MR damper system are also derived. Last, a set of input-output signals for the purpose of the identification and control system design is given.

4. NONLINEAR SYSTEM IDENTIFICATION

4.1 Introduction

One of the most difficult but important tasks in control system design for seismically excited building structures is the development of an accurate explicit mathematical model of the building system to be controlled because precise mathematical information related to the building structure is used for calculation of control forces. However, development of a mathematical model for a nonlinear building system as a dynamic system is still a challenging problem. One example of a nonlinear building structure occurs when magnetorheological (MR) dampers, which are highly nonlinear hysteretic devices, are applied to the building systems for efficient energy dissipation. In this case, the integrated building-MR damper system behaves nonlinearly although the building structure itself is usually assumed to remain linear (Ramallo et al. 2004). The development of an appropriate nonlinear model of the integrated system that includes the interaction between the structural system and the nonlinear MR damper plays a key role in control system design because the building structure equipped with a nonlinear MR damper is intrinsically nonlinear. A solution can be found in nonlinear system identification based on TS fuzzy model.

In this section, a framework for nonlinear system identification is presented through a family of local linear MIMO autoregressive with exogenous (ARX) input-

based TS fuzzy model. In particular, the building-MR damper system that is modeled as a Takagi-Sugeno (TS) fuzzy model can be used to design a parallel distributed compensation (PDC)-based nonlinear controller because the PDC-based nonlinear controller shares linguistic information with the building-damper system that is modeled as the TS fuzzy model. The goal is to achieve optimal estimation of a set of nonlinear MIMO data from building structures equipped with MR dampers. In the following sections, the ARX model and fuzzy models are reviewed briefly. Next, a hybrid multiple ARX-TS fuzzy model is introduced and then its parameters are optimized via clustering and least squares algorithms. To demonstrate the effectiveness of the proposed ARX-TS fuzzy model, a three-story and an eight-story shear type building structure are studied.

4.2 MIMO ARX Model

4.2.1 Single-input-single-output (SISO) ARX Model

An input-output relationship of a linear time-invariant dynamic system can be described via a linear difference equation that is often called an ARX model in which AR represents the autoregressive output and X represents the exogenous input

$$\begin{aligned} &y(kT)+a_1 y(kT-1)+a_2 y(kT-2)+\cdots+a_n y(kT-n) \\ &=b_0 u(kT-1)+b_1 u(kT-2)+b_2 u(kT-3)+\cdots+b_m u(kT-m), \end{aligned} \tag{4.1}$$

where $y(kT)$ is an output signal, $u(kT)$ is an input signal, n is the number of delay steps in the output signals, and m is the number of delay steps in the input signals. In addition, T is the sample period, $1/T$ is the sample rate, and k is the integer value. However, the $y(kT)$ and $u(kT)$ are written simply as $y(k)$ and $u(k)$

$$\begin{aligned} &y(k)+a_1 y(k-1)+a_2 y(k-2)+\cdots+a_n y(k-n) \\ &=b_0 u(k-1)+b_1 u(k-2)+b_2 u(k-3)+\cdots+b_m u(k-m). \end{aligned} \tag{4.2}$$

This difference equation can be considered as an equation to determine the current output in terms of previous inputs and outputs

$$\begin{aligned} &y(k)=-a_1 y(k-1)-a_2 y(k-2)-\cdots-a_n y(k-n) \\ &+b_0 u(k-1)+b_1 u(k-2)+b_2 u(k-3)+\cdots+b_m u(k-m), \end{aligned} \tag{4.3}$$

or

$$y(k)=-\sum_{i=1}^{n} a_i y(k-i)+\sum_{i=1}^{m} b_i u(k-i). \tag{4.4}$$

Eq. (4.4) can be represented in more compact form by defining the following vectors

$$\underline{\boldsymbol{\theta}} = \left[a_1, \ldots, a_n, b_1, \ldots, b_m\right]^T, \tag{4.5}$$

$$\underline{\mathbf{H}}(k) = \left[-y(k-1), \ \ldots \ , -y(k-n), u(k-1), \ \ldots \ , u(k-m)\right]^T. \tag{4.6}$$

Using Eq. (4.5) and Eq. (4.6), Eq. (4.4) can be rewritten as

$$y(k) = \underline{\mathbf{H}}^T(k)\underline{\boldsymbol{\theta}}. \tag{4.7}$$

Eq. (4.7) can be thought as a linear regression expression because $y(k)$ depends on the parameters in $\underline{\boldsymbol{\theta}}$ as

$$\hat{y}(k \,|\, \underline{\boldsymbol{\theta}}) = \underline{\mathbf{H}}^T(k)\underline{\boldsymbol{\theta}}, \tag{4.8}$$

where the vector $\underline{\mathbf{H}}(k)$ is called a regression vector. Also, the SISO ARX model can be generalized as a MIMO ARX model. In what follows, the SISO ARX model is extended into a MIMO ARX model.

4.2.2 MIMO ARX Model

A SISO ARX model that represents a relationship between single input and single output of a linear time-invariant dynamic system can be easily generalized into a MIMO ARX model

$$\begin{aligned}\mathbf{y}(k) &= -\mathbf{a}_1\mathbf{y}(k-1) - \mathbf{a}_2\mathbf{y}(k-2) - \cdots - \mathbf{a}_n\mathbf{y}(k-n) \\ &+\mathbf{b}_0\mathbf{u}(k-1) + \mathbf{b}_1\mathbf{u}(k-2) + \mathbf{b}_2\mathbf{u}(k-3) + \cdots + \mathbf{b}_m\mathbf{u}(k-m),\end{aligned} \tag{4.9}$$

or

$$\mathbf{y}(k) = -\sum_{i=1}^{n}\mathbf{a}_i\mathbf{y}\left(k-i\right) + \sum_{i=1}^{m}\mathbf{b}_i\mathbf{u}\left(k-i\right), \tag{4.10}$$

where

$$\mathbf{y}\left(k\right) = \left[\, y_1\left(k\right), y_2\left(k\right), \cdots, y_p\left(k\right) \,\right]^T, \tag{4.11}$$

$$\mathbf{u}\left(k\right) = \left[\, u_1\left(k\right), u_2\left(k\right), \cdots, u_q\left(k\right) \,\right]^T, \tag{4.12}$$

$$\mathbf{a}_i = \begin{bmatrix} a_i^{1,1} & a_i^{1,2} & \cdots & a_i^{1,n-1} & a_i^{1,n} \\ a_i^{2,1} & a_i^{2,2} & & a_i^{2,n-1} & a_i^{2,n} \\ \vdots & \vdots & & \vdots & \vdots \\ a_i^{p-1,1} & a_i^{p-1,2} & & a_i^{p-1,n-1} & a_i^{p-1,n} \\ a_i^{p,1} & a_i^{p,2} & \cdots & a_i^{p,n-1} & a_i^{p,n} \end{bmatrix}, \tag{4.13}$$

and

$$\mathbf{b}_i = \begin{bmatrix} b_i^{1,1} & b_i^{1,2} & \cdots & b_i^{1,m-1} & b_i^{1,m} \\ b_i^{2,1} & b_i^{2,2} & & b_i^{2,m-1} & b_i^{2,m} \\ \vdots & \vdots & & \vdots & \vdots \\ b_i^{q-1,1} & b_i^{q-1,2} & & b_i^{q-1,m-1} & b_i^{q-1,m} \\ b_i^{q,1} & b_i^{q,2} & \cdots & b_i^{q,m-1} & b_i^{q,m} \end{bmatrix}. \tag{4.14}$$

Eq. (4.10) can be represented in more compact form by defining the following matrices

$$\boldsymbol{\theta} = \left[\mathbf{a}_1, \ldots, \mathbf{a}_n, \mathbf{b}_1, \ldots, \mathbf{b}_m\right]^T, \tag{4.15}$$

$$\mathbf{H}(k) = \left[-\mathbf{y}(k-1),\ \ldots\ , -\mathbf{y}(k-n), \mathbf{u}(k-1),\ \ldots\ , \mathbf{u}(k-m)\right]^T. \tag{4.16}$$

Using Eq. (4.15) and Eq. (4.16), Eq. (4.10) can be rewritten as

$$\mathbf{y}(t) = \mathbf{H}^T(k)\boldsymbol{\theta}. \tag{4.17}$$

This can be also a regression equation

$$\hat{\mathbf{y}}(k|\boldsymbol{\theta}) = \mathbf{H}^T(k)\boldsymbol{\theta}. \tag{4.18}$$

Unfortunately, the ARX model has the limited range of operating regions because it is a linear time-invariant system model; however, a solution on this drawback can be found in multiple ARX models that have a variety of operating regions. In the following sections, fuzzy models are first introduced; then, it is integrated with the multiple ARX models.

4.3 Fuzzy Model

4.3.1 Membership Functions and Fuzzy Sets

Membership functions (MFs) and fuzzy sets are the cornerstone of a fuzzy logic-based system that is appropriate for modeling complex nonlinear systems with uncertain parameters. There exist always a variety of uncertainties in engineering problems; e.g., "the structural damage is very large" and "the performance of a MR damper is sensitive to high temperature." However, questions would arise: "How much damage would be thought as very large quantity?" or "Which degree of temperature is high?" In reality, it is impossible to model variables with these uncertainties in a conventional way; however, MFs can be used for modeling such variables as an element of a fuzzy set.

Fig. 4.1 shows several types of MFs that is generally selected by engineers' judgment depending on given problems.

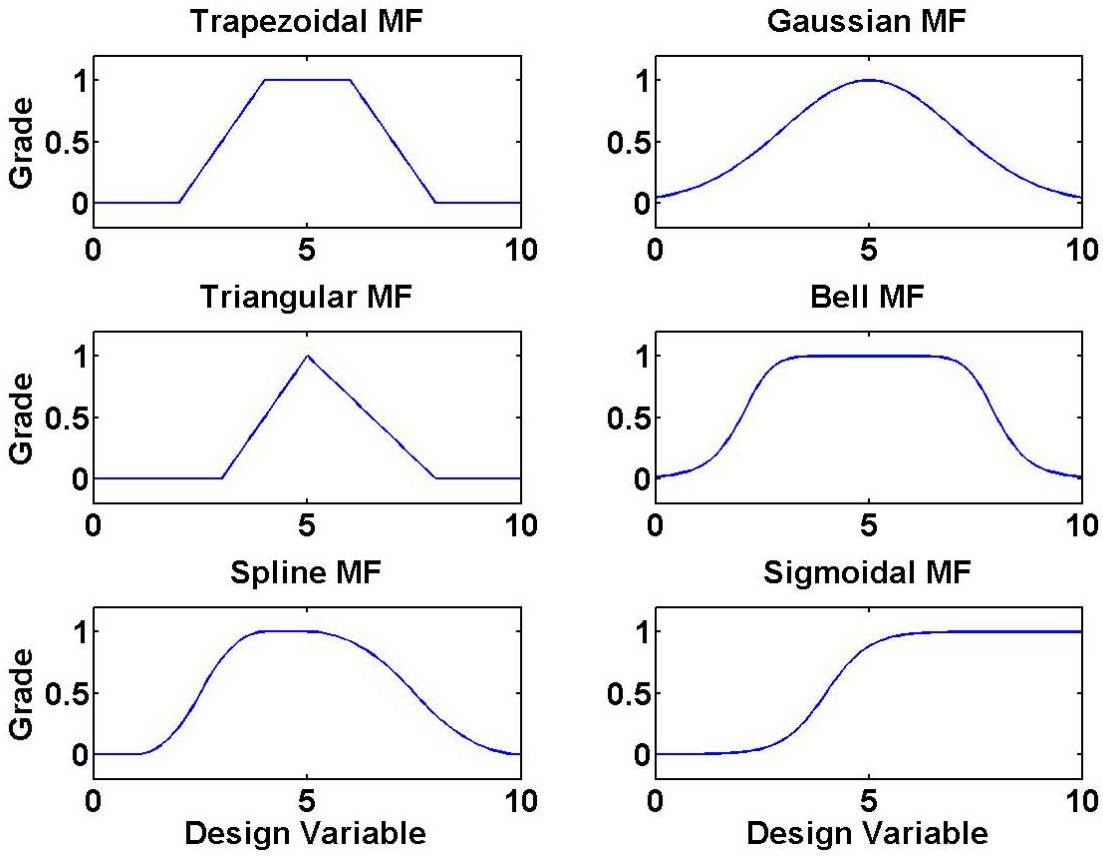

Fig. 4.1. Type of fuzzy membership functions

Fuzzy sets are constructed from the MFs. For example, if the structural damage is categorized into three stages, e.g., small, medium, and large damage, a fuzzy set can be constructed as shown in Fig. 4.2. This fuzzy set is used for constructing a premise part of an IF-THEN rule, i.e., IF STATEMENT.

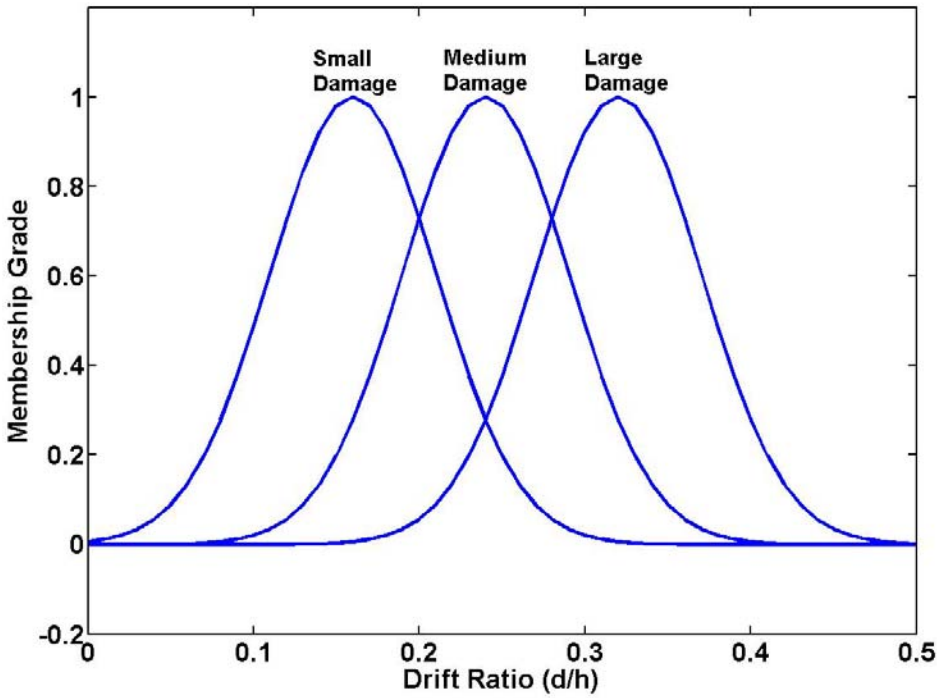

Fig. 4.2. A fuzzy set representing structural damage

4.3.2 Fuzzy Rules

A fuzzy rule base has a family of fuzzy IF-THEN rules; e.g., “if a building structure has large damage, a controller is operated such that an alarm is rung twice”, “if the structural damage is medium, the controller is operated such that the alarm is rung

once", and "if there is no damage in the building structure, the controller is not operated." The set of IF-THEN rules is blended into an integrated system through fuzzy reasoning methods.

4.3.3 Fuzzy Reasoning

Fuzzy reasoning is a mechanism to perform the fuzzy inference system that derives conclusions from a family of IF-THEN rules, i.e., fuzzy reasoning is a methodology to organize a set of the IF-THEN rules. In what follows, two types of fuzzy models that have been extensively applied to a variety of engineering fields are introduced in order to compare different type of reasoning mechanisms: Mamdani and Takagi-Sugeno fuzzy models.

4.3.3.1 Mamdani Fuzzy Model

Mamdani fuzzy model uses fuzzy sets in both IF and THEN STATEMENTS; the IF STATEMENT and THEN STATEMENT are called a premise part and a consequent part, respectively. A typical fuzzy rule of a Mamdani fuzzy model has the form

R_j : If z_{FZ}^1 is $p_{1,j}$ and z_{FZ}^2 is $p_{2,j}$ and$\cdots$ and z_{FZ}^i is $p_{i,j}$

Then, (4.19)

$$y = q,$$

where R_j is the j^{th} fuzzy rule; $\mathbf{z}_{\mathrm{FZ}} = \left[z_{\mathrm{FZ}}^1, \ldots, z_{\mathrm{FZ}}^i \right]$ is a premise vector that can be either a set of system inputs or outputs.

Consider a simple Mamdani fuzzy model that has two rules, two input variables in the premise part, and one output variable in the consequent part in order to describe the Mamdani's reasoning mechanism

$$\begin{aligned} &\mathrm{R}_1 : \text{If } z_{\mathrm{FZ}}^1 \text{ is } p_{11} \text{ and } z_{\mathrm{FZ}}^2 \text{ is } p_{21} \text{ Then } y \text{ is } q_1, \\ &\mathrm{R}_2 : \text{If } z_{\mathrm{FZ}}^1 \text{ is } p_{12} \text{ and } z_{\mathrm{FZ}}^2 \text{ is } p_{22} \text{ Then } y \text{ is } q_2. \end{aligned} \tag{4.20}$$

The Mamdani's reasoning procedure has four main steps: calculating weights, weighing consequent parameters, aggregation, and defuzzification.

Step 1: Computation of weight

The first step is to calculate weighing values of each rule for the input values

$$\begin{aligned} &\text{Weight of } \mathrm{R}_1 : w_1 = \mu_{p_{11}}\left(z_{\mathrm{FZ}}^1\right) \wedge \mu_{p_{21}}\left(z_{\mathrm{FZ}}^2\right) \\ &\text{Weight of } \mathrm{R}_2 : w_2 = \mu_{p_{12}}\left(z_{\mathrm{FZ}}^1\right) \wedge \mu_{p_{22}}\left(z_{\mathrm{FZ}}^2\right), \end{aligned} \tag{4.21}$$

where $\mu_{p_{ij}}\left(z_{\mathrm{FZ}}^{i}\right)$ is a MF for the premise parameter p_{ij}; $\wedge$ represents min-operation (Yen and Langari 1999). These weighting values are applied to consequent parameters to derive conclusions of each fuzzy rule.

Step 2: Apply for the weights of rules to consequent parameters

By applying for weights of rules to the MFs about consequent parameters, the following conclusions of each rule are derived

$$\begin{aligned}&\text{Conclusion of } \mathrm{R}_1 : \mu_{q_1}^{*}\left(z_{\mathrm{FZ}}^{1}, z_{\mathrm{FZ}}^{2}\right) = w_1 \wedge \mu_{q_1}\left(y\right),\\ &\text{Conclusion of } \mathrm{R}_2 : \mu_{q_2}^{*}\left(z_{\mathrm{FZ}}^{1}, z_{\mathrm{FZ}}^{2}\right) = w_2 \wedge \mu_{q_2}\left(y\right).\end{aligned} \tag{4.22}$$

These conclusions of each fuzzy rule are derived as a conclusion via aggregation process.

Step 3: Aggregate the conclusions obtained in Step 2

The conclusions that are derived in Step 2 should be blended as an integrated conclusion using union of fuzzy sets

$$\mu_q\left(y\right) = \mu_{q_1}^{*}\left(y\right) \vee \mu_{q_2}^{*}\left(y\right), \tag{4.23}$$

where $\vee$ represents max-operation (Yen and Langari 1999).

However, values obtained from Eq. (4.23) are not definite values, but fuzzy values. Thus, these fuzzy set values are converted into definite values with a defuzzification process.

Step 4: Defuzzification

Defuzzification is a way of extracting definite values from fuzzy sets. A commonly used method, centroid of area method is used here although there are many defuzzification methodologies, e.g., bisector of area, mean of maximum, smallest of maximum, largest of maximum, etc.

$$y_{\text{final}} = \frac{\int_y \mu_q(y)\, y dy}{\int_y \mu_q(y)\, dy}. \tag{4.24}$$

However, the computational cost of Mamdani fuzzy model is high because the defuzzification procedure is time-consuming. In addition, the model is not appropriate for rigorous mathematical analysis. Those drawbacks have led to development of other types of fuzzy models that are computationally efficient and mathematically meaningful. In what follows, one of such efficient models, TS fuzzy model, is introduced.

4.3.3.2 Takagi-Sugeno (TS) Fuzzy Model

Takagi and Sugeno (1985) developed a systematic methodology for a fuzzy reasoning using linear functions in the consequent part. Because the TS-fuzzy model uses linear functions in the consequent part, the defuzzification procedure is not required. Therefore, the reasoning mechanism of the TS fuzzy model is simpler than the Mamdani fuzzy model, i.e., the lower computational cost is required for the TS fuzzy model than the Mamdani fuzzy model due to much smaller number of fuzzy rules of the TS fuzzy model. Furthermore, the TS fuzzy model provides a systematic framework for rigorous mathematical analysis. A typical fuzzy rule for the TS fuzzy model has the form

R_j : If z_{FZ}^1 is $p_{1,j}$ and z_{FZ}^2 is $p_{2,j}$ and$\cdots$ and z_{FZ}^i is $p_{i,j}$

Then, (4.25)

$$y = f\left(z_{\mathrm{FZ}}^1,...,z_{\mathrm{FZ}}^i\right),$$

where R_j is the j^{th} fuzzy rule; $\mathbf{z}_{\mathrm{FZ}} = \left[z_{\mathrm{FZ}}^1,\ldots,z_{\mathrm{FZ}}^i\right]$ is a premise vector that can be either a set of system inputs or outputs; $y = f\left(z_{\mathrm{FZ}}^1,...,z_{\mathrm{FZ}}^i\right)$ is a linear function in the consequent part. In general, $y = f\left(z_{\mathrm{FZ}}^1,...,z_{\mathrm{FZ}}^i\right)$ is a polynomial function in terms of the premise vector $\mathbf{z}_{\mathrm{FZ}} = \left[z_{\mathrm{FZ}}^1,\ldots,z_{\mathrm{FZ}}^i\right]$ although it can be any type of function.

Differently with the Mamdani's reasoning method with relatively complicated procedure, TS fuzzy model-based reasoning is a simple process to compute weighted mean values

$$y_{\text{final}} = \frac{\sum_{j=1}^{N_r} w_j y_j}{\sum_{j=1}^{N_r} w_j}, \tag{4.26}$$

where

$$w_j = \prod_{i=1}^{n} \mu_{i,j}\left(z_{\text{FZ}}^{i}\right). \tag{4.27}$$

However, this type of polynomial may not be appropriate for modeling dynamic systems. Thus, ARX models are integrated with the TS fuzzy model such that the TS fuzzy model can describe behavior of a dynamic system.

4.4 A Family of MIMO ARX TS Fuzzy Models

A nonlinear dynamic system that has multiple operation regions can be described through multiple linear dynamic models. In this section, multiple ARX models whose

operating regions are blended with a fuzzy interpolation method are introduced (Johansen 1994; Abonyi et al. 2000; Abonyi 2003).

A MIMO dynamic system can be described by the following multivariable nonlinear model

$$\dot{\mathbf{z}} = \mathbf{f}(t, \mathbf{z}, \mathbf{u}), \tag{4.28}$$

where t is the time variable; $\mathbf{z}$ is a state vector; $\mathbf{u}$ is an input vector; and $\mathbf{f}$ represents a multivariable nonlinear dynamic system. This MIMO nonlinear dynamic model can be described by a family of ARX-TS fuzzy models

$$\mathrm{R}_j: \text{ If } z_{\mathrm{FZ}}^1 \text{ is } p_{1,j} \text{ and } z_{\mathrm{FZ}}^2 \text{ is } p_{2,j} \text{ and} \cdots \text{ and } z_{\mathrm{FZ}}^i \text{ is } p_{i,j}$$

Then,

$$\begin{aligned} \mathbf{y}(k) = {} & \mathbf{a}_{1,j}\,\mathbf{y}(k-1) + \mathbf{a}_{2,j}\,\mathbf{y}(k-2) + \cdots + \mathbf{a}_{n,j}\mathbf{y}(k-n) \\ & + \mathbf{b}_{1,j}\,\mathbf{u}(k-1) + \mathbf{b}_{2,j}\,\mathbf{u}(k-2) + \cdots + \mathbf{b}_{m,j}\,\mathbf{u}(k-m), \end{aligned} \tag{4.29}$$

or

R_j : If z_{FZ}^1 is $p_{1,j}$ and z_{FZ}^2 is $p_{2,j}$ and$\cdots$ and z_{FZ}^i is $p_{i,j}$

Then,

$$\mathbf{y}(k) = \sum_{i=1}^{n} \mathbf{a}_{i,j}\, \mathbf{y}(k-i) + \sum_{i=1}^{m} \mathbf{b}_{i,j}\, \mathbf{u}(k-i), \tag{4.30}$$

where R_j is the j^{th} fuzzy rule; $\mathbf{z} = \left[z_{\mathrm{FZ}}^1, ..., z_{\mathrm{FZ}}^i \right]$ is a premise vector that can be either a set of dynamic system inputs or outputs

$$\mathbf{z}_{\mathrm{FZ}} \in \left\{ y_1(k-1), ..., y_1(k-n), ..., y_p(k-n), u_1(k-1), ...u_1(k-m), ..., u_q(k-m) \right\}, \tag{4.31}$$

$$\mathbf{y}(k) = \left[y_1(k), y_2(k), \cdots, y_p(k) \right]^T, \tag{4.32}$$

$$\mathbf{u}(k) = \left[u_1(k), u_2(k), \cdots, u_q(k) \right]^T, \tag{4.33}$$

$$\mathbf{a}_{i,j} = \begin{bmatrix} a_{i,j}^{1,1} & a_{i,j}^{1,2} & \cdots & a_{i,j}^{1,n-1} & a_{i,j}^{1,n} \\ a_{i,j}^{2,1} & a_{i,j}^{2,2} & & a_{i,j}^{2,n-1} & a_{i,j}^{2,n} \\ \vdots & \vdots & & \vdots & \vdots \\ a_{i,j}^{p-1,1} & a_{i,j}^{p-1,2} & & a_{i,j}^{p-1,n-1} & a_{i,j}^{p-1,n} \\ a_{i,j}^{p,1} & a_{i,j}^{p,2} & \cdots & a_{i,j}^{p,n-1} & a_{i,j}^{p,n} \end{bmatrix}, \tag{4.34}$$

and

$$\mathbf{b}_{i,j} = \begin{bmatrix} b_{i,j}^{1,1} & b_{i,j}^{1,2} & \cdots & b_{i,j}^{1,m-1} & b_{i,j}^{1,m} \\ b_{i,j}^{2,1} & b_{i,j}^{2,2} & & b_{i,j}^{2,m-1} & b_{i,j}^{2,m} \\ \vdots & \vdots & & \vdots & \vdots \\ b_{i,j}^{q-1,1} & b_{i,j}^{q-1,2} & & b_{i,j}^{q-1,m-1} & b_{i,j}^{q-1,m} \\ b_{i,j}^{q,1} & b_{i,j}^{q,2} & \cdots & b_{i,j}^{q,m-1} & b_{i,j}^{q,m} \end{bmatrix}, \tag{4.35}$$

where n is the number of delay steps in the output signals; m is the number of delay steps in the input signals, p is the number of output signals, and q is the number of input signals. Note that the number of the fuzzy rules corresponds to the number of local ARX models, i.e., m ARX linear dynamic models represent m fuzzy rules that describe behavior of a nonlinear dynamic system. However, a question would arise on how to blend the multiple ARX dynamic models as an integrated system model, i.e., how to make a bridge for communication among each ARX models. One of solutions is found in fuzzy logic-based interpolation. The multiple ARX local models at the specific operating point z_{FZ}^{i} can be blended

$$\hat{\mathbf{y}}(k) = \sum_{i=1}^{n}\sum_{j=1}^{N_r} w_j\left(z_{\mathrm{FZ}}^{i}\right)\mathbf{a}_{i,j}\mathbf{y}(k-i) + \sum_{i=1}^{m}\sum_{j=1}^{N_r} w_j\left(z_{\mathrm{FZ}}^{i}\right)\mathbf{b}_{i,j}\mathbf{u}(k-i), \tag{4.36}$$

where $0 \le w_j\left(z_{\mathrm{FZ}}^{i}\right) \le 1$ is the normalized true value of the j^{th} rule,

$$w_j(z_{\mathrm{FZ}}^i) = \frac{\prod_{i=1}^{n} \mu_{i,j}(z_{\mathrm{FZ}}^i)}{\sum_{j=1}^{N_r} \prod_{i=1}^{n} \mu_{i,j}(z_{\mathrm{FZ}}^i)}. \tag{4.37}$$

Once the multiple ARX-TS fuzzy model is set up, the premise parameters $p_{i,j}$ and the consequent parameters $\mathbf{a}_{i,j}$ and $\mathbf{b}_{i,j}$ are determined such that the multiple ARX-TS fuzzy model describes behavior of a nonlinear dynamic system. In this research, the premise parameters are determined through clustering techniques and the consequent part is optimized using a weighted least squares estimation algorithm. In what follows, clustering algorithms are introduced.

4.5 Clustering Algorithms

For efficient determination of the premise part, (i.e., the small number of membership functions but reasonable pattern recognition), grouping of data with similar patterns would be desirable. In this research, subtractive and fuzzy C-means clustering algorithms are used to extract information on center of groups from a large data set.

4.5.1 Fuzzy C-means Clustering

As a generalized version of K-means clustering algorithm (Jang et al. 1997), fuzzy C-means clustering algorithm has been widely applied to a variety of engineering

problems (Wang and Langari 1996). This algorithm generates fuzzy sets in an automatic way and does not require any previous knowledge about the data structure of a given problem.

The fuzzy C-means clustering algorithm is formulated as a constraint optimization problem

$$\underset{\sigma_k-\sigma_i\neq 0}{\text{Minimize}} \quad J(\mathbf{U},\sigma_1,...,\sigma_c)=\sum_{i=1}^{c}\sum_{j=1}^{n}\left(\mu_{i,j}\right)^m\left\|\sigma_i-\sigma_j\right\| \tag{4.38}$$

subject to

$$\sum_{i=1}^{c}\mu_{i,j}=1, \quad j=1,2,...,n,$$

where $\mu_{i,j}$ is membership for σ_j in the i^{th} cluster whose values in between 0 and 1; σ_i is the cluster center of each group i; σ_j is i^{th} data point; $m>1$ is a design parameter; and $\mathbf{U}=\left[\mu_{i,j}\right]$ is the partition matrix with $c\times n$ dimension.

Using Lagrange multipliers, the constrained optimization can be transformed into an unconstrained optimization problem

$$\bar{J}(\mathbf{U},\sigma_1,...,\sigma_c,\lambda_1,...,\lambda_n)=\sum_{i=1}^{c}\sum_{j=1}^{n}\left(\mu_{i,j}\right)^m\left\|\sigma_i-\sigma_j\right\|+\sum_{j=1}^{n}\lambda_j\left(\sum_{i=1}^{c}\mu_{i,j}-1\right). \tag{4.39}$$

Differentiation of the augmented objective function leads to the necessary conditions

$$\sigma_i = \frac{\sum_{j=1}^{n} \left(\mu_{i,j}\right)^m \sigma_j}{\sum_{j=1}^{n} \left(\mu_{i,j}\right)^m}, \tag{4.40}$$

where

$$\mu_{i,j} = \sum_{k=1}^{c} \left(\frac{\left\| \sigma_i - \sigma_j \right\|}{\left\| \sigma_k - \sigma_j \right\|} \right)^{-2/(m-1)} . \tag{4.41}$$

This fuzzy C-means clustering procedure is a simple iterative algorithm: first, generate the initial membership function matrix $\mathbf{U} = \left[\mu_{i,j} \right]$ using a random number generator such that the constraint condition $\sum_{i=1}^{c} \mu_{i,j} = 1$ is satisfied; second, calculate a cluster center using Eq. (4.40); third, compute the cost function value using Eq. (4.38) and stop if iteration stopping criteria is satisfied; and fourth, calculate a new membership function matrix $\mathbf{U} = \left[\mu_{i,j} \right]$ using Eq. (4.41) and then go to the second step.

However, the fuzzy C-means clustering algorithm is sensitive to initialization of the membership function matrix $\mathbf{U} = \left[\mu_{i,j} \right]$ that might fall into local minima. In such a case, uncountable trial-and-error simulations would be required. Thus, a different

clustering algorithm that is not sensitive to initial values is introduced in the following section: subtractive clustering.

4.5.2 Subtractive Clustering

Differently with the fuzzy C-means clustering algorithm, subtractive clustering is not sensitive to initial values because it considers all the data points as a candidate for a cluster center. In addition, it is independent of the data dimension.

In the subtractive clustering, a data point with the highest density neighborhood is selected as a cluster center. The density measure at data point σ_i is given by (Liu et al. 2003)

$$D_i = \sum_{j=1}^{n} \exp\left(\frac{\left\| \sigma_i - \sigma_j \right\|^2}{\left(R_a / 2 \right)^2} \right), \tag{4.42}$$

where σ_i is the i^{th} data point, n is the total number of data points, and R_a, which is chosen by the user, represents range of data neighborhood to be considered or the degree to which a cluster center contributes to the density measure. After a data point is selected as the first cluster center with the highest potential, the selected cluster center and its neighborhood data points are subtracted in the following selection procedure

$$D_i = D_i - D_{c_j} \sum_{j=1}^{n} \exp\left(\frac{\left\| \sigma_i - \sigma_{c_j} \right\|^2}{\left(R_b / 2 \right)^2} \right), \tag{4.43}$$

where D_{c_j} is the j^{th} density measure, σ_{c_j} is the j^{th} cluster center, and R_b is a parameter used to avoid closely spaced centers that is specified by $R_b = \eta R_a$, where η is a positive constant greater than 1. After subtraction procedure, the next density measure is calculated and the cluster center is selected. This procedure is repeated until a sufficient number of cluster centers are found in the input space. The cluster centers that have been calculated via either fuzzy C-means or subtractive clustering algorithms are used to construct the linguistic part, i.e., premise part, of a TS fuzzy model, e.g., the cluster center information is used as a center value of a Gaussian or triangular MFs. Once the premise part of the TS fuzzy model is determined by either fuzzy C-means or subtractive clustering algorithms, weighted least squares algorithm is applied to find optimum solutions of the consequent parameters of the TS fuzzy model.

4.6 Weighted Least Squares

Once the premise part is determined, the consequent parameters can be optimized with weighted least squares algorithms. A least squares algorithm can be formulated as a quadratic optimization problem that minimizes difference between true values and estimated values

$$\text{Min } J = \frac{1}{2}\mathbf{e}(k)^{\mathrm{T}}\mathbf{e}(k), \tag{4.44}$$

where $\mathbf{e}(k) = \hat{\mathbf{y}}(k) - \tilde{\mathbf{y}}(k)$; i.e., the error $\mathbf{e}(k)$ is difference between the estimation model $\hat{\mathbf{y}}(k)$ and true values $\tilde{\mathbf{y}}(k)$.

A linear estimation model for used with the linear least squares algorithm is

$$\hat{\mathbf{y}}(k) = \mathbf{H}(k)\boldsymbol{\theta}_j. \tag{4.45}$$

On the other hand, the true model can be thought as a contaminated estimation model

$$\tilde{y}(k) = \mathbf{H}(k)\boldsymbol{\theta}_j + \mathbf{e}(k). \tag{4.46}$$

From Eq. (4.46), the error dynamics is given by

$$\mathbf{e}(k) = \tilde{\mathbf{y}}(k) - \mathbf{H}(k)\boldsymbol{\theta}_j. \tag{4.47}$$

Substituting Eq. (4.47) into Eq. (4.44) leads to the following objective function

$$J = J(\boldsymbol{\theta}_j) = \frac{1}{2}\left[\tilde{\mathbf{y}}(k)^{\mathrm{T}}\tilde{\mathbf{y}}(k) - 2\tilde{\mathbf{y}}(k)^{\mathrm{T}}\mathbf{H}(k)\boldsymbol{\theta}_j + \boldsymbol{\theta}_j{}^{\mathrm{T}}\mathbf{H}(k)^{\mathrm{T}}\mathbf{H}(k)\boldsymbol{\theta}_j\right]. \tag{4.48}$$

In this problem, the objective is to find $\boldsymbol{\theta}_j$ such that the objective function, J is minimized. For minimization of the quadratic function of Eq. (4.48), the necessary condition can be derived

$$\nabla_{\boldsymbol{\theta}_j} J = \mathbf{H}(k)^{\mathrm{T}} \mathbf{H}(k) \boldsymbol{\theta}_j - \mathbf{H}(k)^{\mathrm{T}} \tilde{\mathbf{y}}(k) = 0, \tag{4.49}$$

where $\nabla_{\boldsymbol{\theta}_j} J$ is a Jacobian matrix, the 1st partial derivative of J about $\boldsymbol{\theta}_j$. For solution of this equation, the following analytical least squares estimator is available (Wang and Langari 1996)

$$\boldsymbol{\theta}_j = \left[\mathbf{H}(k)^{\mathrm{T}} \mathbf{H}(k) \right]^{-1} \mathbf{H}(k)^{\mathrm{T}} \tilde{\mathbf{y}}(k). \tag{4.50}$$

This linear least squares estimation can be easily extended into a weighted least squares estimator

$$\boldsymbol{\theta}_j = \left[\mathbf{H}(k)^{\mathrm{T}} w_j \mathbf{H}(k) \right]^{-1} \mathbf{H}(k)^{\mathrm{T}} w_j \tilde{\mathbf{y}}(k), \tag{4.51}$$

where

$$\mathbf{H}(k) = [\mathbf{y}(k-1)^{\mathrm{T}}, ..., \mathbf{y}(k-n)^{\mathrm{T}}, \mathbf{u}(k-1)^{\mathrm{T}}, ..., \mathbf{u}(k-m)^{\mathrm{T}}], \tag{4.52}$$

and

$$\boldsymbol{\theta}_j = [\mathbf{a}_{1,j}, ..., \mathbf{a}_{n,j}, \mathbf{b}_{1,j}, ..., \mathbf{b}_{m,j}]. \tag{4.53}$$

In summary, the proposed nonlinear MIMO ARX fuzzy modeling approach is: 1) nonlinear behavior of a building-MR damper system is represented by a family of multiple ARX LTI models that are integrated into a nonlinear time-varying model via fuzzy rules; 2) the premise part of the multiple ARX-TS fuzzy model are partitioned to subdivide the input space into several operating regions using either subtractive or fuzzy C-means clustering techniques; 3) the consequent parameters are optimized by a family of linear weighted least squares. Finally, the effectiveness of the proposed multiple ARX-TS fuzzy model is demonstrated from numerical simulations in the following section. Note that the nonlinear multiple ARX-TS fuzzy model will be used for design of a parallel distributed compensation (PDC)-based active nonlinear fuzzy control system. The control system design is presented in the following section.

4.7 Examples

In this section, two benchmark building structures are investigated in order to demonstrate the effectiveness of the proposed nonlinear multiple ARX-TS fuzzy model. They include a three story and an eight story shear type building structures.

4.7.1 A Three Story Shear Type Building Structure

As explained in Section 2, the three story shear type building structure is a scaled model of a prototype building structure in the National Center for Earthquake Engineering Research (NCEER) at SUNY-Buffalo (Dyke et al. 1996). The reason to choose this structure is that many researchers have used this model as a benchmark test model.

A SD-1000 MR damper (Spencer et al. 1997) whose approximate capacity is 1500 N is installed into the 1st floor using a Chevron brace, which leads to a nonlinear dynamic model, i.e., a building-MR damper system. A configuration that shows how a MR damper is implemented into a building structure is shown in the figure on page 33. The equations of motion for the three-story shear type building-MR damper system are given by the equation on page 36. Note that once the MR damper is added into the building structure, behavior of the integrated building-MR damper system does not remain linear, i.e., it may not easy to derive equations of motion of the integrated building-MR damper system in an analytical way. In other words, it may not be

reasonable to identify $\mathbf{M}^*$, $\mathbf{C}^*$, and $\mathbf{K}^*$ through linear time invariant (LTI) model framework because m_1^*, c_1^*, and k_1^* are nonlinear time-varying values. However, a solution can be found in nonlinear system identification using a set of input and output data.

To date, only a few papers have been published on system identification for building structures equipped with nonlinear MR dampers (Dyke et al. 1998; Ramallo et al. 2004). In their approaches, identification of a building structure is first carried out in the frequency domain; a MR damper is next identified in the time domain; then, the identified building structure and the MR damper are integrated in the time domain; and finally, parameters of the combined building structure-MR damper model are modified. In this dissertation, this method is called joint frequency-time identification (JFTI) methodology.

However, the JFTI method is available only for linear building structures. In fact, dynamic characteristics such as the mass, stiffness, and damping of the building structure are changed by installing MR dampers into the building structure. In other words, it may not be reasonable to assume that the building system is a linear time-invariant system, i.e., a linear building model-based identification may not be effective to catch time-varying nonlinearity of a building-MR damper system. A nonlinear model-based identification for building-MR damper systems can circumvent this drawback. However, no systematic nonlinear identification methodology for a building-MR damper system has been investigated. Thus, this research addresses the development

of a new nonlinear identification methodology for building structures employing MR dampers in a systematic manner.

In this example, two input and two output signals are used for the purpose of the system identification. One of the inputs is an external disturbance, e.g., an earthquake-type random signal. The other input is a MR damper force signal. Differently with input signals that should be selected carefully, a variety of two output signals of interest can be used. Once a set of input-output signal is given, a nonlinear system identification algorithm, the nonlinear multiple ARX-TS fuzzy model can be applied to the given data set.

Fig. 4.3 and Fig 4.4 depict the comparison between the responses obtained by implementing the MR damper in the building structure and the response of the nonlinear identified model. Fig. 4.3 shows the comparison of the 1st floor displacement response with the identified model; Fig. 4.4 presents the comparison of the 3rd floor acceleration response with the identified model. As can be seen, good agreement between the original values and the identified model is found in both displacement and acceleration responses. The reason to choose these 1st floor displacement and 3rd floor acceleration responses as output signals to be identified is: 1) the response at the 3rd (top) floor is the largest one; 2) acceleration is readily available as absolute values; 3) the responses at the 1st floor are feedback to a MR damper because the MR damper is added into the 1st floor.

However, this is a small-scaled model; it might be necessary to investigate a larger-scale building structure. Therefore, an eight story shear type building structure is studied in the following section.

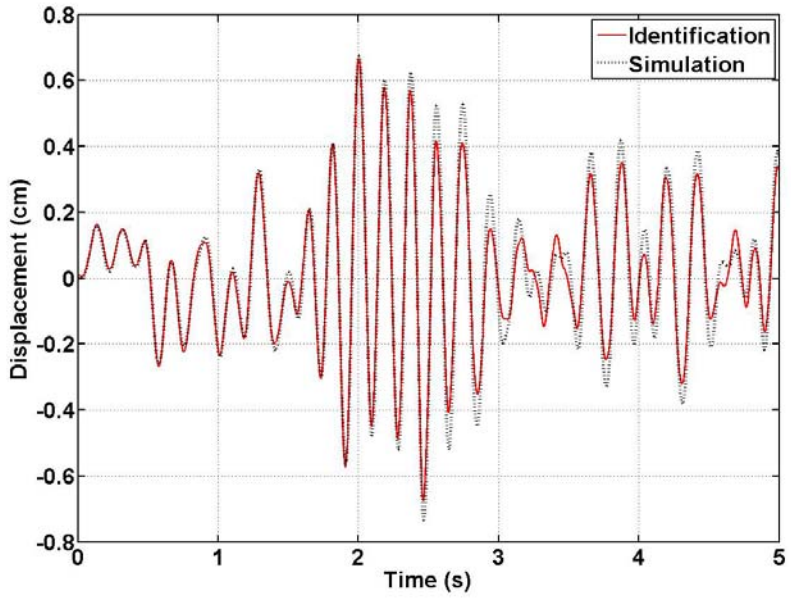

Fig. 4.3. Comparison of the 1st floor displacement relative to the ground of the original responses with the responses using the nonlinear fuzzy identification model

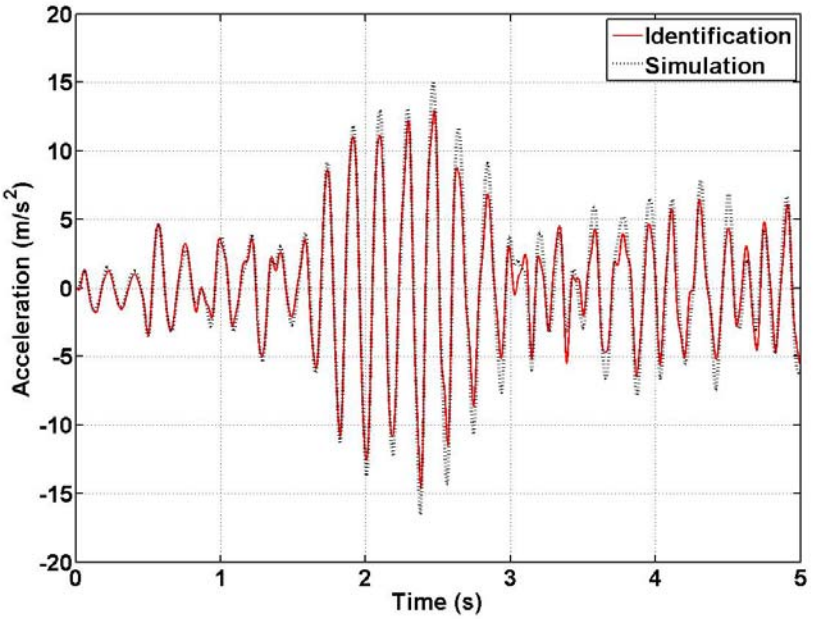

Fig. 4.4. Comparison of the 3rd floor acceleration of the original responses with the responses using the nonlinear fuzzy identification model

4.7.2 An Eight Story Shear Type Building Structure

To demonstrate the effectiveness of the proposed nonlinear multiple ARX-TS fuzzy model with a larger scale building structure, an eight story building structure that is explained in detail in Section 3 is studied here. Two 1000 kN MR dampers are installed on the 5^{th} and 8^{th} floors using Chevron braces. A configuration that shows how MR dampers are implemented into a building structure is shown in the figure on page 42. The equations of motion for the eight-story shear type building-MR damper system are given by the equation on page 38.

In this example, two identified models that represent behaviors of the eight story building employing MR dampers are developed: (1) ARX-TS Fuzzy 801 (2) ARX-TS Fuzzy 802. Each model is identified independently. For each model, two input and two output signals are used for the purpose of the system identification. One of the inputs is an external disturbance, i.e., an earthquake-type random signal. The other input is a MR damper force signal. On the other hand, a variety of two output signals of interest can be used: acceleration and drift at the floor where a MR damper is added are selected as output signals.

Once a set of input-output signal is given, a nonlinear system identification algorithm, the nonlinear multiple ARX-TS fuzzy model can be applied to the given data set. Detailed description on this eight story building-MR damper system is presented in Section 3.

Fig. 4.5 and Fig. 4.6 compare the original simulated values with a nonlinear fuzzy identified model. Fig. 4.5 is comparison of the 7^{th}-8^{th} floor drift response with the identified model; Fig. 4.6 is the comparison of the 8^{th} floor acceleration response with the identified model. As can be seen, good agreement between original simulated values and the identified model is found in both drift and acceleration responses. The reason to choose the 7^{th}-8^{th} floor drift and 8^{th} floor acceleration responses as output signals to be identified is: 1) the response at the 8^{th} (Top) floor is the largest one; 2) acceleration is readily available as absolute values; 3) the 7^{th}-8^{th} floor drift information are feedback to the MR damper because the MR damper is added into the 8^{th} floor. This model, which is called ARX-TS Fuzzy 801, is used for a MISO semiactive nonlinear control system.

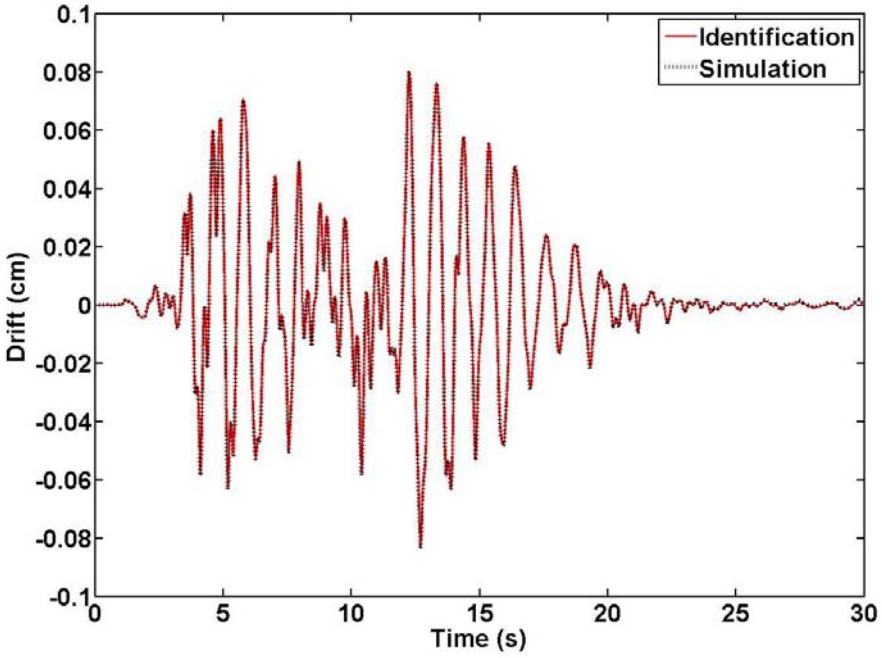

Fig. 4.5. Comparison of the 8th floor drift relative to the 7th floor level of the original responses with the responses using the nonlinear fuzzy identification model

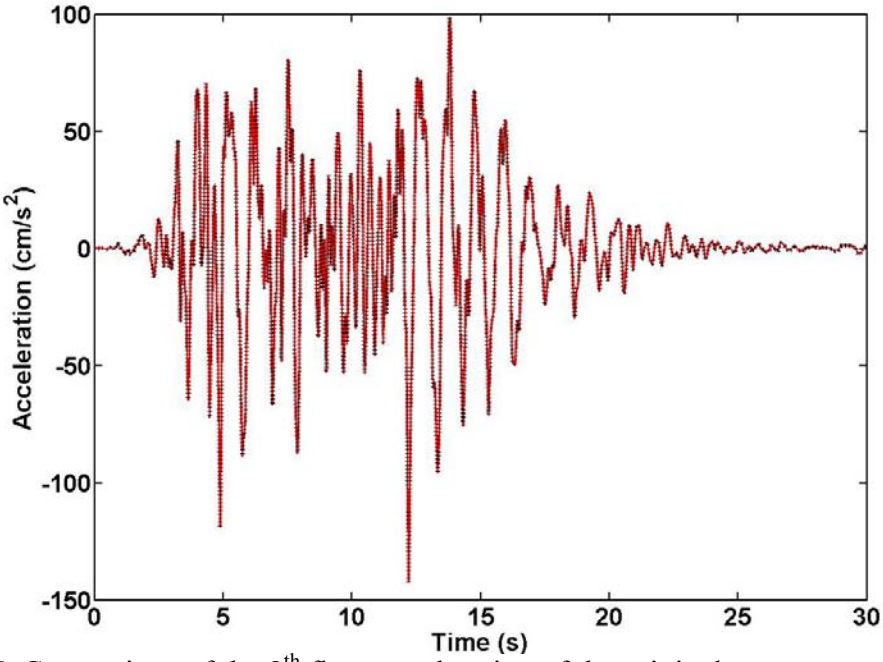

Fig. 4.6. Comparison of the 8th floor acceleration of the original responses with the responses using the nonlinear fuzzy identification model

Fig. 4.7 and Fig. 4.8 compare the original simulated values with another nonlinear fuzzy identified model. Fig. 4.7 is comparison of the 4^{th}-5^{th} floor drift response with the identified model; Fig. 4.8 is comparison of the 5^{th} floor acceleration response with the identified model. As can be seen, good agreement between the original simulated values and the identified model is found in both drift and acceleration responses. The reason to choose these 4^{th}-5^{th} floor drift and 5^{th} floor acceleration responses as another output signal to be identified is that additional MR damper is implemented into the 5^{th} floor. This model called ARX-TS Fuzzy 802 is used for a MIMO semiactive nonlinear control system with the ARX-TS Fuzzy 801.

In summary, two 1000 kN MR dampers are added on the 5^{th} and the 8^{th} floors whose locations are found through numerical simulations. The identified models, which include ARX-TS Fuzzy 801 and ARX-TS Fuzzy 802, are used for a MIMO semiactive nonlinear control system via decentralized control concepts.

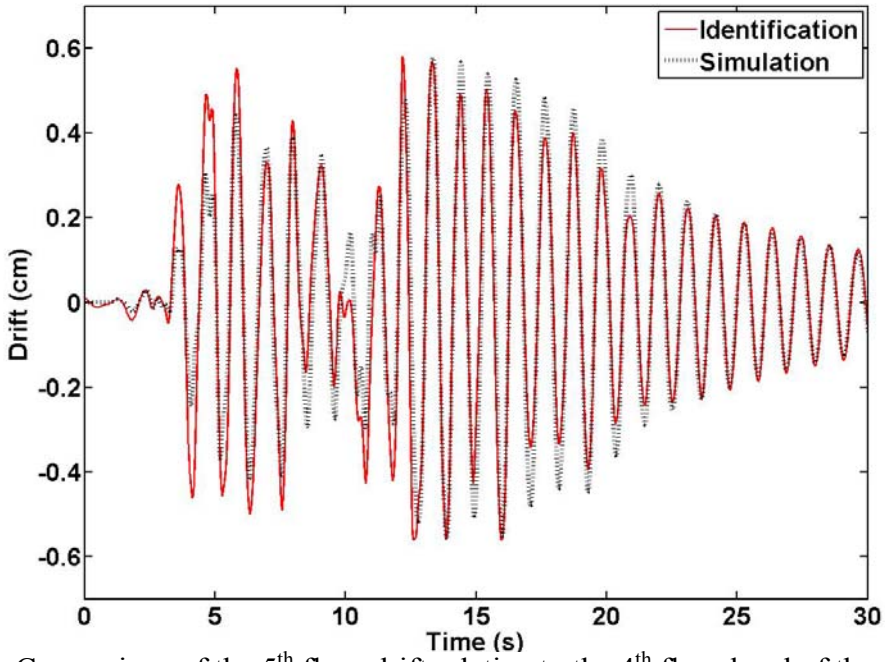

Fig. 4.7. Comparison of the 5th floor drift relative to the 4th floor level of the original responses with the responses using the nonlinear fuzzy identification model

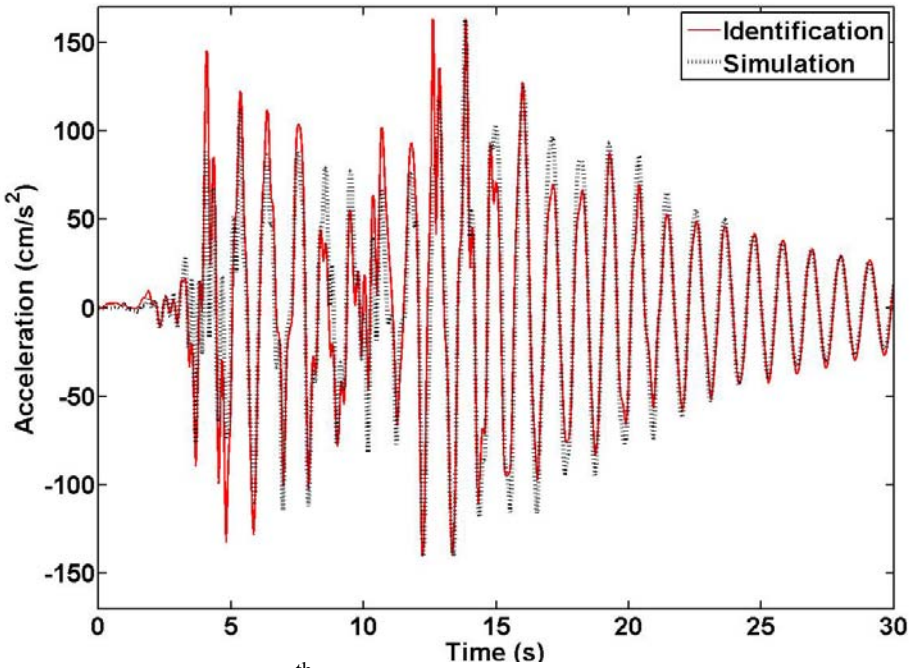

Fig. 4.8. Comparison of the 5th floor acceleration of the original responses with the responses using the nonlinear fuzzy identification model

4.8 Concluding Remarks

In this section, a nonlinear multiple autoregressive exogenous (ARX) input based Takagi-Sugeno (TS) fuzzy model was proposed to identify nonlinear behavior of building-magnetorheological (MR) damper systems. The premise part of the multiple ARX-TS fuzzy model was determined through either subtractive or fuzzy C-means clustering algorithm; the consequent parameters were optimized using weighted least squares estimation.

This nonlinear identification methodology provides a framework that a parallel distributed compensation (PDC)-based TS fuzzy controller can be applied to large-scale civil engineering building structures equipped with MR dampers.

To demonstrate the effectiveness of this framework, a three story shear type building structure equipped with a MR damper and an eight-story shear type building structure employing two MR dampers were investigated. It was demonstrated from numerical simulations that the proposed multiple ARX-TS fuzzy model is effective to identify nonlinear behavior of building-MR damper systems.

However, the performance of the nonlinear multiple ARX-TS models should be judged based on the performance of control systems to be designed because the objective of the system identification is in control system design.

5. SEMIACTIVE NONLINEAR CONTROL SYSTEM

5.1 Introduction

In recent years, attention has attracted to systematic applications of semiactive linear control (SLC) algorithms for vibration control of building structures subjected to natural hazards, e.g., earthquakes and strong winds. In particular, many design methodologies for the SLC have been developed for use with low-, mid-, and high-rise building structures employing magnetorheological (MR) dampers. In addition, semiactive nonlinear control (SNC), mainly semiactive nonlinear fuzzy control (SNFC), has been successively applied to the building-MR damper systems due to the effectiveness and robustness of the SNFC systems.

However, the SNFC systems have been designed by trial and error approaches that use either investigators' experience or high-cost computation, i.e., as a model-free controller, they are trained using a set of input-output data. Although useful for the performance purpose, the ad-hoc approach may not provide a design guideline in a systematic way. Furthermore, it is difficult for the ad-hoc approach-based SNFC systems to guarantee stability because stability conditions can not be formulated using the ad-hoc design approach. Unfortunately, no systematic study has been conducted to design a SNFC system for structural vibration control of building structures such that stability conditions are guaranteed. Therefore, a new research is recommended to

develop a systematic design methodology for the SNFC system of large scale building structures employing MR dampers.

An active nonlinear fuzzy control (ANFC) system design has been carried out in a systematic way via the so called parallel distributed compensation (PDC) approach, which employs multiple linear controllers (Hong and Langari 2000; Joh et al. 1997). The linear controllers correspond to the local linear structural models with automatic scheduling performed through fuzzy rule base. The PDC-based ANFC system provides sufficient conditions to be globally asymptotically stable (GAS) by finding a common symmetric positive definite matrix such that a set of simultaneous Lyapunov inequalities are satisfied. However, no systematic design framework has been investigated to design a SNFC for building structures equipped with nonlinear MR dampers for reduction of response to earthquake events.

Section 5.2 describes the design framework. It includes Takagi-Sugeno fuzzy model, PDC, and LMIs. In Section 5.3, a LMI-based systematic design framework for the ANFC system design is described. Section 5.4 describes an optimal estimator and converting algorithms to derive a SNFC system. The proposed SNFC system is demonstrated in Section 5.5 with an illustrating example. Finally, concluding remarks are given in the last section.

5.2 Design Framework

Takagi-Sugeno fuzzy model, PDC, and LMIs are the backbone for the proposed SNFC system. In this section, Takagi-Sugeno fuzzy model is briefly represented in terms of state space equations first. Its detail is described in Section 4. Then, fundamentals of the PDC and LMIs are discussed.

5.2.1 Takagi-Sugeno (TS) Fuzzy Model

In 1985, Takagi and Sugeno suggested an effective way for modeling complex nonlinear dynamic systems by introducing linear equations in consequent parts of a fuzzy model, which is called Takagi-Sugeno (TS) fuzzy model. It has led to reduction of computational cost because it does not need any defuzzification procedure. However, a more important value of the TS fuzzy model is that it provides a framework for a rigorous mathematical analysis, i.e., many modern linear system theories can be applied to nonlinear system models in terms of IF-THEN rules. A typical fuzzy rule for a TS fuzzy model is of the form

R_j : If z_{FZ}^1 is $p_{1,j}$ and z_{FZ}^2 is $p_{2,j}$ and $\cdots$ and z_{FZ}^i is $p_{i,j}$

Then, (5.1)

$$y = f\left(z_{\mathrm{FZ}}^1, \ldots, z_{\mathrm{FZ}}^i\right),$$

where the equation of the consequent part, $y = f\left(z_{\mathrm{FZ}}^{1},...,z_{\mathrm{FZ}}^{i}\right)$, can be any type of linear equation. However, it is advantageous to represent the consequent part in terms of state space equations in order to apply for modern control theories; a typical rule of the TS fuzzy model that is expressed in terms of state space equations in the consequent part is of the form

$$\begin{aligned} &\mathrm{R}_j : \text{If } z_{\mathrm{FZ}}^{1} \text{ is } p_{1,j} \text{ and} ... \text{and } z_{\mathrm{FZ}}^{n} \text{ is } p_{n,j} \\ &\text{Then} \quad \begin{cases} \dot{\mathbf{x}} = \mathbf{A}_j \mathbf{x} + \mathbf{B}_j \mathbf{u} \\ \mathbf{y} = \mathbf{C}_j \mathbf{x} + \mathbf{D}_j \mathbf{u} \end{cases}, \qquad j = 1, 2, ..., r, \end{aligned} \tag{5.2}$$

where r is the number of fuzzy rules, $p_{i,j}$ are fuzzy sets centered at the i^{th} operating point, z_{FZ}^{i} is are premise variables that can be either input or output values, $\mathbf{x}$ is the state vector, $\mathbf{u}$ is the input vector, $\mathbf{y}$ is the output vector, and $\mathbf{A}_j$, $\mathbf{B}_j$, $\mathbf{C}_j$, $\mathbf{D}_j$ are system matrices.

Note that Eq. (5.2) represents the j^{th} local linear subsystem of a nonlinear dynamic system, i.e., a linear dynamic system model that is operated in only a limited region. Therefore, all the local subsystems should be integrated into a global nonlinear dynamic system by blending operating regions of each local subsystem. Such a blending job is performed through interpolation of all the local subsystem models. Note that the local subsystem involves only linear combinations of input and output vectors; however,

the integrated subsystem is truly nonlinear. The blended TS fuzzy model is of the following form

$$\dot{\mathbf{x}} = \frac{\sum_{j=1}^{N_r} w_j\left(z_{\mathrm{FZ}}^i\right)\left[\mathbf{A}_j\mathbf{x} + \mathbf{B}_j\mathbf{u}\right]}{\sum_{j=1}^{N_r} w_j\left(z_{\mathrm{FZ}}^i\right)}, \tag{5.3}$$

where $w_j\left(z_{\mathrm{FZ}}^i\right) = \prod_{i=1}^{n} \mu_{p_{i,j}}(z_{\mathrm{FZ}}^i)$ and $\mu_{p_{i,j}}(z_{\mathrm{FZ}}^i)$ is the grades of membership of z_{FZ}^i in $p_{i,j}$. More detailed description of the TS fuzzy is discussed in Section 4.

To control the responses of the blended TS fuzzy model, an effective control law associated with Eq. (5.3), i.e., $\mathbf{u}$ should be designed. In this research, multiple optimal linear controllers associated with each local subsystem are designed and then blended through a fuzzy interpolation method.

5.2.2 Parallel Distributed Compensation (PDC)

Development of systematic design procedures for a nonlinear feedback control is still challenging due to its complexity. Thus, a curious question would be arising: “Can linear system theories be applied to nonlinear control system design?” One of reasonable answers can be found in the parallel distributed compensation (PDC). In the PDC approach, linear system theories can be applied to state feedback controllers

associated with each local subsystem; in particular, the PDC approach is appropriate for the ANFC system because the subsystem in the consequent part of the fuzzy rules is described by a linear state space equation.

The control rule j of an ANFC system is of the form

$$\begin{aligned} &\mathrm{R}_j : \text{If } z_{\mathrm{FZ}}^1 \text{ is } p_{1,j} \text{ and} \ldots \text{and } z_{\mathrm{FZ}}^n \text{ is } p_{n,j} \\ &\text{Then} \quad \mathbf{u} = -\mathbf{K}_j \mathbf{x}. \end{aligned} \tag{5.4}$$

The state feedback controller in the consequent part of the j^{th} IF-THEN rule is a local linear controller associated with a local subsystem to be controlled. All the local state feedback controllers are integrated into a global nonlinear controller using fuzzy sets

$$\mathbf{u} = \frac{\sum_{j=1}^{N_r} w_j\left(z_{\mathrm{FZ}}^i\right)\left[-\mathbf{K}_j \mathbf{x}\right]}{\sum_{j=1}^{N_r} w_j\left(z_{\mathrm{FZ}}^i\right)}. \tag{5.5}$$

Notice that the blended state feedback controller is truly nonlinear. By substituting Eq. (5.5) into Eq. (5.3), the final closed loop control system is derived

$$\dot{\mathbf{x}} = \frac{\sum_{j}^{N_r}\sum_{q=1}^{N_r} w_j\left(z_{\mathrm{FZ}}^i\right) w_q\left(z_{\mathrm{FZ}}^i\right)\left[\mathbf{A}_j - \mathbf{B}_j\mathbf{K}_q\right]\mathbf{x}}{\sum_{j}^{N_r}\sum_{q=1}^{N_r} w_j\left(z_{\mathrm{FZ}}^i\right) w_q\left(z_{\mathrm{FZ}}^i\right)}. \tag{5.6}$$

To implement the ANFC system Eq. (5.6), the next step is to compute the multiple state feedback gains, $\mathbf{K}_q$, $q = 1,...,r$ such that the nonlinear dynamic system to be controlled is globally asymptotically stable (GAS) while the performance on transient responses is also satisfied. Next, they are integrated with a Kalman filter to convert the state feedback mode into the output feedback mode and then are integrated with a converting algorithm to convert the active mode into semi-active one.

Although there might be many methodologies to design the state feedback gains $\mathbf{K}_q$, $q = 1,...,r$, LMI-based control formulations are carried out here because the LMI technique is appropriate to the formulation of multiple objectives and constraints. Basic background on LMIs is discussed and then stability issues are described.

5.2.3 Linear Matrix Inequalities (LMIs)

In recent years, LMI techniques have attracted significant attention because a great variety of engineering problems can be re-formulated as convex or pseudo-convex optimization problems in terms of LMIs. Such problems include control system design, system identification, structural design, etc. In particular, many control problems can be

recast in terms of LMIs because design objectives and constraint conditions can be formulated in numerically tractable manner.

An LMI has the form of (Boyd et al. 1994)

$$\mathbf{Q}(\mathbf{x}) \triangleq \mathbf{Q}_0 + \sum_{i=1}^{m} x_i \mathbf{Q}_i < 0, \tag{5.7}$$

where $\mathbf{Q}_i = \mathbf{Q}_i^T \in \Re^{n\times n}, i = 0,...,m$ are given as the symmetric matrices and $x_i \in \Re^m$, $i = 1,...,m$ are the design variable to be solved. The inequality symbol of < 0 represents negative definite, i.e., the largest eigenvalue of $\mathbf{Q}(\mathbf{x})$ is negative.

Finding a solution of the LMI Eq. (5.7) is a convex optimization problem because the LMI Eq. (5.7) is a convex constraint on $\mathbf{x}$. One of the main advantages of the LMI formulation is that design objectives and design constraints that can arise in control system design can be combined in numerically tractable manner. Note that multiple LMIs that can arise in control system design can be considered as a single LMI, i.e.,

$$\left\{\begin{array}{c} \mathbf{Q}_1(\mathbf{x}) < 0 \\ \vdots \\ \mathbf{Q}_n(\mathbf{x}) < 0 \end{array}\right\} \text{ is equal to } \mathbf{Q}(\mathbf{x}) := \operatorname{diag}\left\{\mathbf{Q}_1(\mathbf{x}),...,\mathbf{Q}_n(\mathbf{x})\right\} < 0. \tag{5.8}$$

A typical example in control engineering using LMIs is the Lyapunov inequality (Khalil 2002),

$$\mathbf{A}^{\mathrm{T}}\mathbf{P} + \mathbf{P}\mathbf{A} < 0, \tag{5.9}$$

where $\mathbf{A} \in \Re^{n \times n}$ is the given system matrix of a dynamic system, $\mathbf{P} = \mathbf{P}^{\mathrm{T}}$ is a symmetric positive definite matrix as a design variable:

$$\text{Find } \mathbf{P} = \mathbf{P}^{\mathrm{T}} \text{ such that } \mathbf{A}^{\mathrm{T}}\mathbf{P} + \mathbf{P}\mathbf{A} < 0. \tag{5.10}$$

In this research, from the Lyapunov inequality equation, a convex optimization problem to find a set of feasible solution is formulated.

5.3 Formulations for LMI-based Control System Design

This section presents an LMI-based systematic design approach for an ANFC system. This approach considers global asymptotical stability as well as transient response characteristics in a unified framework.

5.3.1 Stability Conditions

Stability analysis is one of the most essential issues in system and control engineering fields. However, a critical question would often arise; "Should a stability issue be formulated for a semiactive control system design?" The reason to ask this question is that it is generally said that a semiactive control system is inherently stable in bounded input and bounded output (BIBO) sense because a semiactive device does not add mechanical energy into a structural system (Jung et al. 2003). This might be true for open loop systems; however, it is not always necessarily true for feedback control systems because a semiactive control system can be destabilized due to structure-semiactive device interaction, inaccurate plant or actuator modeling, etc. (Kuehn and Stalford 2000; Jin et al. 2005). However, what should be more stressed here is that actually the statement that a semiactive control system is stable in the BIBO sense can not be automatically generalized. Note that the building-MR damper system is a nonlinear time-varying (NTV) dynamic system. Therefore, stability should be necessarily considered for a semiactive control system design. In particular, it might be much more important issue in a semiactive nonlinear control system.

In general, it is difficult to include a stability condition for the design of a typical fuzzy logic-based controller, e.g., Mamdani fuzzy model-based controller (Casciati 1997). The reason is that a Mamdani fuzzy system does not provide a rigorous mathematical framework for stability analysis. However, such a drawback of the Mamdani fuzzy system can be solved by a TS fuzzy model. Advanced system theories

such as Lyapunov theorems can be applied to the TS fuzzy model to address stability conditions because the consequent part of the TS fuzzy model is expressed in terms of linear functions, e.g., state space equations.

Consider the following LTI dynamic system

$$\dot{\mathbf{x}} = \mathbf{A}\mathbf{x}, \tag{5.11}$$

where $\mathbf{x}$ is the state vector and $\mathbf{A}$ is a system matrix. The stability of this LTI dynamic system can be checked via eigenvalue analysis. The asymptotic stability can be also investigated using Lyapunov theorem:

Theorem 1 (Khalil 2002). The equilibrium point of the LTI dynamic system is asymptotically stable if there exist a symmetric positive definite matrix $\mathbf{P}$ and a positive definite matrix $\mathbf{Q}_{\text{Ly}}$ such that

$$\mathbf{A}^{\text{T}}\mathbf{P} + \mathbf{P}\mathbf{A} = -\mathbf{Q}_{\text{Ly}}. \tag{5.12}$$

Based on this Lyapunov equation, Tanaka and Sugeno (1992) suggested a stability condition for a nonlinear Takagi-Sugeno (TS) fuzzy model.

Theorem 2 (Tanaka and Sugeno 1992). The equilibrium point at the origin of the continuous nonlinear TS fuzzy model is globally asymptotically stable if there exist a common symmetric positive definite matrix $\mathbf{P}$ such that

$$\mathbf{A}_j^{\mathrm{T}}\mathbf{P} + \mathbf{P}\mathbf{A}_j < 0 \text{ for all } j = 1, 2, ..., r, \tag{5.13}$$

where r is the number of the fuzzy rules. This stability condition for an open loop system can be extended into a stability condition for a closed loop dynamic system.

Theorem 3 (Wang et al. 1995). The equilibrium point at the origin of the continuous closed loop TS fuzzy model is globally asymptotically stable if there exists a common symmetric positive definite matrix $\mathbf{P}$ such that

$$(\mathbf{A}_j + \mathbf{B}_j\mathbf{K}_q)^{\mathrm{T}}\mathbf{P} + \mathbf{P}(\mathbf{A}_j + \mathbf{B}_j\mathbf{K}_q) < 0 \text{ for all } j, q = 1, 2, ..., r. \tag{5.14}$$

Note, to determine the common symmetric positive definite matrix $\mathbf{P}$, r^2 LMI formulations should be solved; however, the computational cost can be reduced by approximately a half by grouping terms.

Corollary 1 (Wang et al. 1995). The equilibrium point at the origin of the continuous closed loop TS fuzzy model is globally asymptotically stable if there exists a common symmetric positive definite matrix $\mathbf{P}$ such that

$$(\mathbf{A}_j + \mathbf{B}_j\mathbf{K}_j)^{\mathrm{T}}\mathbf{P} + \mathbf{P}(\mathbf{A}_j + \mathbf{B}_j\mathbf{K}_j) < 0 \text{ for all } j = 1,2,...,r, \tag{5.15}$$

$$\mathbf{G}_{jq}^{\mathrm{T}}\mathbf{P} + \mathbf{P}\mathbf{G}_{jq} < 0 \text{ for all } j,q = 1,2,...,r, \tag{5.16}$$

where

$$\mathbf{G}_{jq} = \frac{(\mathbf{A}_j + \mathbf{B}_j\mathbf{K}_q) + (\mathbf{A}_q + \mathbf{B}_q\mathbf{K}_j)}{2}, j < q \le r. \tag{5.17}$$

Using Eq. (5.15) to Eq. (5.17), the number of LMIs to be solved is reduced from r^2 of Eq. (5.14) to $r(r+1)/2$. Note that from Eq. (5.15) to Eq. (5.17), control gains are not automatically obtained; the equations are only used to check if the *designed* control systems are stable, i.e., the system matrices $\mathbf{A}_j$ and $\mathbf{B}_j$ are given, the control matrix $\mathbf{K}_j$ should be designed first. Then, they are checked to determine whether the controllers $\mathbf{K}_j^{'}s,\ j = 1,2,...,r$ stabilize the closed loop systems. This procedure generally requires many trial-and-errors; therefore, it is desirable to integrate the stability conditions with the control system design procedure. In other words, it is necessary to formulate $\mathbf{K}_j^{'}s$ and $\mathbf{P}$ as design matrix variables at the same time.

5.3.2 LMI Formulation of Stabilizing Control

In this subsection, the control system design procedure is integrated with the stability condition checking process (Farinwata et al. 2000). Substitution of Eq. (5.17) into Eq. (5.15) and Eq. (5.16) yields Eq. (5.18) and Eq. (5.19), respectively

$$(\mathbf{A}_j + \mathbf{B}_j\mathbf{K}_j)^{\mathrm{T}}\mathbf{P} + \mathbf{P}(\mathbf{A}_j + \mathbf{B}_j\mathbf{K}_j) < 0, \quad j = 1,2,...,r, \tag{5.18}$$

$$\begin{aligned}&(\mathbf{A}_j + \mathbf{B}_j\mathbf{K}_q)^{\mathrm{T}}\mathbf{P} + (\mathbf{A}_q + \mathbf{B}_q\mathbf{K}_j)^{\mathrm{T}}\mathbf{P} + \\ &\mathbf{P}(\mathbf{A}_j + \mathbf{B}_j\mathbf{K}_q) + \mathbf{P}(\mathbf{A}_q + \mathbf{B}_q\mathbf{K}_j) < 0, \;\; j < q \le r = 1,2,...,r.\end{aligned} \tag{5.19}$$

By pre-and post-multiplying Eq. (5.18) and Eq. (5.19) by $\mathbf{P}^{-1} > 0$, Eq. (5.20) and Eq. (5.21) are obtained

$$\mathbf{P}^{-1}(\mathbf{A}_j + \mathbf{B}_j\mathbf{K}_j)^{\mathrm{T}}\mathbf{P}\mathbf{P}^{-1} + \mathbf{P}^{-1}\mathbf{P}(\mathbf{A}_j + \mathbf{B}_j\mathbf{K}_j)\mathbf{P}^{-1} < 0, \quad j < q \le r = 1,2,...,r, \tag{5.20}$$

$$\begin{aligned}&\mathbf{P}^{-1}(\mathbf{A}_j + \mathbf{B}_j\mathbf{K}_q)^{\mathrm{T}}\mathbf{P}\mathbf{P}^{-1} + \mathbf{P}^{-1}(\mathbf{A}_q + \mathbf{B}_q\mathbf{K}_j)^{\mathrm{T}}\mathbf{P}\mathbf{P}^{-1} + \\ &\mathbf{P}^{-1}\mathbf{P}(\mathbf{A}_j + \mathbf{B}_j\mathbf{K}_q)\mathbf{P}^{-1} + \mathbf{P}^{-1}\mathbf{P}(\mathbf{A}_q + \mathbf{B}_q\mathbf{K}_j)\mathbf{P}^{-1} < 0, \;\; j < q \le r = 1,2,...,r.\end{aligned} \tag{5.21}$$

In the numerical simulation, it is not desirable to have an inverse matrix term such as $\mathbf{P}^{-1}$; the following LMIs are derived by defining a new matrix variable $\mathbf{Q} = \mathbf{P}^{-1}$

$$\mathbf{Q}\mathbf{A}_j^{\mathrm{T}} + \mathbf{A}_j\mathbf{Q} + \mathbf{Q}\mathbf{K}_j^{\mathrm{T}}\mathbf{B}_j^{\mathrm{T}} + \mathbf{B}_j\mathbf{K}_j\mathbf{Q} < 0, \quad j = 1,2,...,r, \tag{5.22}$$

$$\begin{aligned}&\mathbf{Q}\mathbf{A}_j^{\mathrm{T}} + \mathbf{A}_j\mathbf{Q} + \mathbf{Q}\mathbf{A}_q^{\mathrm{T}} + \mathbf{A}_q\mathbf{Q} + \mathbf{Q}\mathbf{K}_q^{\mathrm{T}}\mathbf{B}_j^{\mathrm{T}} + \\ &\mathbf{B}_j\mathbf{K}_q\mathbf{Q} + \mathbf{Q}\mathbf{K}_j^{\mathrm{T}}\mathbf{B}_q^{\mathrm{T}} + \mathbf{B}_q\mathbf{K}_j\mathbf{Q} < 0, \quad j < q \le r = 1,2,...,r.\end{aligned} \tag{5.23}$$

However, Eq. (5.22) and Eq. (5.23) are not LMIs because there exist nonlinear matrix terms $\mathbf{Q}\mathbf{K}_j^{T}$ and $\mathbf{K}_j\mathbf{Q}$. Thus, these coupled nonlinear terms are transformed into LMIs by defining a new matrix $\mathbf{K}_j\mathbf{Q} = \mathbf{M}_j$

$$\mathbf{Q}\mathbf{A}_j^{T} + \mathbf{A}_j\mathbf{Q} + \mathbf{M}_j^{\mathrm{T}}\mathbf{B}_j^{\mathrm{T}} + \mathbf{B}_j\mathbf{M}_j < 0, \quad j = 1,2,...,r, \tag{5.24}$$

$$\begin{aligned}&\mathbf{Q}\mathbf{A}_j^{\mathrm{T}} + \mathbf{A}_j\mathbf{Q} + \mathbf{Q}\mathbf{A}_q^{\mathrm{T}} + \mathbf{A}_q\mathbf{Q} + \mathbf{M}_q^{\mathrm{T}}\mathbf{B}_j^{\mathrm{T}} + \mathbf{B}_j\mathbf{M}_q + \mathbf{M}_j^{\mathrm{T}}\mathbf{B}_q^{\mathrm{T}} + \mathbf{B}_q\mathbf{M}_j < 0, \\ &j < q \le r = 1,2,...,r.\end{aligned} \tag{5.25}$$

Eq. (5.24) and Eq. (5.25) are used to design stabilizing feedback control gains. However, the stabilizing control formulations do not directly address transient response characteristics. The performance-based design can be achieved through integration of a pole-placement algorithm with the stabilizing controllers.

5.3.3 LMI Formulation of Pole-assignment Control

In large-scale civil engineering structures, the performance on transient response is an important issue; however, the stability LMI formulation does not directly address that issue. Therefore, in this section, the pole-assignment concept is recast by LMI formulation. The formulation of the pole-placement in terms of LMI is motivated by Chilali and Gahinet (1996). A *D*-stable region is defined by first.

Definition 1: Let *D* be a subset of left half plane (LHP) in the complex plane that represents behavior of a dynamic system $\dot{\mathbf{x}} = \mathbf{A}\mathbf{x}$. If all the poles (or eigenvalues) of the dynamic system are located in the subset region *D*, the dynamic system (or the system matrix $\mathbf{A}$) is *D*-stable.

Definition 2: LMI Stability Region

The closed loop poles (or eigenvalues) of a dynamic system are located in the LMI stability region

$$D = \left\{ s \in C : f_D(s) := \alpha + \beta s + \beta^{\mathrm{T}} \overline{s} < 0 \right\} \tag{5.26}$$

if and only if there exist a symmetric positive definite matrix $\alpha = [\alpha_{kl}] \in \Re^{m \times m}$ and a matrix $\beta = [\beta_{kl}] \in \Re^{m \times m}$. The characteristic function $f_D(s)$ is a $m \times m$ Hermitian matrix.

Based on Chilali and Gahinet (1996) theorem, Hong and Langari (2000) applied for a circular LMI region *D* that is convex and symmetric with respect to real axis to the pole-assignment control formulation. Let consider the following circular LMI region that has a center at $(-q_c, 0)$ and radius $r_c > 0$

$$D = \{x + jy \in C : (x + q_c)^2 + y^2 < r_c^2\}. \tag{5.27}$$

The associated characteristic function $f_D(s)$ is given by

$$f_D(s) = \begin{pmatrix} -r_c & \overline{s} + q_c \\ s + q_c & -r_c \end{pmatrix}. \tag{5.28}$$

Fig. 5.1 shows a schematic of the circular LMI region. This circular LMI region can be related to a LMI stability region described in terms of an *m* × *m* block matrix.

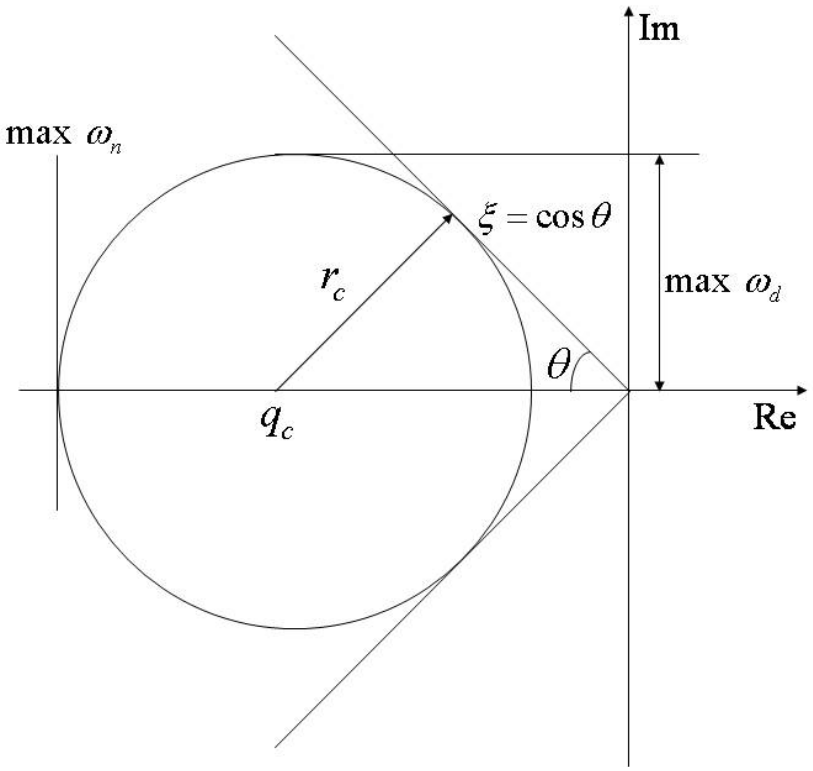

Fig. 5.1. Circular region (*D*) for pole location (Hong and Langari 2000)

Theorem 4 (Chilali and Gahinet 1996). The system dynamics of $\dot{\mathbf{x}} = \mathbf{A}\mathbf{x}$ is *D*-stable if and only if there exists a symmetric matrix $\mathbf{Q}$ such that

$$\begin{aligned} M_D(\mathbf{A},\mathbf{X}) &:= \alpha \otimes \mathbf{Q} + \beta \otimes (\mathbf{A}\mathbf{Q}) + \beta^{\mathrm{T}} \otimes (\mathbf{A}\mathbf{Q})^{\mathrm{T}} \\ &= [\alpha_{kl}\mathbf{Q} + \beta_{kl}\mathbf{A}\mathbf{Q} + \beta_{lk}\mathbf{Q}\mathbf{A}^{\mathrm{T}}]_{1\le k,l\le m} < 0, \quad \mathbf{Q} > 0. \end{aligned} \tag{5.29}$$

It should be noted that $M_D(\mathbf{A},\mathbf{Q})$ and $f_D(s)$ have close relationship, i.e., replacing $(1, s, \bar{s})$ of $f_D(s)$ by $(\mathbf{Q}, \mathbf{A}\mathbf{Q}, \mathbf{Q}\mathbf{A}^{\mathrm{T}})$ of $M_D(\mathbf{A},\mathbf{Q})$ yields

$$\begin{pmatrix} -r_c\mathbf{Q} & q_c\mathbf{Q} + \mathbf{Q}\mathbf{A}^{\mathrm{T}} \\ q_c\mathbf{Q} + \mathbf{A}\mathbf{Q} & -r_c\mathbf{Q} \end{pmatrix} < 0, \ \mathbf{Q} > 0. \tag{5.30}$$

From Eq. (5.30), a LMI for the pole-placement controller is derived.

Theorem 5 (Hong and Langari 2000). The continuous closed loop TS fuzzy control system is *D*-stable if and only if there exists a positive symmetric matrix $\mathbf{Q}$ such that

$$\begin{pmatrix} -r_c\mathbf{Q} & q_c\mathbf{Q} + \mathbf{Q}(\mathbf{A}_j + \mathbf{B}_j\mathbf{K}_q)^{\mathrm{T}} \\ q_c\mathbf{Q} + (\mathbf{A}_j + \mathbf{B}_j\mathbf{K}_q)\mathbf{Q} & -r_c\mathbf{Q} \end{pmatrix} < 0. \tag{5.31}$$

Remark: It should be noted that the inequality Eq. (5.31) is not a LMI because the matrices $\mathbf{Q}$ and $\mathbf{K}_j$ are coupled. This nonlinear matrix inequality can be transformed into a LMI by defining a new matrix variable $\mathbf{M}_j = \mathbf{K}_j\mathbf{Q}$.

Corollary 2: The continuous closed loop TS fuzzy control system is *D*-stable if and only if there exists a positive symmetric matrix $\mathbf{Q}$ and $\mathbf{M}_j$ such that

$$\begin{pmatrix} -r_c\mathbf{Q} & q_c\mathbf{Q} + \mathbf{Q}\mathbf{A}_j^{\mathrm{T}} + \mathbf{M}_j^{\mathrm{T}}\mathbf{B}_j^{\mathrm{T}} \\ q_c\mathbf{Q} + \mathbf{A}_j\mathbf{Q} + \mathbf{B}_j\mathbf{M}_j & -r_c\mathbf{Q} \end{pmatrix} < 0. \tag{5.32}$$

This LMI (5.32) directly addresses the performance on transient response of the dynamic system.

In summary, three LMIs Eq. (5.24), Eq. (5.25), and Eq. (5.32) are solved simultaneously to obtain $\mathbf{Q}$ and $\mathbf{M}_j$. Then the common symmetric positive definite matrix $\mathbf{P}$ and state feedback control gains $\mathbf{K}_j$ are determined

$$\begin{aligned} &\mathbf{P} = \mathbf{Q}^{-1} \\ &\mathbf{K}_j = \mathbf{M}_j\mathbf{Q}^{-1} = \mathbf{M}_j\mathbf{P}, \;\; j = 1, 2, ..., r. \end{aligned} \tag{5.33}$$

These state feedback control gains are integrated with a state estimator to construct output feedback controllers.

5.4 Output Feedback-based Semiactive Nonlinear Fuzzy Control

In this section, two more design units, which are a state estimator and clipped algorithms, are introduced to convert the full state feedback-based active nonlinear control system into output feedback-based semiactive nonlinear control system.

5.4.1 State Estimator

From practical point of view, it is not always available to measure all the states. Therefore, state estimators are designed to implement the full state feedback control systems as output feedback control systems.

Consider the following state space equation

$$\dot{\mathbf{x}} = \mathbf{A}_j \mathbf{x} + \mathbf{B}_j \mathbf{u}, \tag{5.34}$$

$$\mathbf{y} = \mathbf{C}_j \mathbf{x} + \mathbf{D}_j \mathbf{u}. \tag{5.35}$$

By adding and subtracting a term $\mathbf{L}_j \mathbf{y}$ into Eq. (5.34),

$$\dot{\mathbf{x}} = \mathbf{A}_j \mathbf{x} + \mathbf{B}_j \mathbf{u} + \mathbf{L}_j \mathbf{y} - \mathbf{L}_j \mathbf{y}. \tag{5.36}$$

Substitution of Eq. (5.35) into Eq. (5.36) yields

$$\dot{\mathbf{x}} = (\mathbf{A}_j + \mathbf{L}_j\mathbf{C}_j)\mathbf{x} + (\mathbf{B}_j + \mathbf{L}_j\mathbf{D}_j)\mathbf{u} - \mathbf{L}_j\mathbf{y}. \tag{5.37}$$

Consider a negative feedback controller

$$\mathbf{u} = -\mathbf{K}_j\mathbf{x}. \tag{5.38}$$

By substituting Eq. (5.38) into Eq. (5.37),

$$\dot{\mathbf{x}} = (\mathbf{A}_j + \mathbf{L}\mathbf{C}_j)\mathbf{x} - (\mathbf{B}_j + \mathbf{L}\mathbf{D}_j)\mathbf{K}_j\mathbf{x} - \mathbf{L}_j\mathbf{y}. \tag{5.39}$$

Then a continuous time state observer model of a dynamic system is derived

$$\hat{\mathbf{x}} = (\mathbf{A}_j + \mathbf{L}\mathbf{C}_j)\mathbf{x} - (\mathbf{B}_j + \mathbf{L}\mathbf{D}_j)\mathbf{K}_j\mathbf{x} - \mathbf{L}_j\mathbf{y}, \tag{5.40}$$

$$\mathbf{u} = -\mathbf{K}_j\hat{\mathbf{x}}. \tag{5.41}$$

In this research, the optimal observer gains $\mathbf{L}_j$ are obtained by Kalman filter estimation procedure (Crassidis and Junkins 2004) Fig. 5.2 is a schematic of a combined control law and observer system.

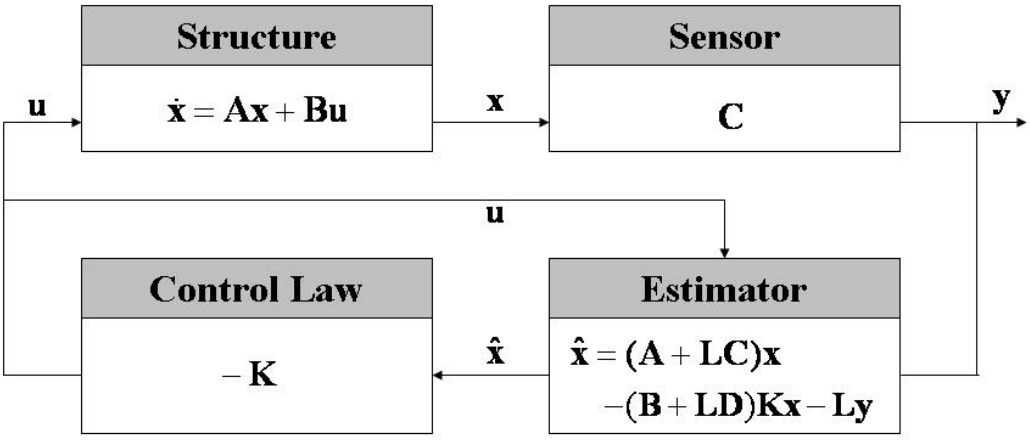

Fig. 5.2. Mechanism of combined controller and estimator

5.4.2 Clipped Algorithms

Once the output feedback-based active nonlinear fuzzy controller (ANFC) is designed, a converting algorithm and a MR damper are integrated with the output ANFC to develop a SNFC system. In general, a MR damper can not be directly controlled by a control algorithm. The reason is that a controller generates force signals, while a MR damper requires voltage or current signals to be operated. Therefore, a unit that converts from a control force signal to a voltage signal should be integrated with the ANFC system to construct a SNFC system. Such a unit would be either to use an inverse MR damper model or to implement a converting algorithm. Candidates for the inverse MR damper models may include a Bingham, a polynomial, a Bouc-Wen, and a modified Bouc-Wen model whose detailed description is presented in Section 2. Another good candidate for the conversion is a clipped algorithm

$$v = V_{\max} \mathrm{H}\left(\{f_{\mathrm{ANFC}} - f_{\mathrm{m}}\} f_{\mathrm{m}}\right), \tag{5.42}$$

where v is the voltage level, $V_{\max}$ is the maximum voltage level, H is a Heaviside step function, f_{m} is a measured MR damper force, and f_{ANFC} is a control force signal generated by an active nonlinear fuzzy controller.

However, this clipped algorithm generates only either a maximum or a zero value. Therefore, this algorithm can be modified such that it takes any value between 0 and the maximum values (Yoshida and Dyke 2004)

$$v = V_a \mathrm{H}\left(\{f_{\mathrm{ANFC}} - f_{\mathrm{m}}\} f_{\mathrm{m}}\right), \tag{5.43}$$

where

$$V_a = \begin{cases} \mu \cdot f_{\mathrm{ANFC}} & \text{for } f_{\mathrm{ANFC}} \le f_{\max,} \\ V_{\max} & \text{for } f_{\mathrm{ANFC}} > f_{\max,} \end{cases} \tag{5.44}$$

where μ is a value relating the MR damper force to the voltage. Fig. 5.3 and Fig. 5.4 show the graphical representation for the modified clipped algorithm.

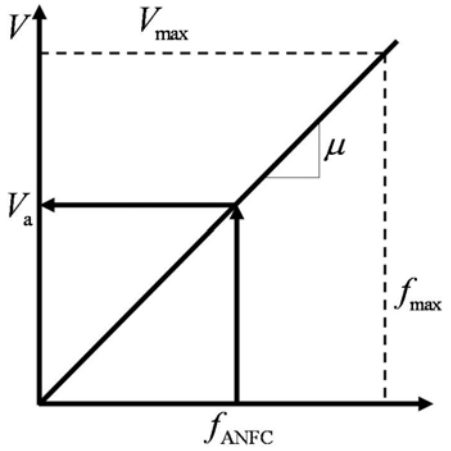

Fig. 5.3. The function of the modified clipped algorithm

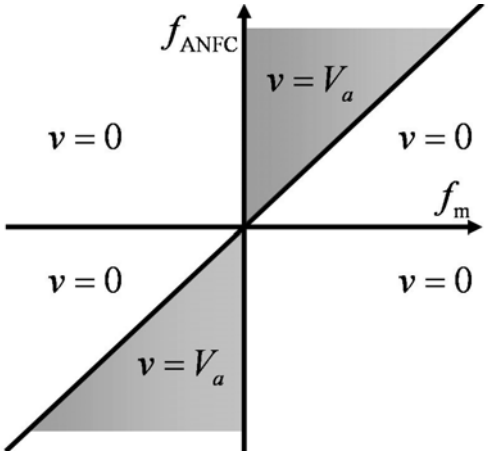

Fig. 5.4. Operation regions of the modified clipped algorithm

Recall the active nonlinear fuzzy controller

$$f_{\text{ANFC}} = \frac{\sum_{j=1}^{N_r} \prod_{i=1}^{n} \mu_{i,j}(z_{\text{FZ}}^{i}) \left[\mathbf{K}_j \hat{\mathbf{x}} \right]}{\sum_{j=1}^{N_r} \prod_{i=1}^{n} \mu_{i,j}(z_{\text{FZ}}^{i})}. \tag{5.45}$$

By substitution of Eq. (5.45) into Eq. (5.42), the final voltage equation can be written as

$$v = V_a \text{H} \left(\left\{ \frac{\sum_{j=1}^{N_r} \prod_{i=1}^{n} \mu_{i,j}(z_{\text{FZ}}^{i}) \left[\mathbf{K}_j \hat{\mathbf{x}} \right]}{\sum_{j=1}^{N_r} \prod_{i=1}^{n} \mu_{i,j}(z_{\text{FZ}}^{i})} - f_{\text{m}} \right\} f_{\text{m}} \right). \tag{5.46}$$

This SNFC system is applied to a three-story shear type building structure equipped with a MR damper to demonstrate its performance.

5.5 Examples

The proposed SNFC system is tested within two different situations: without sensor noise and with sensor noises.

5.5.1 Control Performance Evaluation: Noise Free Case

To evaluate the performance of the proposed SNFC system, a three-story building structure is investigated. The equation of motion is given by Eq. (3.10). Detailed description on the building structure is provided in Section 3. A SD-1000 MR damper model is employed at the first floor. To synthesis the MR damper to the SNFC system, a modified Bouc-Wen model is used. The applied modified Bouc-Wen model and its properties are described in detail in Section 2. The 1940 El-Centro earthquake record is applied as a ground motion shown in the figure on page 53.

The time history responses that are controlled by the SNFC system at the entire floor are compared with the performance of a traditional optimal controller, i.e., H2/LQG, while the uncontrolled system response is used as the baseline. The parameters of the LQR and the Kalman filter are adopted from Dyke et al. (1996). Fig. 5.5 and Fig. 5.6 compare displacement and acceleration responses at the 1st floor of an uncontrolled, a H2/LQG controlled, and a SNFC controlled system. According to the time history responses,

both displacement and acceleration responses are dramatically reduced when either H2/LQG or SNFC systems are applied.

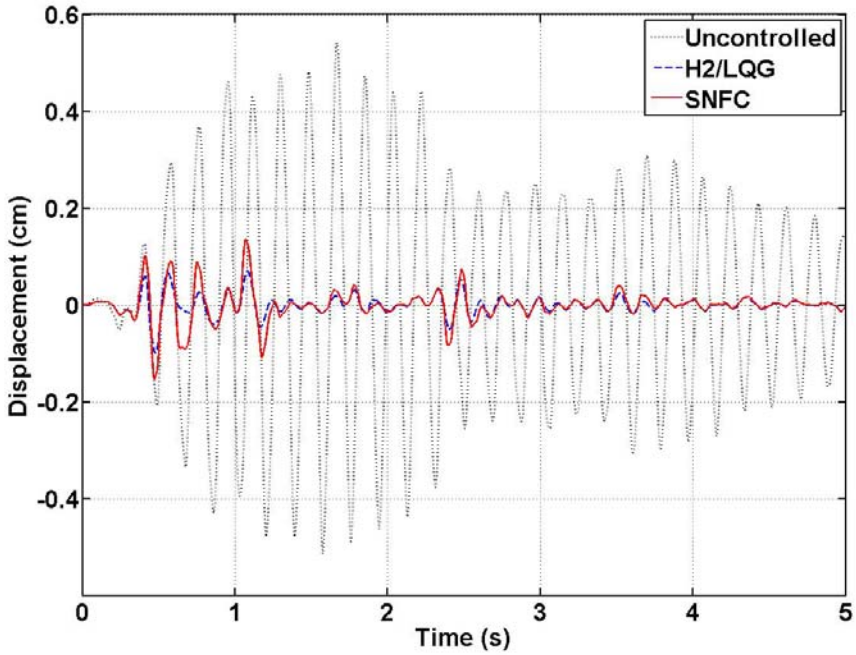

Fig. 5.5. Time history displacement responses of an uncontrolled, a H2/LQG control, and a SNFC systems at the 1st floor

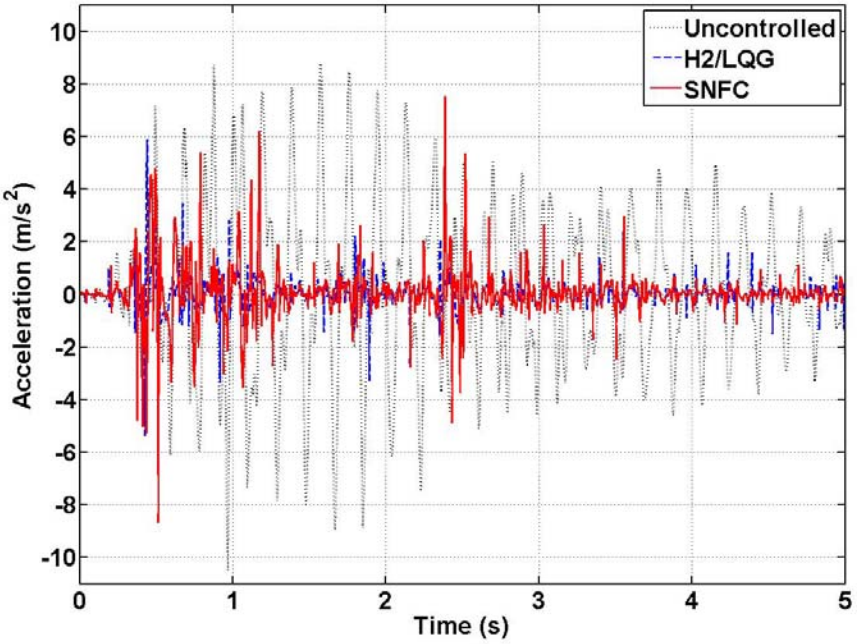

Fig. 5.6. Time history acceleration responses of an uncontrolled, a H2/LQG control, and a SNFC systems at the 1st floor

Fig. 5.7 and Fig. 5.8 compare displacement and acceleration responses at the 2nd floor of an uncontrolled, a H2/LQG controlled, and a SNFC controlled system. According to the time history responses, both displacement and acceleration responses are dramatically reduced when either H2/LQG or SNFC systems are applied.

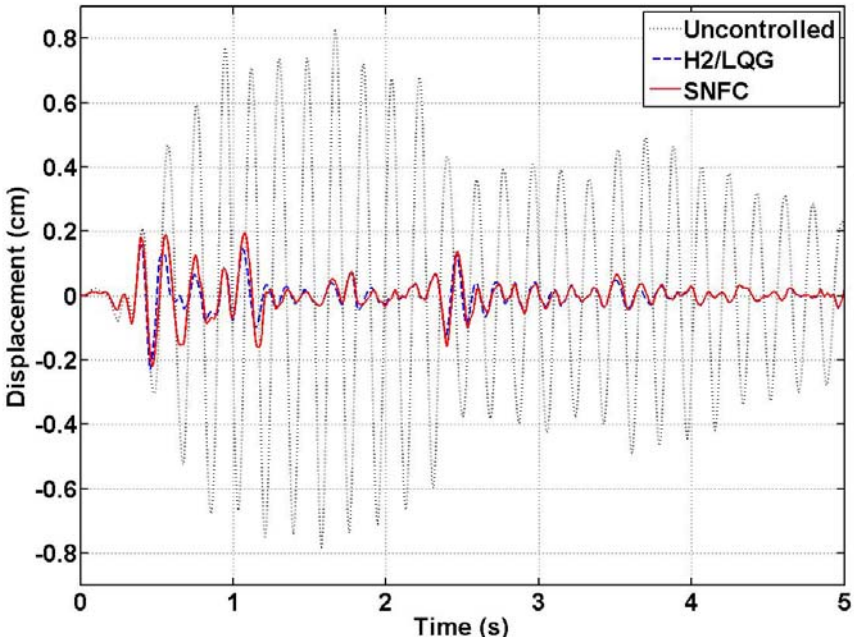

Fig. 5.7. Time history displacement responses of an uncontrolled, a H2/LQG control, and a SNFC systems at the 2nd floor

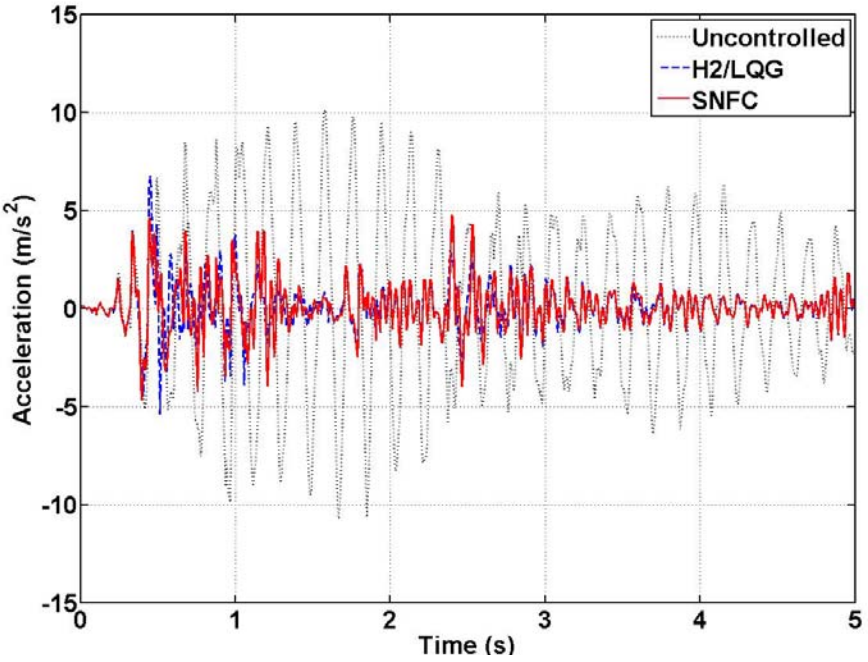

Fig. 5.8. Time history acceleration responses of an uncontrolled, a H2/LQG control, and a SNFC systems at the 2nd floor

Fig. 5.9 and Fig. 5.10 compare displacement and acceleration responses at the 3rd floor of an uncontrolled, a H2/LQG controlled, and a SNFC controlled system. According to the time history responses, both displacement and acceleration responses are dramatically reduced when either H2/LQG or SNFC systems are applied.

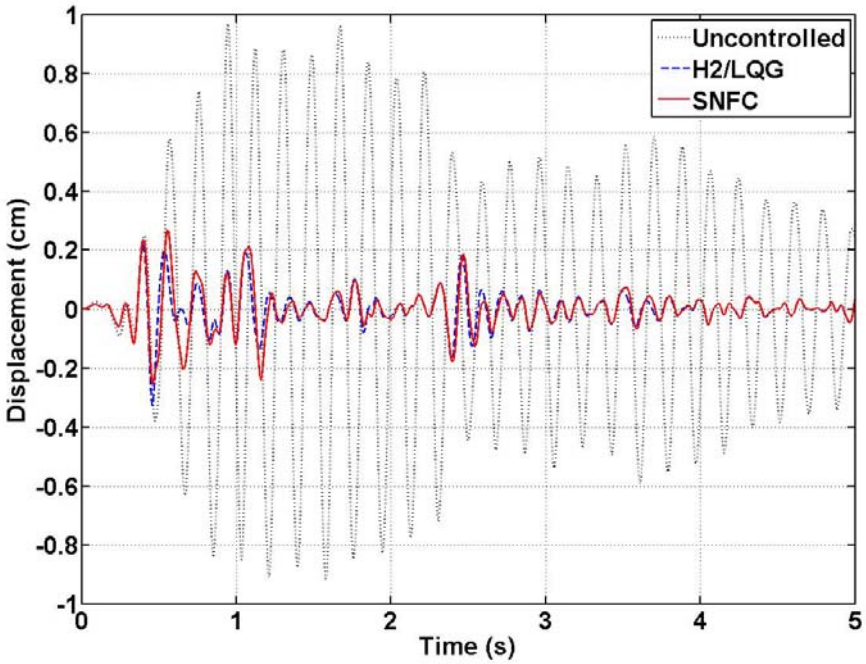

Fig. 5.9. Time history displacement responses of an uncontrolled, a H2/LQG control, and a SNFC systems at the 3rd floor

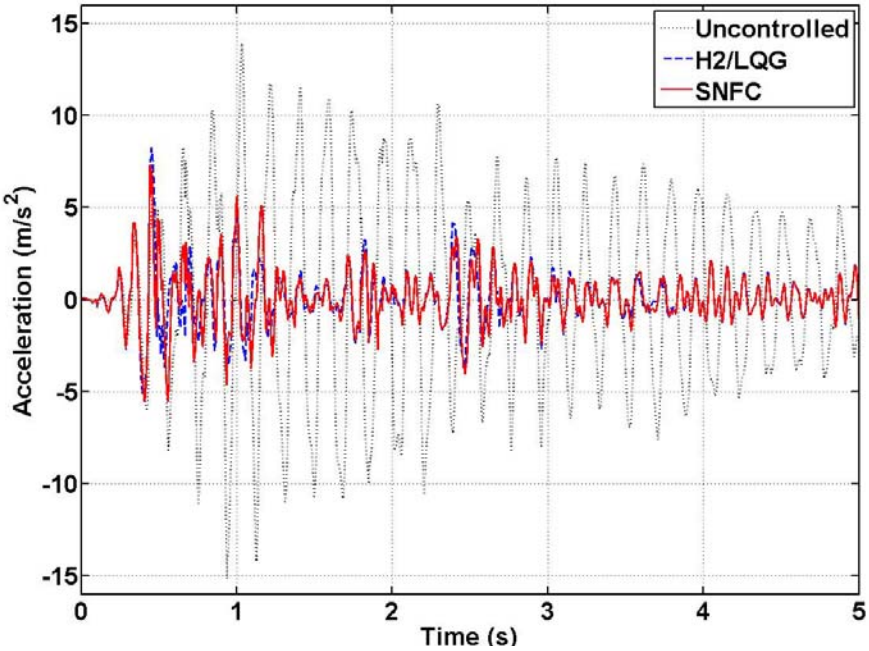

Fig. 5.10. Time history acceleration responses of an uncontrolled, a H2/LQG control, and a SNFC systems at the 3rd floor

Fig. 5.11 compares maximum interstory responses of the uncontrolled, the H2/LQG controlled, and the SNFC controlled responses: The graph (a) is about the comparison of the maximum displacement responses; (b) compares maximum drift responses; and (c) compares maximum acceleration responses. In terms of the 2nd and the 3rd maximum responses, the SNFC system is better than the H2/LQG controller, while the H2/LQG controller shows better performance than the SNFC system in the 1st floor response. Furthermore, the normalized maximum MR damper force, which is a value normalized by the total weight of the given building structure (Jansen and Dyke 2000), of the SNFC system is evaluated

$$J = \max_{t}\left(\frac{\left|f_{\mathrm{MR}}(t)\right|}{W_{\mathrm{s}}}\right), \tag{5.47}$$

where $f_{\mathrm{MR}}(t)$ is the applied MR damper force and W_{s} is the seismic weight of the building structure. The result is that the proposed SNFC system is 0.0289, while the H2/LQG control system is 0.0350, i.e., the SNFC system is more efficient than the H2/LQG controller.

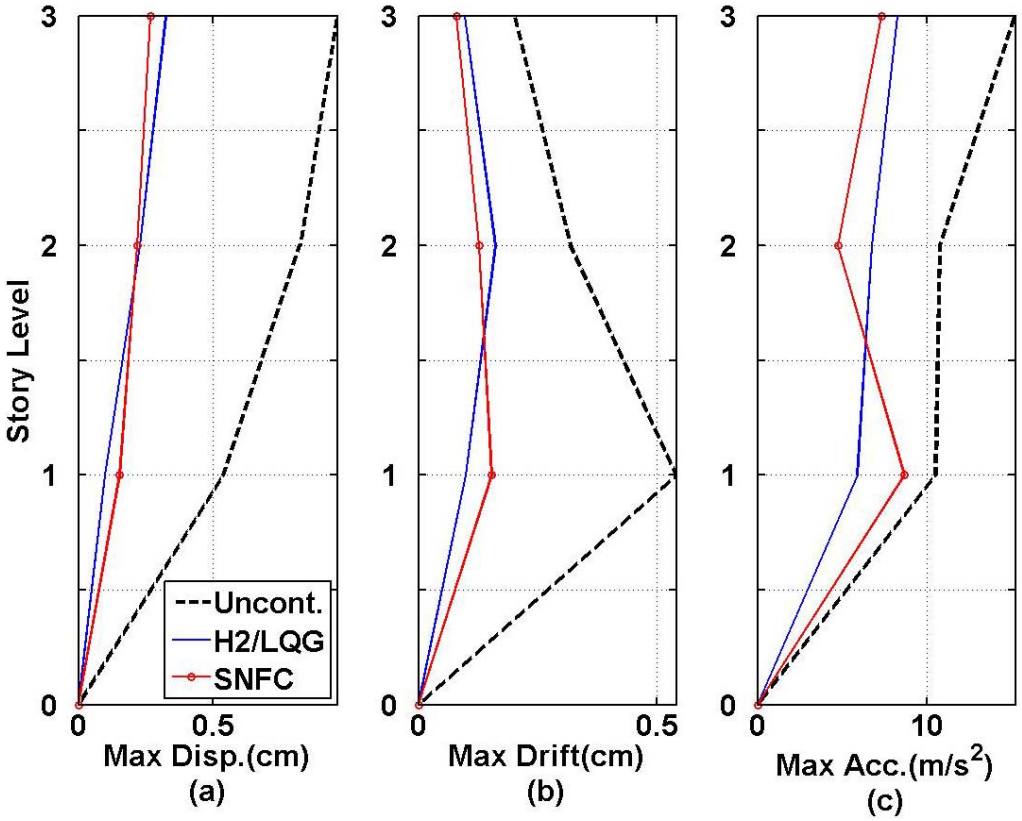

Fig. 5.11. Interstory responses of an uncontrolled, a H2/LQG control, and a SNFC systems

5.5.2 Control Performance Evaluation: Noise Contaminated Case

In addition to the normal case, the robustness of the SNFC system is compared with that of the H2/LQG control system using the 30 % zero-mean Gaussian white noise. According to the time history responses, both displacement and acceleration responses are dramatically reduced when either H2/LQG or SNFC systems are applied.

Fig. 5.12 and Fig. 5.13 compare displacement and acceleration responses at the 1st floor of an uncontrolled, a H2/LQG controlled, and a SNFC controlled system. According to the time history, the performance of the H2/LQG control system is degraded when the sensor noise is applied. It is even destabilized for the 1st floor acceleration. However, the SNFC control system is very robust with respect to the sensor noise.

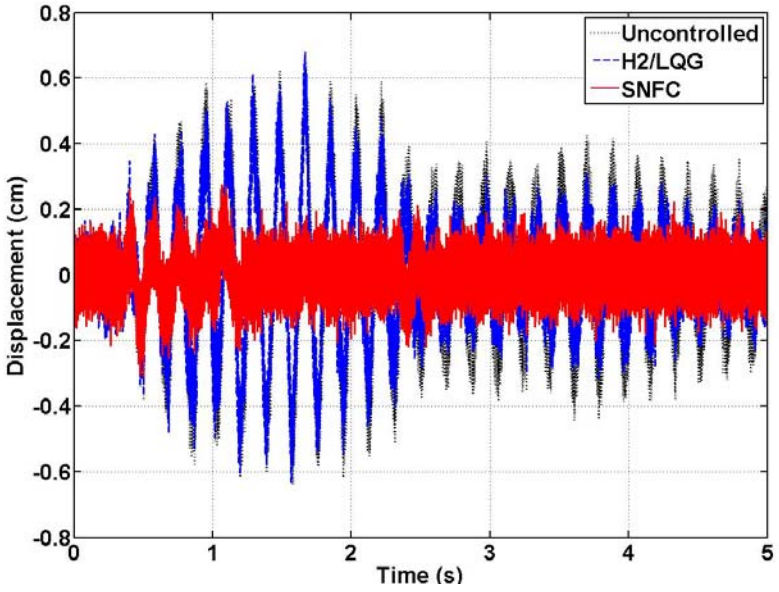

Fig. 5.12. Time history displacement responses at the 1st floor (disturbed by 30 % sensor noise from a zero-mean Gaussian white noise generator)

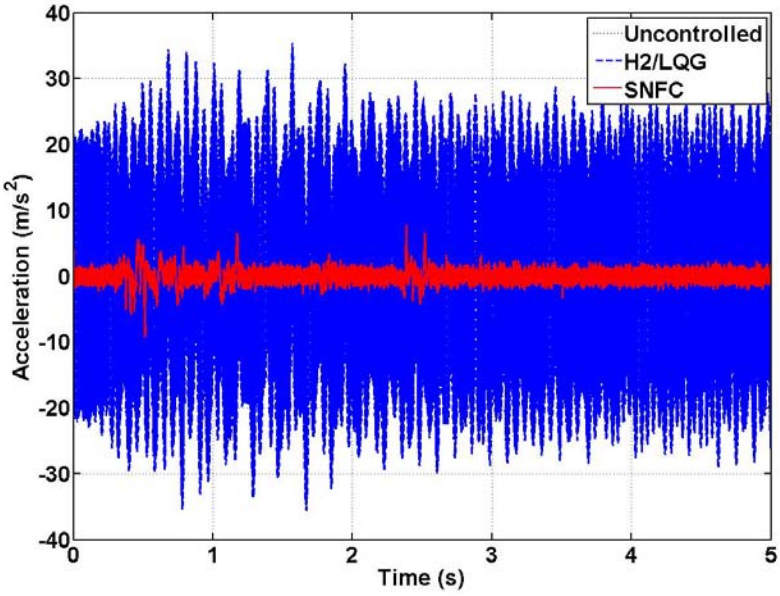

Fig. 5.13. Time history acceleration responses at the 1st floor (disturbed by 30 % sensor noise from a zero-mean Gaussian white noise generator)

Fig. 5.14 and Fig. 5.15 compare displacement and acceleration responses at the 2nd floor of an uncontrolled, a H2/LQG controlled, and a SNFC controlled system. According to the time history, the performance of the H2/LQG control system is degraded when the sensor noise is applied.

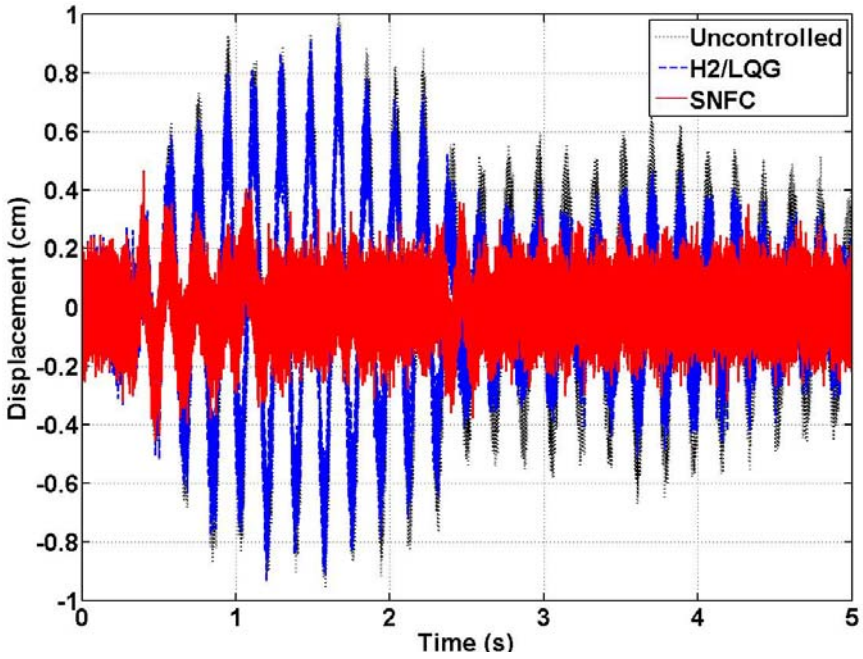

Fig. 5.14. Time history displacement responses at the 2nd floor (disturbed by 30 % sensor noise from a zero-mean Gaussian white noise generator)

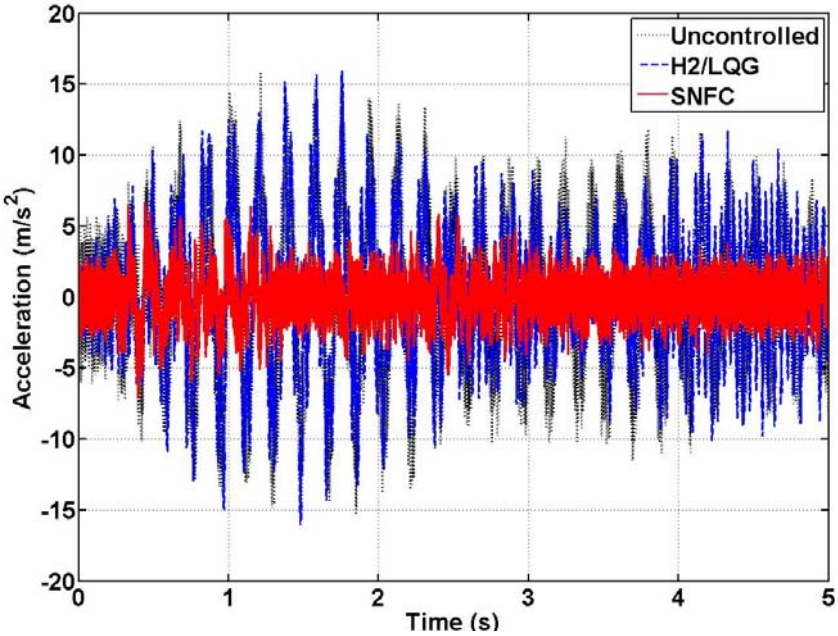

Fig. 5.15. Time history acceleration responses at the 2nd floor (disturbed by 30 % sensor noise from a zero-mean Gaussian white noise generator)

Fig. 5.16 and Fig. 5.17 compare displacement and acceleration responses at the 3rd floor of an uncontrolled, a H2/LQG controlled, and a SNFC controlled system. According to the time history, the performance of the H2/LQG control system is degraded when the sensor noise is applied. However, the SNFC control system is very robust with respect to the sensor noise.

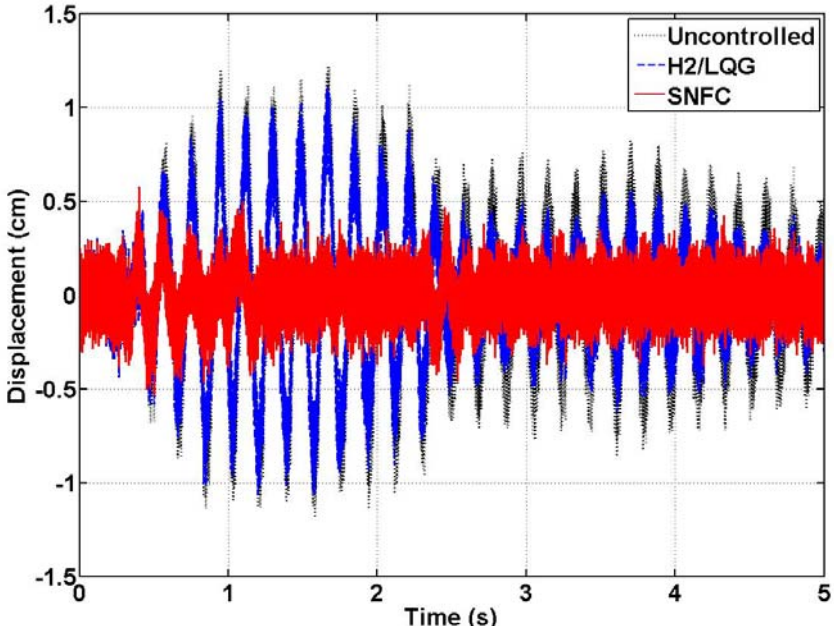

Fig. 5.16. Time history responses at the 3rd floor (disturbed by 30 % sensor noise from a zero-mean Gaussian white noise generator)

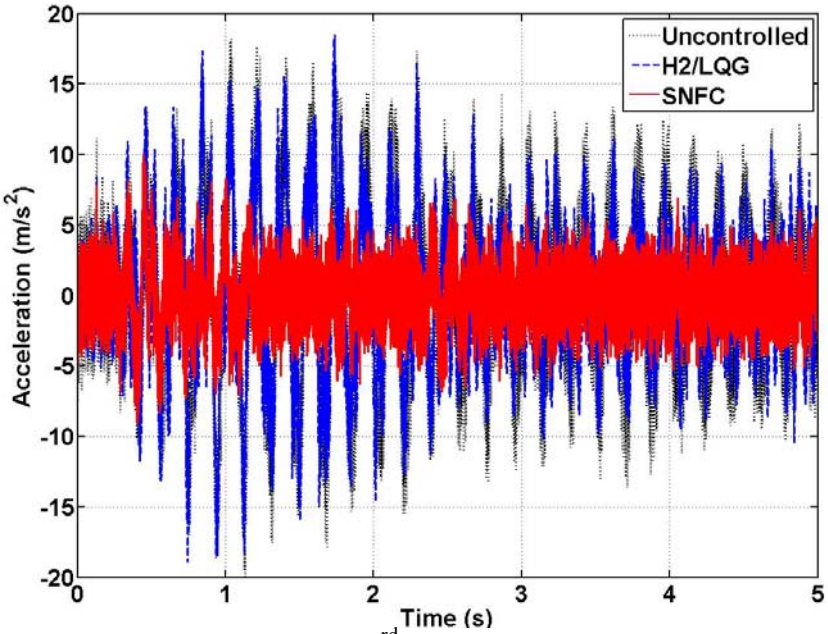

Fig. 5.17. Time history responses at the 3rd floor (disturbed by 30 % sensor noise from a zero-mean Gaussian white noise generator)

Fig. 5.18 compares maximum interstory responses of the uncontrolled, the H2/LQG controlled, and the SNFC controlled responses. The graph (a) is about the comparison of the maximum displacement responses; (b) compares maximum drift responses; and (c) compares maximum acceleration responses. The H2/LQG controller is not effective in reducing the maximum interstory displacement and acceleration responses of the three story building structure with sensor noise. It also allows the 1st floor acceleration responses to vibrate significantly, even more than the uncontrolled system. However, the SNFC system is effective in reducing all the interstory displacement and acceleration responses of the entire floor levels of the three story building structure with sensor noises. Furthermore, the normalized maximum MR damper force of the SNFC system is 0.0299, while that of the H2/LQG control system is 0.0692, i.e., the SNFC system is more efficient than the H2/LQG controller. Therefore, it is demonstrated that the SNFC system is effective and efficient to control responses of a low-rise building structure subjected to the 1940 El Centro earthquake disturbance.

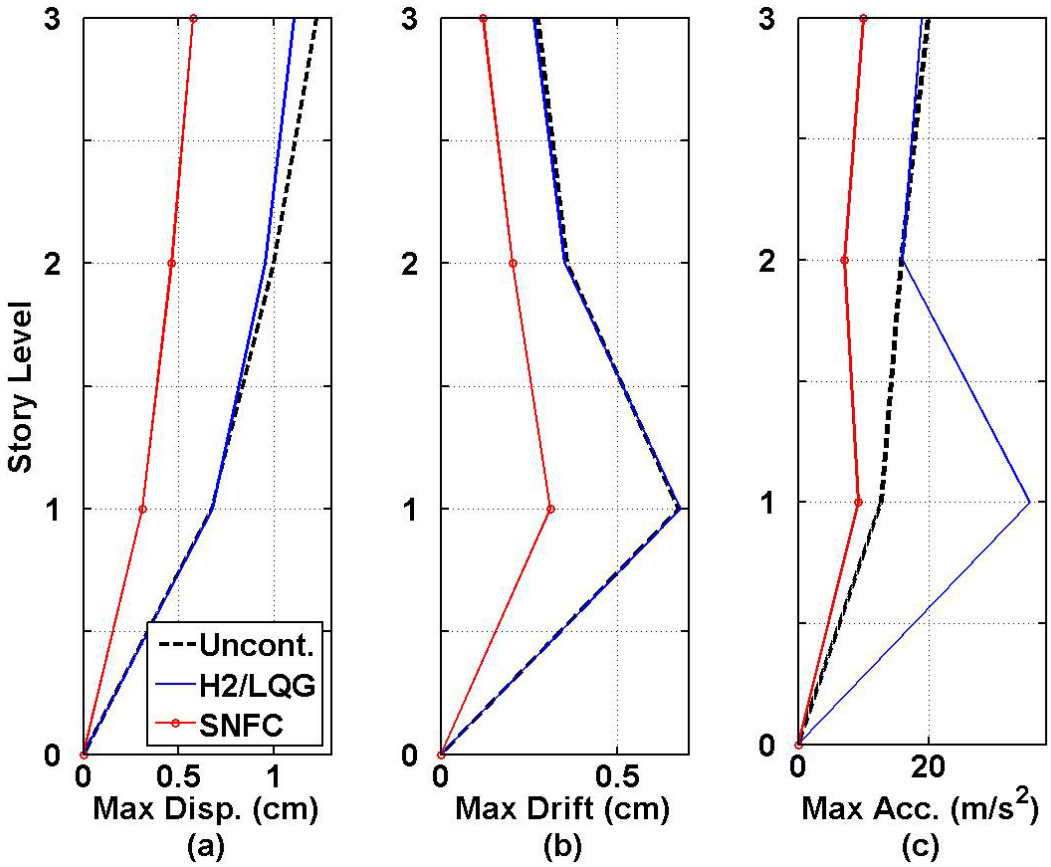

Fig. 5.18. Interstory responses of an uncontrolled, a LQG control, and a SNFC systems (disturbed by 30 % sensor noise from a zero-mean Gaussian white noise generator)

5.6 Concluding Remarks

In this section, a systematic design methodology was proposed for the semiactive nonlinear fuzzy control (SNFC) of a class of building-magnetorheological damper systems with multi-objective requirements in a unified framework based on parallel distributed compensation. Linear matrix inequality (LMI)-based state feedback controllers were derived by first such that the closed loop system is globally asymptotically stable and the performance on transient responses is also satisfied. Then, a Kalman filter was designed to construct output feedback control systems. Next, such output feedback controllers were integrated into an active nonlinear fuzzy control (ANFC) system through a fuzzy interpolation method. Finally, a clipped algorithm was integrated with the output feedback-based ANFC system for a SNFC system. In order to prove the effectiveness of the SNFC system, a benchmark three-story building frame is investigated. Furthermore, the robustness performance of the proposed SNFC system was compared with a traditional semiactive linear control system, in particular, with respect to sensor noise. It was demonstrated from the examples that the suggested SNFC system is effective to control vibration of an earthquake-excited mid-scale building-MR damper system. In addition, the proposed SNFC system is close or better than the H2/linear quadratic Gaussian (LQG) controller. However, the performance of the H2/LQG control system is degraded when noise is added into the sensing unit, even much worse than the uncontrolled system, while the SNFC system is operated effectively in both sensor noise free and sensor noise contaminated cases.

6. SUPERVISORY SEMIACTIVE NONLINEAR CONTROL

6.1 Introduction

In recent years, advanced control technologies, which include passive, active, and semiactive control systems, have been applied to large-scale civil engineering structures for mitigation of natural hazards such as earthquakes and strong winds. However, these control systems have been implemented as the so-called centralized controllers. In the centralized control system, there exist only a single central control unit to operate many actuators and sensors. One of the severe problems for the centralized control technologies is that the overall control system of the large-scale civil engineering structures will be broken down if the main central control unit mal-functions for some reasons during an earthquake event, e.g., shut down of power sources, broken sensors and wires. A solution to solve this problem is to use so-called decentralized control concept.

In general, a decentralized control is to divide the large-scale civil engineering structure into a number of sub-structures by first and then to implement several sub-controllers that are associated with each sub-structure, i.e., each sub-structure is controlled by a sub-controller independently (Hashemian and Ryaciotaki-Roussalis 1995). This decentralized control system increases fail-safe reliability of the overall control system. Thus, the decentralized control systems have attracted attention for use

with large-scale civil engineering building structures (Lynch and Law 2000; Rofooei and Monajemi-nezhad 2006). However, they have been mostly implemented based on linear control theories. Concurrently with the linear control-based decentralized control techniques, nonlinear decentralized controllers have been also applied to the large-scale civil structural systems, in particular, neuro, fuzzy, and neuro-fuzzy control systems because they are easy to handle with nonlinearity and are inherently robust with respect to uncertainties (Xu et al. 2003; Park et al. 2005). However, their applications are limited to active control system implementations. Later, as a breakthrough, Reigles and Symans (2006) suggested a supervisory nonlinear fuzzy control system for use with a base-isolated building structure employing controllable fluid viscous dampers. They designed two decentralized fuzzy controllers for a far- and a near-field earthquake disturbance and the control gains of the decentralized sub-controllers are adapted according to the command of a supervisor fuzzy logic system. However, their systems have been designed by a trial-and-error approach that uses either investigators' experience or high-cost computation, i.e., as a model-free controller, they are trained using a set of input-output data. Although useful for the performance purpose, the ad-hoc approach may not provide a design guideline in a systematic way. Unfortunately, no systematic study has been conducted to design a decentralized fuzzy control system for structural vibration control of building structures equipped with nonlinear semiactive control devices. Therefore, research is needed to develop a systematic design methodology for the decentralized semiactive nonlinear fuzzy control (DSNFC) system of large scale building structures employing MR dampers.

6.2 Decentralized Semiactive Nonlinear Fuzzy Control

In this research, a multi-input-multi-output (MIMO) semiactive nonlinear fuzzy control (SNFC) system is developed as a diagonal or a block-diagonal controller that consists of a set of multi-input-single-output (MISO) controllers. In what follows, fundamentals on decentralized control techniques are discussed. Then, the decentralized control concept is applied to a MIMO SNFC system implementation.

6.2.1 Concept of Decentralized Control

In a decentralized control system, it is assumed that the building structure to be controlled is close to diagonal, i.e., the building structure is a collection of a number of independent sub-structures. Fig. 6.1 shows a schematic of the decentralized control implementation for the large-scale civil engineering building structure. As shown in Fig. 6.1, each sub-controller does not use all the state or output feedback information from the structural system to be controlled, i.e., each local controller that is independently operated uses local feedback information.

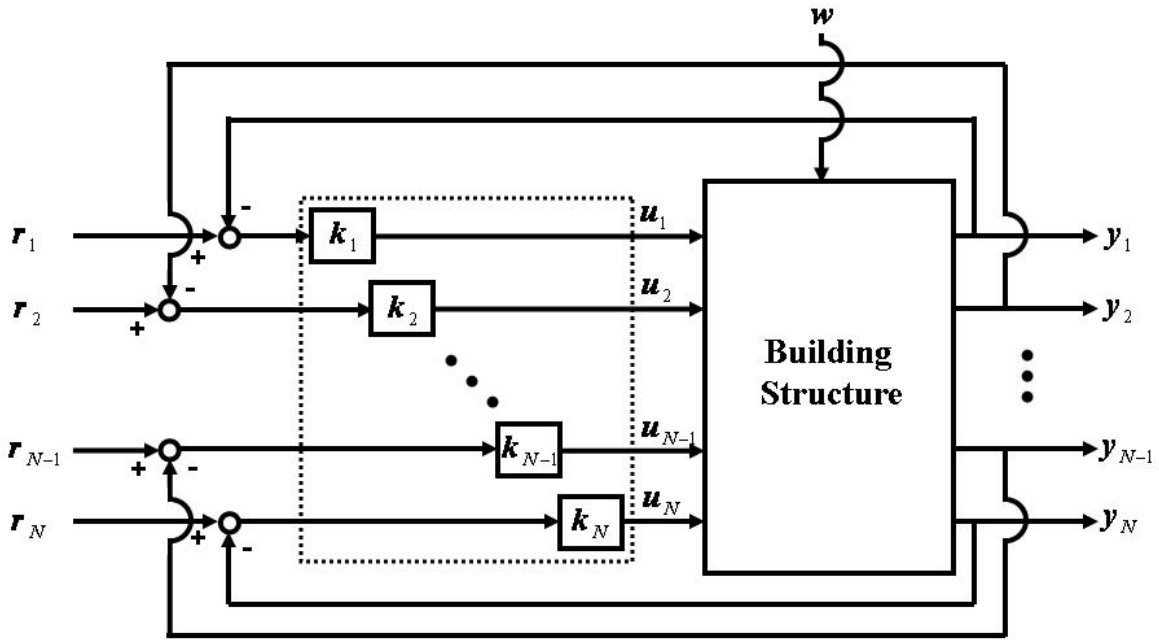

Fig. 6.1. Decentralized diagonal control concept

The decentralized diagonal controller is given by

$$\mathbf{K} = \operatorname{diag}\{k_i\} = \begin{bmatrix} k_1 & 0 & 0 & 0 & 0 \\ 0 & k_2 & 0 & 0 & 0 \\ 0 & 0 & \ddots & 0 & 0 \\ 0 & 0 & 0 & k_N & 0 \\ 0 & 0 & 0 & 0 & k_{N-1} \end{bmatrix}, \tag{6.1}$$

control signals u_i are generated by the local sub-controllers k_i, y_i are output signals, r_i are reference signals, and w is an external disturbance, i.e., earthquake acceleration record. A procedure to design the decentralized control system consists of four steps.

Step 1: Selection of locations to be controlled within the given building structure.

Step 2: Development of a mathematical model for each sub-structure related to the locations to be controlled.

Step 3: Design of each local sub-controller k_i that is associated with each sub-structure.

Step 4: Implementation of the independent sub-controllers into the given building.

In this research, each local sub-controller is independently designed as a SNFC system whose design procedure is described in detail in Section 5. In the following section, the MISO SNFC system is generalized into a MIMO SNFC system via the decentralized control concept.

6.2.2 Decentralized Semiactive Nonlinear Fuzzy Control (DSNFC)

Based on Eq. (6.1), a decentralized MIMO SNFC system is implemented as shown in Fig. 6.2. As shown in Fig. 6.2, a SNFC system is used as a sub-controller of the decentralized semiactive nonlinear fuzzy control (DSNFC). In other words, each sub-controller is designed such that globally asymptotically stable is guaranteed and the performance on transient responses is satisfied, i.e., the sub-controller is developed as the state feedback controller through solving Eq. (5.24), Eq. (5.25), and Eq. (5.32) simultaneously. Then, the state feedback-based sub-controllers are integrated with Eq. (5.40) and Eq. (5.42) to construct the output feedback-based semiactive controller.

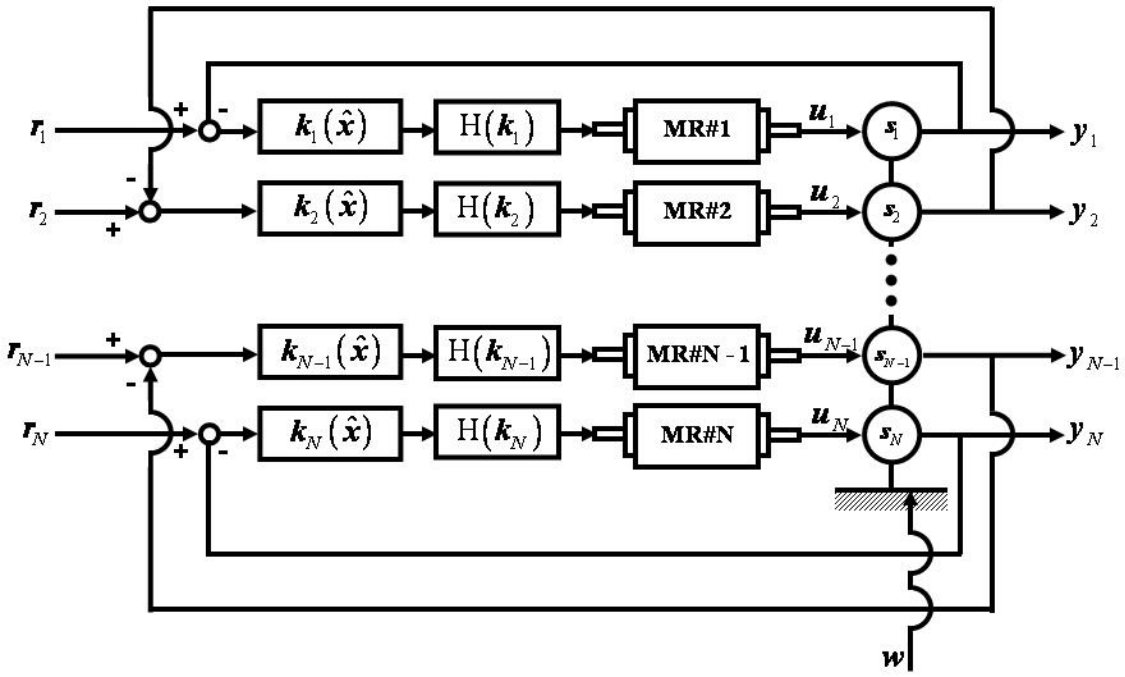

Fig. 6.2. A schematic of a decentralized semiactive nonlinear control system

In Fig. 6.2, $k_i(\hat{\mathbf{x}})$ is the output feedback gain associated with the sub-structure; $\mathrm{H}(k_i)$ is the semiactive converter that is implemented via either a clipped algorithm or an inverse MR damper model; $\mathrm{MR}\#i$ is the MR damper; u_i is the control force that is applied to the sub-structure; y_i is the output; r_i is the reference; w is the external disturbance, i.e., earthquake excitation signals; s_i is the sub-structure. Each DSNFC system is designed based on acceleration and drift feedback information. In this DSNFC system, any information between the local control units is not communicated. However, global performance of the closed loop system can be improved by adding the higher level of a controller, so-called supervisor controller (Lei and Langari 2000). It might be called a supervisory semiactive nonlinear fuzzy control (SSNFC).

6.2.3 Supervisory Semiactive Nonlinear Fuzzy Control (SSNFC)

In the DSNFC system, any information among the local sub-controllers is not communicated. However, the performance of the DSNFC system can be improved by adding the higher level of a controller, so-called a coordinate controller into the DSNFC system. The supervisor controller is first developed as a state feedback controller through solving Eq. (5.24), Eq. (5.25), and Eq. (5.32) simultaneously such that globally asymptotically stable is guaranteed and the performance on transient responses is satisfied. Then, the state feedback-based supervisor controller is integrated with Eq. (5.40) to construct the output feedback-based supervisor controller. The supervisor controller adapts the magnitude of control gains of the sub-controllers according to velocity feedback information. Fig. 6.3 shows a schematic of the SSNFC system configuration. To demonstrate the effective of the proposed DSNFC and SSNFC systems, an eight story shear type building structure is investigated.

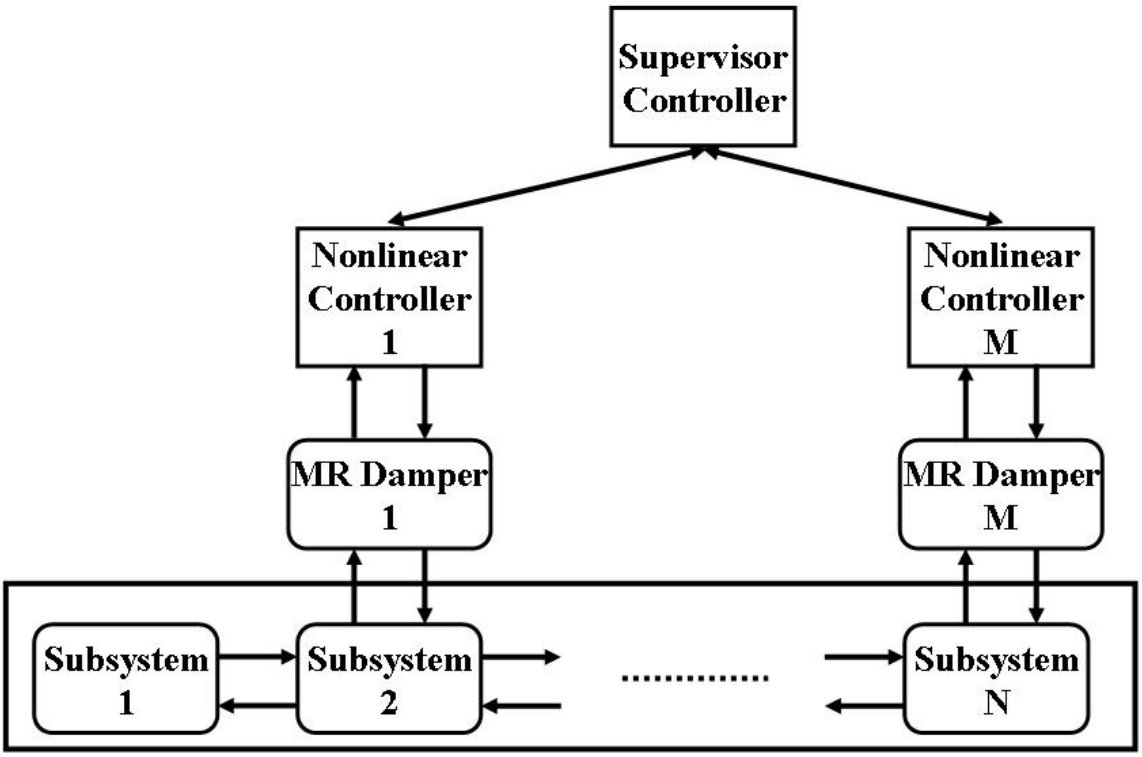

Fig. 6.3. A schematic of a supervisory semiactive nonlinear control system

6.3 Examples

To demonstrate the effectiveness of the developed DSNFC and SSNFC systems, an eight story shear type building structure equipped with two 1000 kN MR dampers is investigated here. The equation of motion of the eight story building-MR damper system is given by the equation on page 43. Detailed description on the building-MR damper system is provided in Section 3. Two 1000 kN-MR damper models are employed at the 5^{th} and 8^{th} floors. To synthesis the MR damper to the SNFC system, two modified Bouc-Wen models are used. The applied modified Bouc-Wen model is

described in Section 2 and its optimum parameters are given in Appendix B. The 1940 El-Centro earthquake acceleration record with 25 % intensity is applied as a ground motion.

The performance of the DSNFC and SSNFC is compared with a centralized semiactive nonlinear fuzzy control (CSNFC) system, while the uncontrolled system response is used as the baseline. Note that all the MR dampers are installed on the same floor for the CSNFC system in this research. Fig. 6.4 and Fig. 6.5 show comparison of displacement and drift time history responses at the 1^{st} floor level of the eight story shear type building structure employing two MR dampers that are controlled by the CSNFC, DSNFC, and SSNFC systems, while the uncontrolled system response is used as the baseline. According to the time history responses, the CSNFC, DSNFC, and SSNFC system are all effective in vibration reduction of displacements and drift at all the floors.

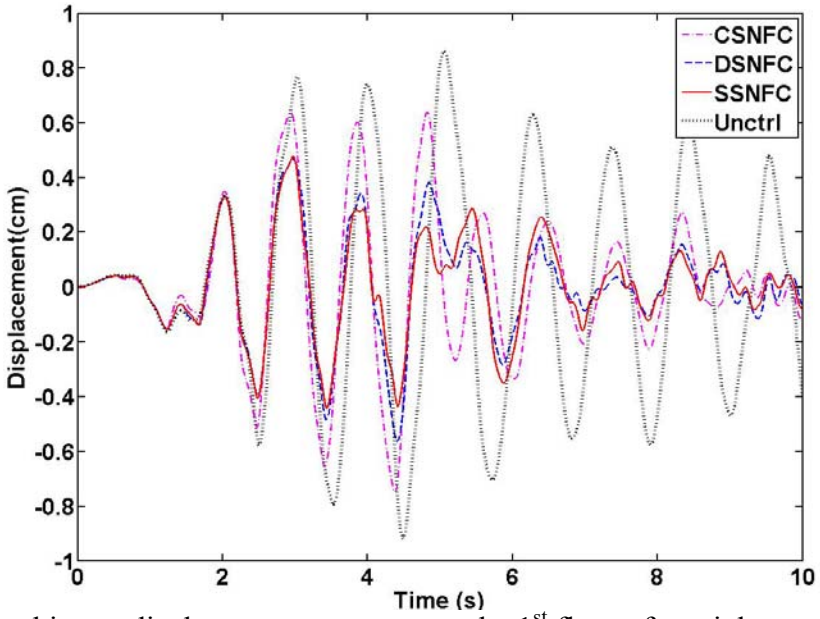

Fig. 6.4. Time history displacement responses at the 1st floor of an eight story shear type building structure equipped with two MR dampers controlled by a CSNFC, a DSNFC, and a SSNFC systems

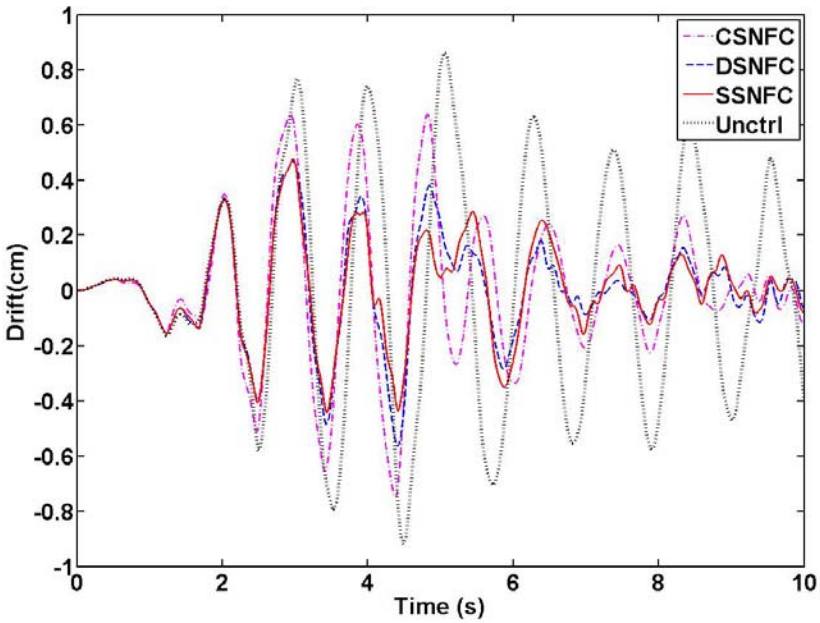

Fig. 6.5. Time history drift responses at the 1st floor of an eight story shear type building structure equipped with two MR dampers controlled by a CSNFC, a DSNFC, and a SSNFC systems

Fig. 6.6 and Fig. 6.7 show comparison of displacement and drift time history responses at the 2nd floor level of the eight story shear type building structure employing two MR dampers that are controlled by the CSNFC, DSNFC, and SSNFC systems, while the uncontrolled system response is used as the baseline. According to the time history responses, the CSNFC, DSNFC, and SSNFC system are all effective in vibration reduction of displacements and drift at all the floors.

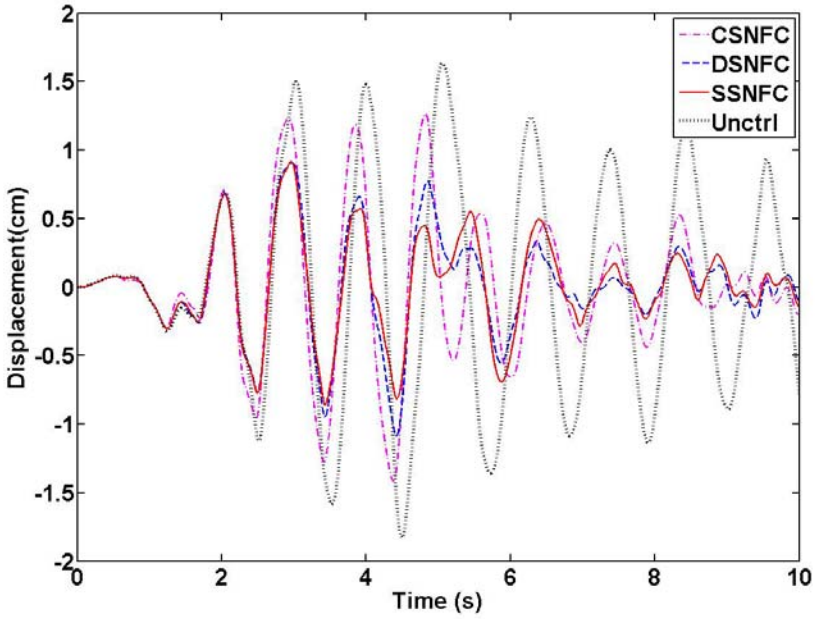

Fig. 6.6. Time history displacement responses at the 2nd floor of an eight story shear type building structure equipped with two MR dampers controlled by a CSNFC, a DSNFC, and a SSNFC systems

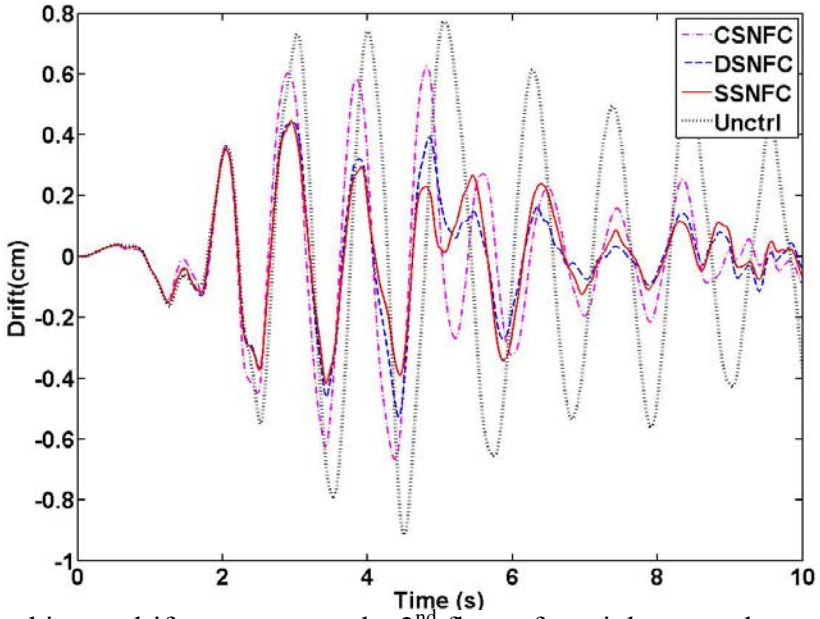

Fig. 6.7. Time history drift responses at the 2nd floor of an eight story shear type building structure equipped with two MR dampers controlled by a CSNFC, a DSNFC, and a SSNFC systems

Fig. 6.8 and Fig. 6.9 show comparison of displacement and drift time history responses at the 3rd floor level of the eight story shear type building structure employing two MR dampers that are controlled by the CSNFC, DSNFC, and SSNFC systems, while the uncontrolled system response is used as the baseline. According to the time history responses, the CSNFC, DSNFC, and SSNFC system are all effective in vibration reduction of displacements and drift at all the floors.

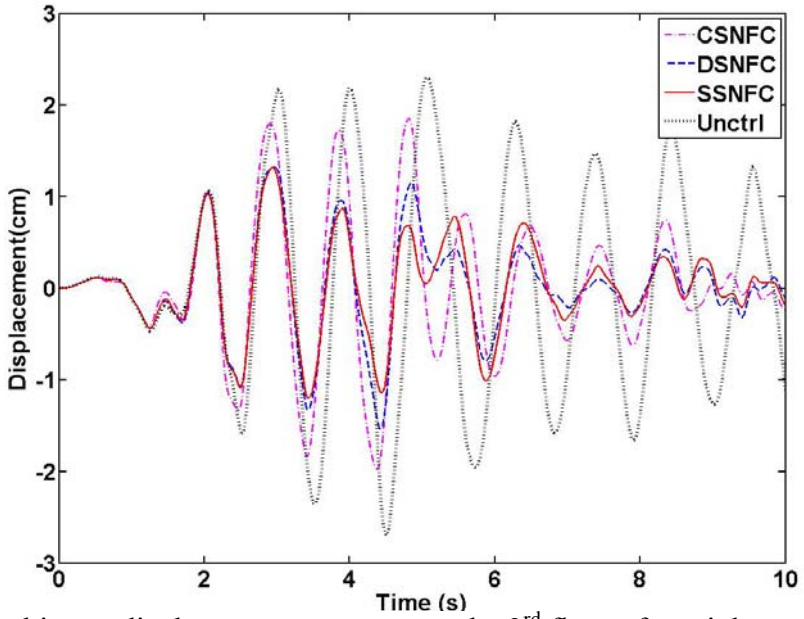

Fig. 6.8. Time history displacement responses at the 3rd floor of an eight story shear type building structure equipped with two MR dampers controlled by a CSNFC, a DSNFC, and a SSNFC systems

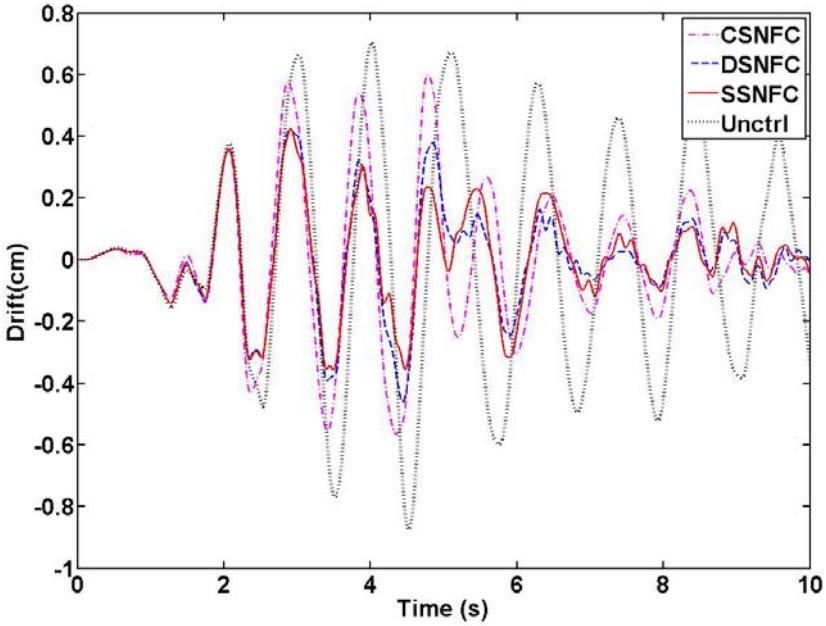

Fig. 6.9. Time history drift responses at the 3rd floor of an eight story shear type building structure equipped with two MR dampers controlled by a CSNFC, a DSNFC, and a SSNFC systems

Fig. 6.10 and Fig. 6.11 show comparison of displacement and drift time history responses at the 4th floor level of the eight story shear type building structure employing two MR dampers that are controlled by the CSNFC, DSNFC, and SSNFC systems, while the uncontrolled system response is used as the baseline. According to the time history responses, the CSNFC, DSNFC, and SSNFC system are all effective in vibration reduction of displacements and drift at all the floors.

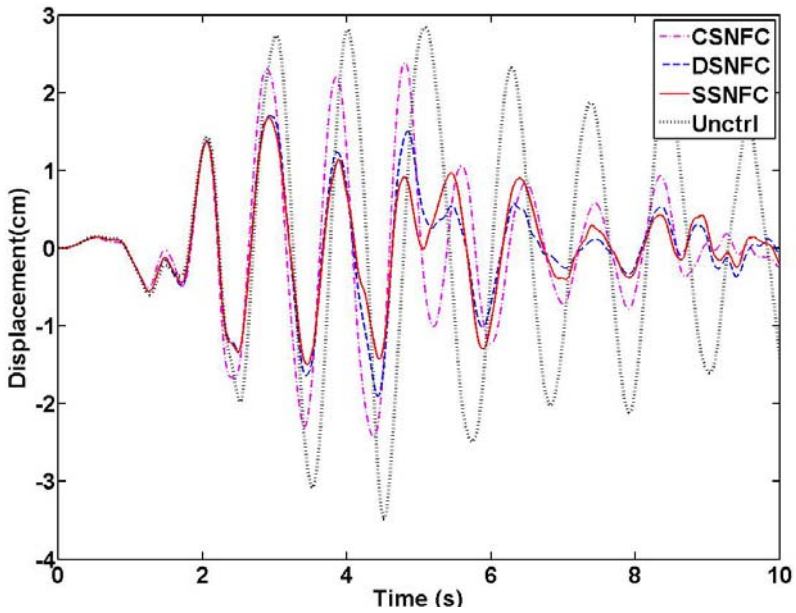

Fig. 6.10. Time history displacement responses at the 4th floor of an eight story shear type building structure equipped with two MR dampers controlled by a CSNFC, a DSNFC, and a SSNFC systems

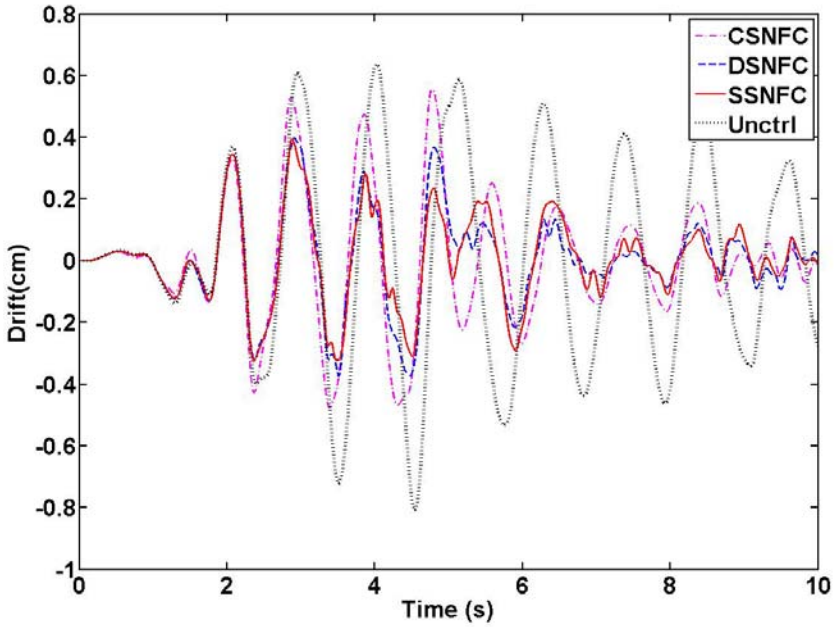

Fig. 6.11. Time history drift responses at the 4th floor of an eight story shear type building structure equipped with two MR dampers controlled by a CSNFC, a DSNFC, and a SSNFC systems

Fig. 6.12 and Fig. 6.13 show comparison of displacement and drift time history responses at the 5th floor level of the eight story shear type building structure employing two MR dampers that are controlled by the CSNFC, DSNFC, and SSNFC systems, while the uncontrolled system response is used as the baseline. According to the time history responses, the CSNFC, DSNFC, and SSNFC system are all effective in vibration reduction of displacements and drift at all the floors.

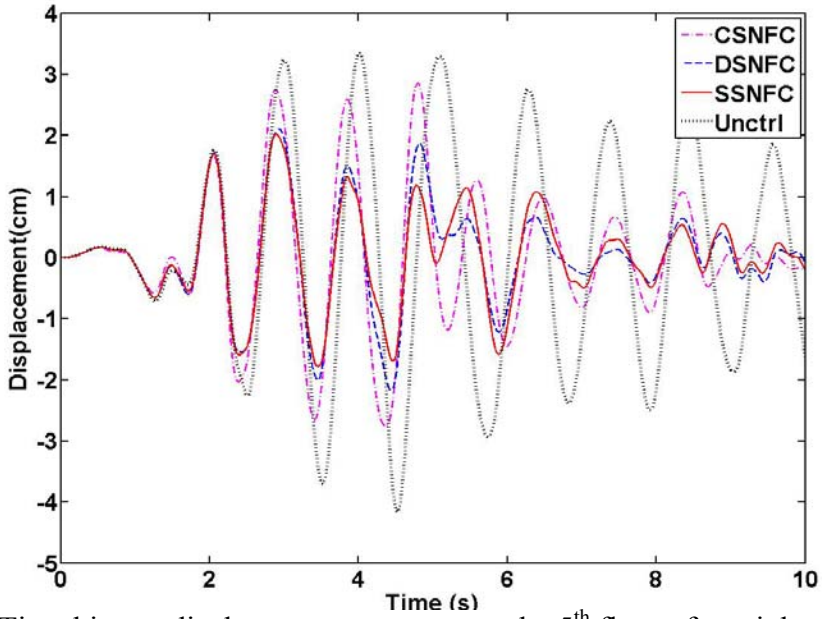

Fig. 6.12. Time history displacement responses at the 5th floor of an eight story shear type building structure equipped with two MR dampers controlled by a CSNFC, a DSNFC, and a SSNFC systems

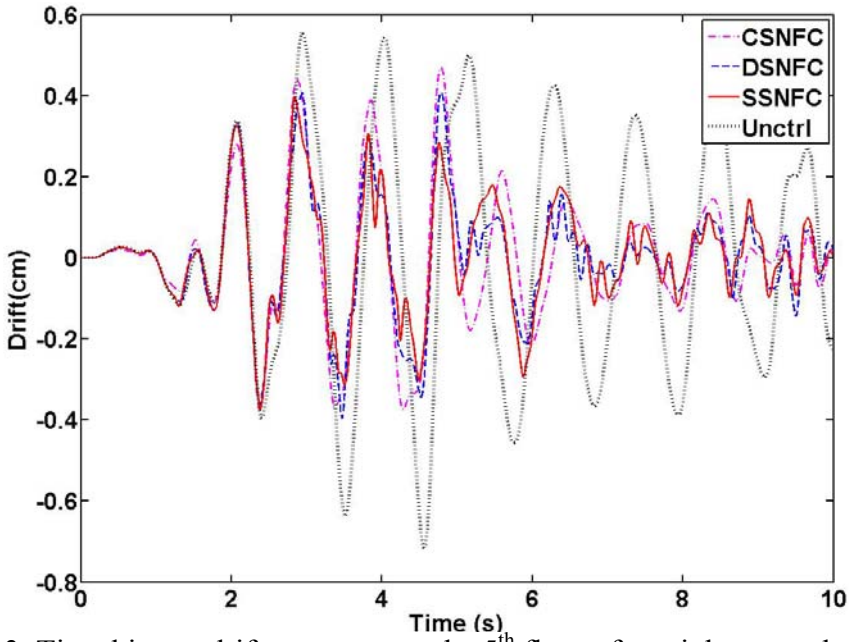

Fig. 6.13. Time history drift responses at the 5th floor of an eight story shear type building structure equipped with two MR dampers controlled by a CSNFC, a DSNFC, and a SSNFC systems

Fig. 6.14 and Fig. 6.15 show comparison of displacement and drift time history responses at the 6th floor level of the eight story shear type building structure employing two MR dampers that are controlled by the CSNFC, DSNFC, and SSNFC systems, while the uncontrolled system response is used as the baseline. According to the time history responses, the CSNFC, DSNFC, and SSNFC system are all effective in vibration reduction of displacements and drift at all the floors.

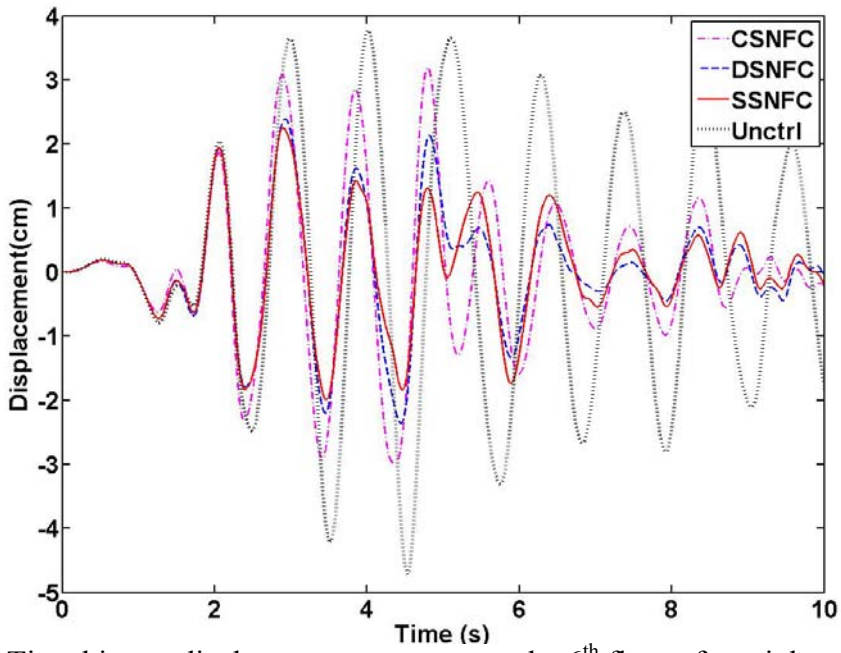

Fig. 6.14. Time history displacement responses at the 6th floor of an eight story shear type building structure equipped with two MR dampers controlled by a CSNFC, a DSNFC, and a SSNFC systems

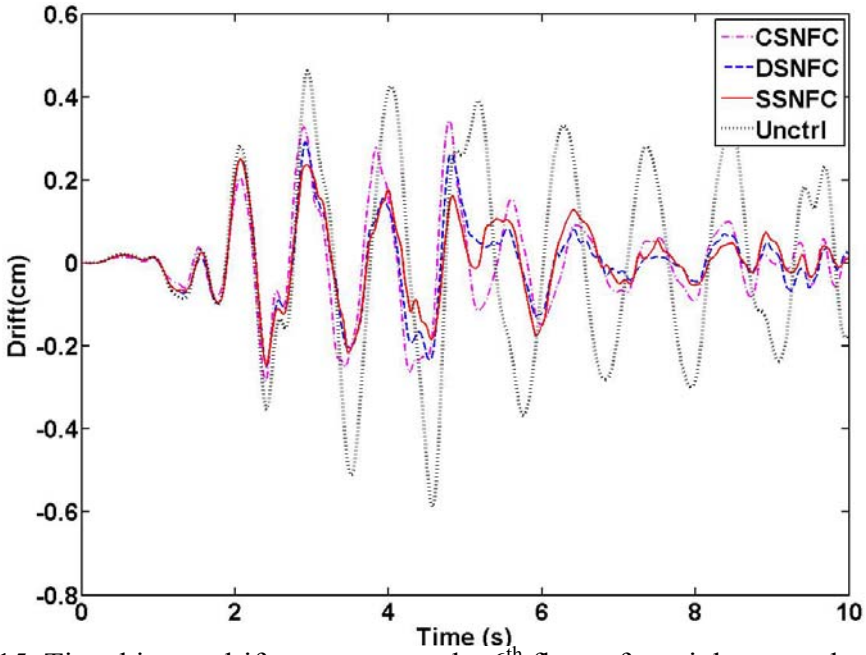

Fig. 6.15. Time history drift responses at the 6th floor of an eight story shear type building structure equipped with two MR dampers controlled by a CSNFC, a DSNFC, and a SSNFC systems

Fig. 6.16 and Fig. 6.17 show comparison of displacement and drift time history responses at the 7th floor level of the eight story shear type building structure employing two MR dampers that are controlled by the CSNFC, DSNFC, and SSNFC systems, while the uncontrolled system response is used as the baseline. According to the time history responses, the CSNFC, DSNFC, and SSNFC system are all effective in vibration reduction of displacements and drift at all the floors.

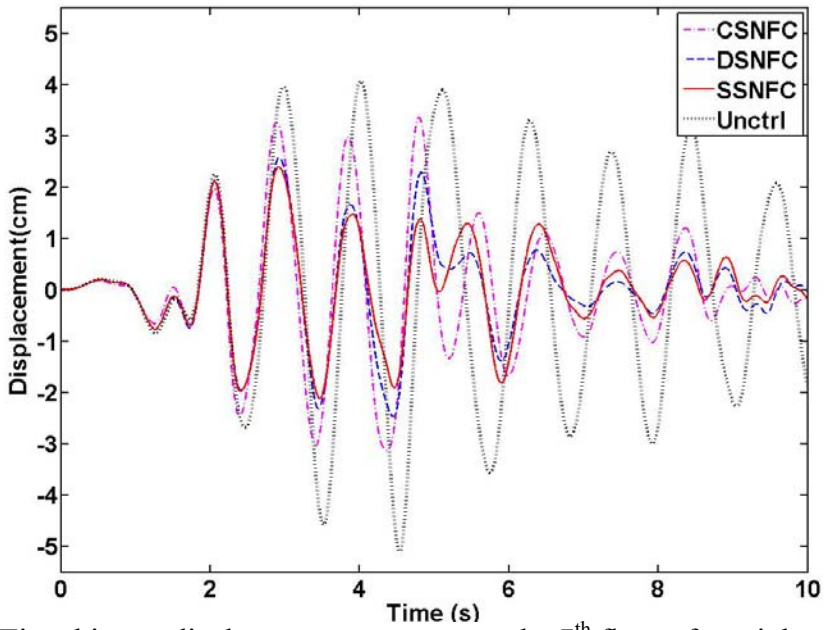

Fig. 6.16. Time history displacement responses at the 7th floor of an eight story shear type building structure equipped with two MR dampers controlled by a CSNFC, a DSNFC, and a SSNFC systems

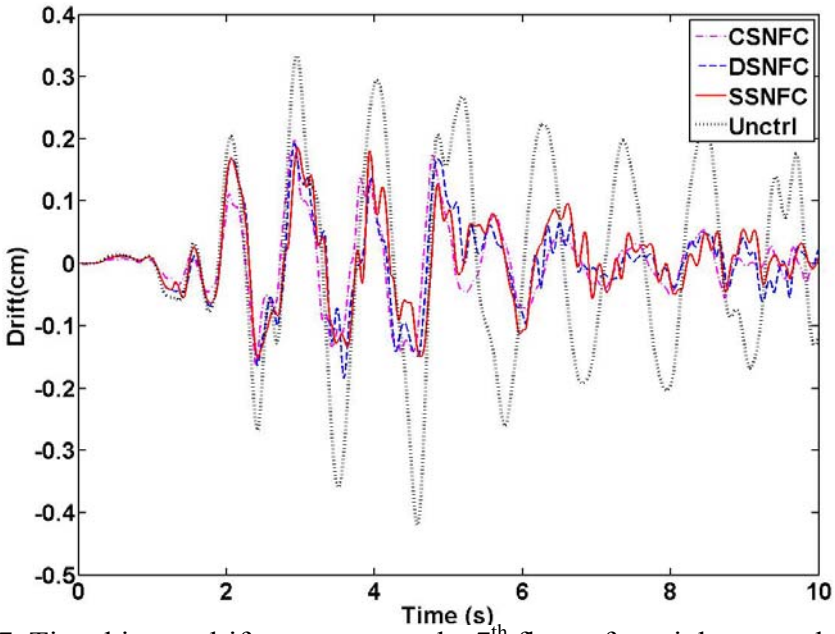

Fig. 6.17. Time history drift responses at the 7th floor of an eight story shear type building structure equipped with two MR dampers controlled by a CSNFC, a DSNFC, and a SSNFC systems

Fig. 6.18 and Fig. 6.19 show comparison of displacement and drift time history responses at the 8th floor level of the eight story shear type building structure employing two MR dampers that are controlled by the CSNFC, DSNFC, and SSNFC systems, while the uncontrolled system response is used as the baseline. According to the time history responses, the CSNFC, DSNFC, and SSNFC system are all effective in vibration reduction of displacements and drift at all the floors.

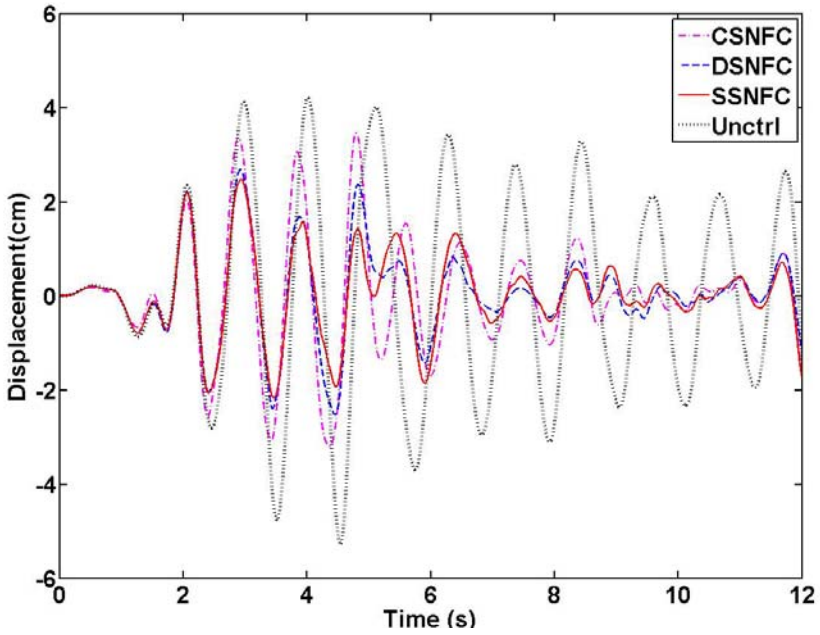

Fig. 6.18. Time history displacement responses at the 8th floor of an eight story shear type building structure equipped with two MR dampers controlled by a CSNFC, a DSNFC, and a SSNFC systems

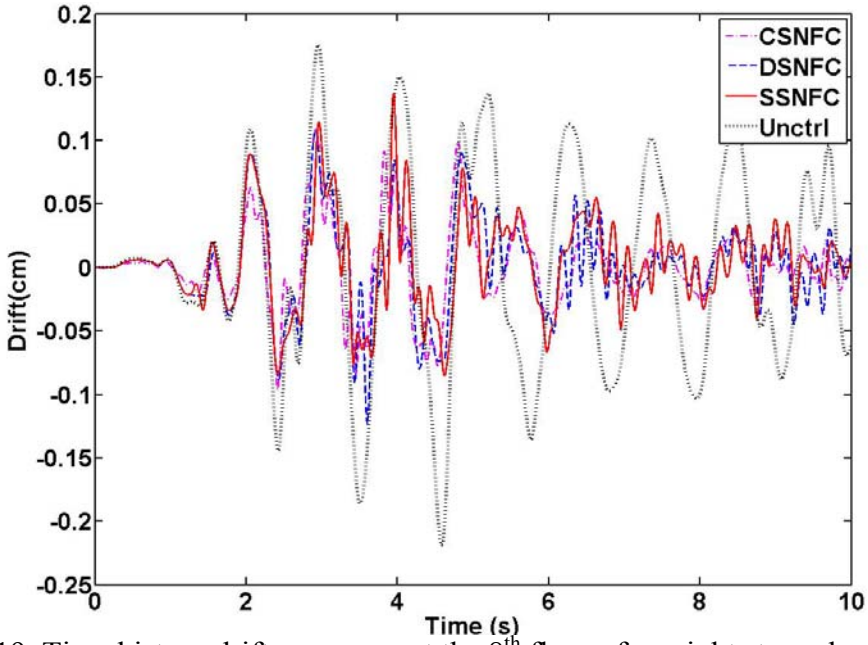

Fig. 6.19. Time history drift responses at the 8th floor of an eight story shear type building structure equipped with two MR dampers controlled by a CSNFC, a DSNFC, and a SSNFC systems

Fig. 6.20 to Fig. 6.22 shows comparison of maximum/mean responses of the uncontrolled, CSNFC, DSNFC, and SSNFC controlled systems. In terms of maximum and mean values of the displacement and the drift at the entire floor levels, all the CSNFC, DSNFC, and SSNFC systems are all effective in vibration reduction. In addition to the displacement and drift, the developed control systems are effective to diminish acceleration responses of almost all floor levels.

As can be seen, the SSNFC is the most effective to control the drift, displacement, acceleration responses and the DSNFC system has better performance than the CSNFC system. According to Eq. (5.47) that represents how much MR damper force is used, CSNFC = 0.0202; DSNFC = 0.0149; and SSNFC = 0.0209, i.e. DSNFC system uses the lowest capacity of the MR damper, while SSNFC system applies for the most capacity of the MR damper to the eight story building structure. Note that MR dampers, differently with actuators that require high cost of power sources, require small amount of power sources for the operation. In other words, a relatively small difference of the applied MR damper capacities does not critically affect the total cost of MR damper implementation. Therefore, practical point of view, it is recommended that the DSNFC and SSNFC systems be chosen as controllers for the eight story building structures because their performances are much better than the CSNFC system.

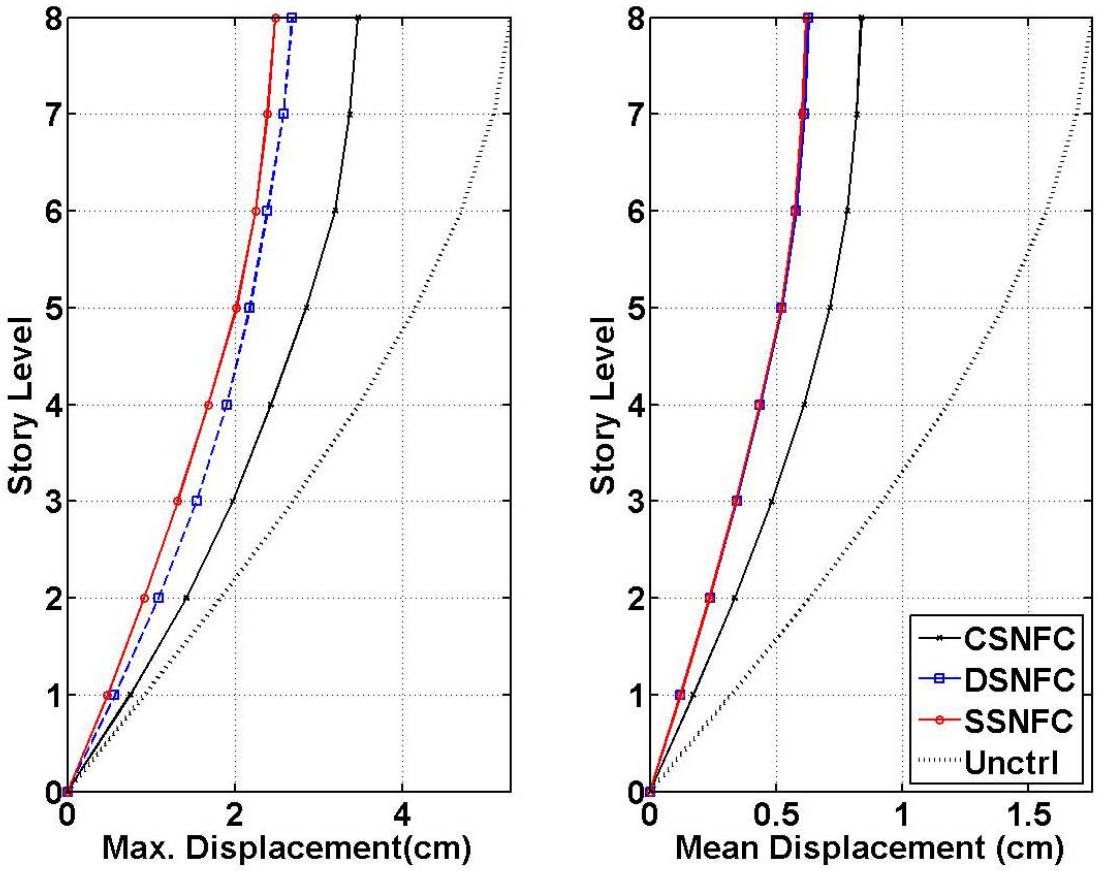

Fig. 6.20. Comparisons of maximum/mean displacement responses of an eight story shear type building structure equipped with two MR dampers controlled by a CSNFC, a DSNFC, and a SSNFC systems

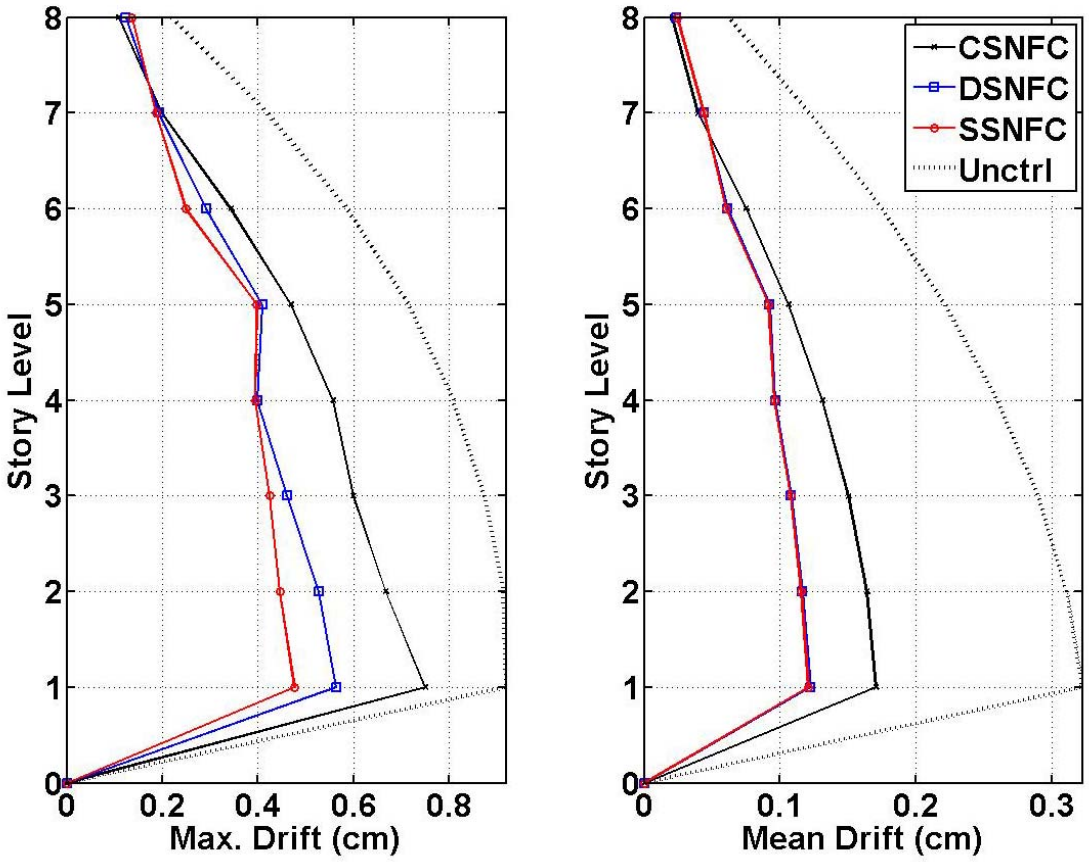

Fig. 6.21. Comparisons of maximum/mean drift responses of an eight story shear type building structure equipped with two MR dampers controlled by a CSNFC, a DSNFC, and a SSNFC systems

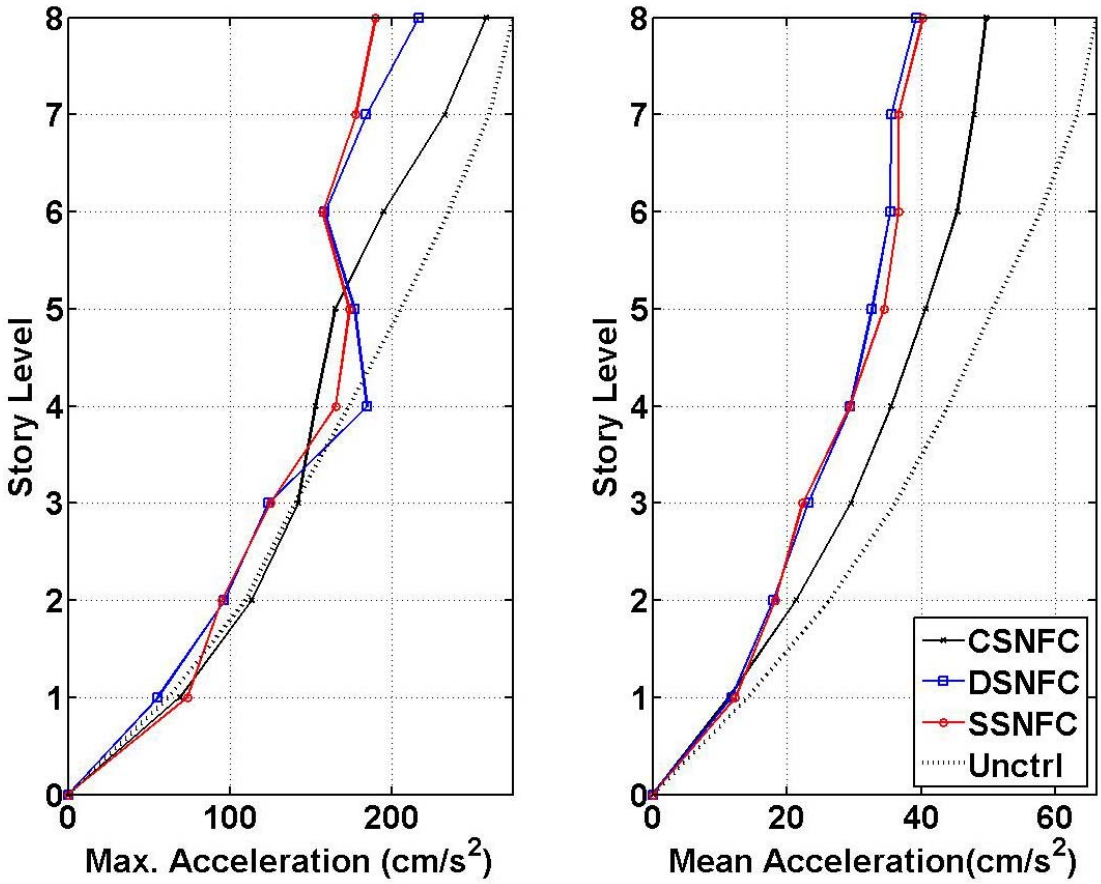

Fig. 6.22. Comparisons of maximum/mean acceleration responses of an eight story shear type building structure equipped with two MR dampers controlled by a CSNFC, a DSNFC, and a SSNFC systems

6.4 Concluding Remarks

In this section, a decentralized semiactive nonlinear fuzzy control (DSNFC) and a supervisory semiactive nonlinear fuzzy control (SSNFC) are proposed for vibration control of a seismically excited eight story building structure equipped with magnetorheological (MR) dampers in the multi-input-multi-output (MIMO) variable sense. The performance of the DSNFC and SSNFC systems were compared with that of the multi-input-single-output (MISO) semiactive nonlinear fuzzy control (SNFC) system, while uncontrolled responses are used as the baseline. It was from numerical examples demonstrated that both DSNFC and SSNFC systems are more effective than the MISO SNFC system (CSNFC) to control responses of the seismically excited building structure employing MR dampers. Furthermore, the performance of the DSNFC system is able to be improved by adding a supervisory controller into the DSNFC system, i.e., the SSNFC system is better than the DSNFC and CSNFC systems.

7. VERIFICATION EXAMPLE

7.1 Introduction

In this section, the effectiveness of the proposed autoregressive exogenous (ARX) inputs based Takagi-Sugeno (TS) fuzzy model and the semiactive nonlinear fuzzy control (SNFC) algorithm, discussed in previous sections, are further studied here for nonlinear control of seismically excited high-rise building structures. A benchmark full-scale building structure is selected as a target model that meets seismic code for Los Angeles, California region designed by Brandow & Johnston Associates for the SAC Phase 2 Steel Project (Spencer et al. 1999; Ohtori et al. 2004). The reason to choose the building structure as a target model is that it has been chosen as a benchmark building structure to compare the performance of structural control algorithms by many other researchers (Spencer et al. 1999; Lynch and Law 2002). To evaluate the effectiveness of the proposed control system with respect to earthquake, four real-recorded earthquake signals which are El Centro, Kobe, Northridge, and Hachinohe are used.

To implement semiactive control systems, a modified clipped algorithm and a Bingham model-based inverse MR damper approach are considered here. In addition, the performance of the proposed SNFC system is compared with that of a linear quadratic Gaussian (LQG)-based semiactive control system. In what follows, a finite element model for the Los Angeles 20 story building structure is discussed first.

7.2 Los Angeles 20 Story Building Model

As a full-scale 20 story building structure in Fig. 7.1 is a moment-resisting frame (MRF), the dimension is 30.48 m (100 ft) by 36.58 m (120 ft) in plane and 80.77 m (265 ft) in height. It has five bays in the north-south (N-S) direction while six bays in the east-west (E-W) direction. The dimension of the bay is 6.10 m (20 ft) on center in both N-S and E-W directions. The floor-to-floor height measured from center of beam to center of beam is 3.96 m (13 ft).

The seismic mass of the structure is: the first floor is 5.32×10^5 kg ($36.4\,\text{kips-sec}^2/\text{ft}$); the second floor is 5.65×10^5 kg ($38.7\,\text{kips-sec}^2/\text{ft}$); the third floor to the 20^{th} floor is 5.51×10^5 kg ($37.7\,\text{kips-sec}^2/\text{ft}$); and the roof level is 5.83×10^5 kg ($39.9\,\text{kips-sec}^2/\text{ft}$). The total seismic mass of the entire structure is 1.16×10^7 kg ($794\,\text{kips-sec}^2/\text{ft}$). However, it is modeled using a plane frame element that contains two nodes in which each node has three degrees-of-freedom (DOFs), i.e., it is an in-plane finite element model of N-S MRF. Therefore, the seismic mass of the structure is modified: the first floor is 2.66×10^5 kg ($18.2\,\text{kips-sec}^2/\text{ft}$); the second floor is 2.83×10^5 kg ($19.4\,\text{kips-sec}^2/\text{ft}$); the third floor to the 20^{th} floor is 2.76×10^5 kg ($18.9\,\text{kips-sec}^2/\text{ft}$); and the roof level is 2.92×10^5 kg ($20.0\,\text{kips-sec}^2/\text{ft}$).

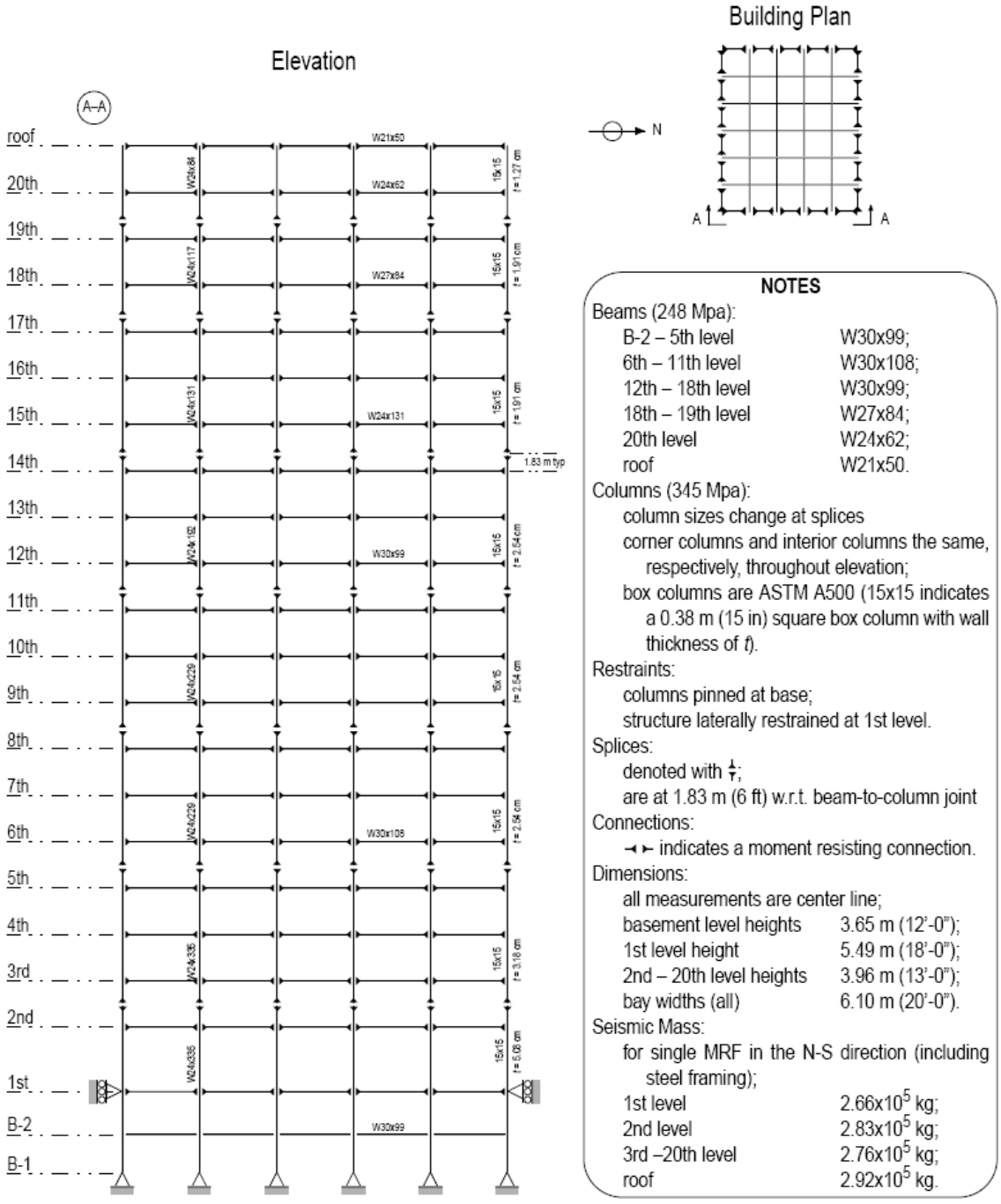

Fig. 7.1. Los Angeles 20 story building structure (Spencer et al. 1999)

Each node of the plane frame element includes horizontal, vertical, and rotational DOFs. The total number of nodes and elements is 180 and 284, respectively. The total DOFs is 540 DOFs before boundary conditions and subsequent model reduction are applied. The boundary constrained DOFs at the horizontal direction are nodes of 1, 2, 3, 4, 5, 6, 13 and 18 and the vertical constrained DOFs are 1, 2, 3, 4, 5 and 6 (see Fig. 7.2). Then, the total DOFs are reduced to 526. However, more DOFs can be reduced because the floor slab in each horizontal plane is assumed to be rigid, i.e., each floor has the same horizontal displacements. Using a Ritz transformation (Craig 1981), the total DOFs are reduced to 418. However, this finite element model with 418 DOFs is too large to analyze/design a control system design. Therefore, the 418 DOF analysis model is reduced to a 106 DOF model using Guyan reduction (Craig 1981) of all the rotational and almost all vertical DOFs. Based on modal damping, the damping matrix is defined using the reduced 106 DOF model: the maximum value of a critical damping is 10 % and the damping in the first mode is assumed to be 2 %. The first ten eigen frequencies of the benchmark building are: 0.29, 0.83, 1.43, 2.01, 2.64, 3.08, 3.30, 3.53, 3.99 and 4.74 Hz. The associated mode shapes are given in Fig. 7.3. In what follows, evaluation criteria for the performance evaluation of the LA 20 story building structure are addressed.

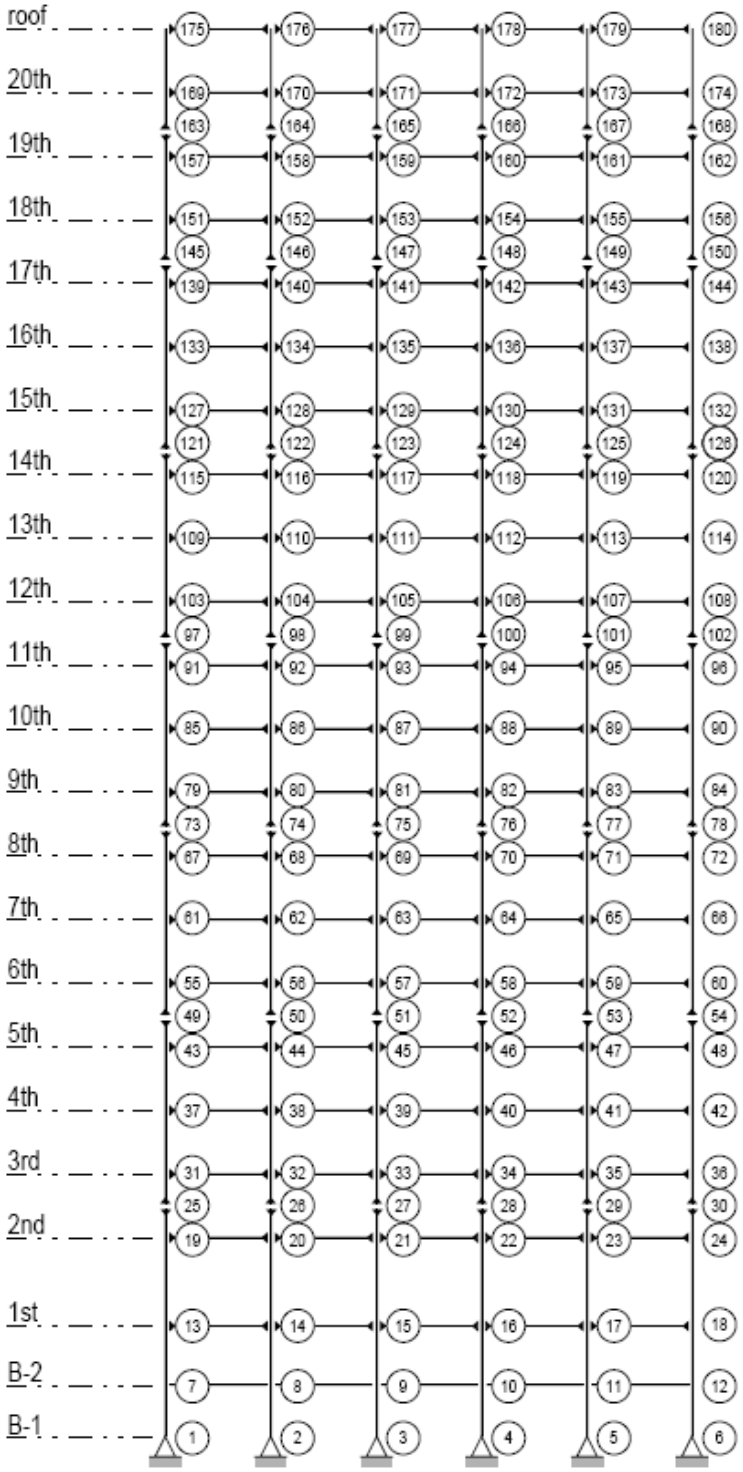

Fig. 7.2. Node numbers of an in-plane FEM for the LA 20 story building (Spencer et al. 1999)

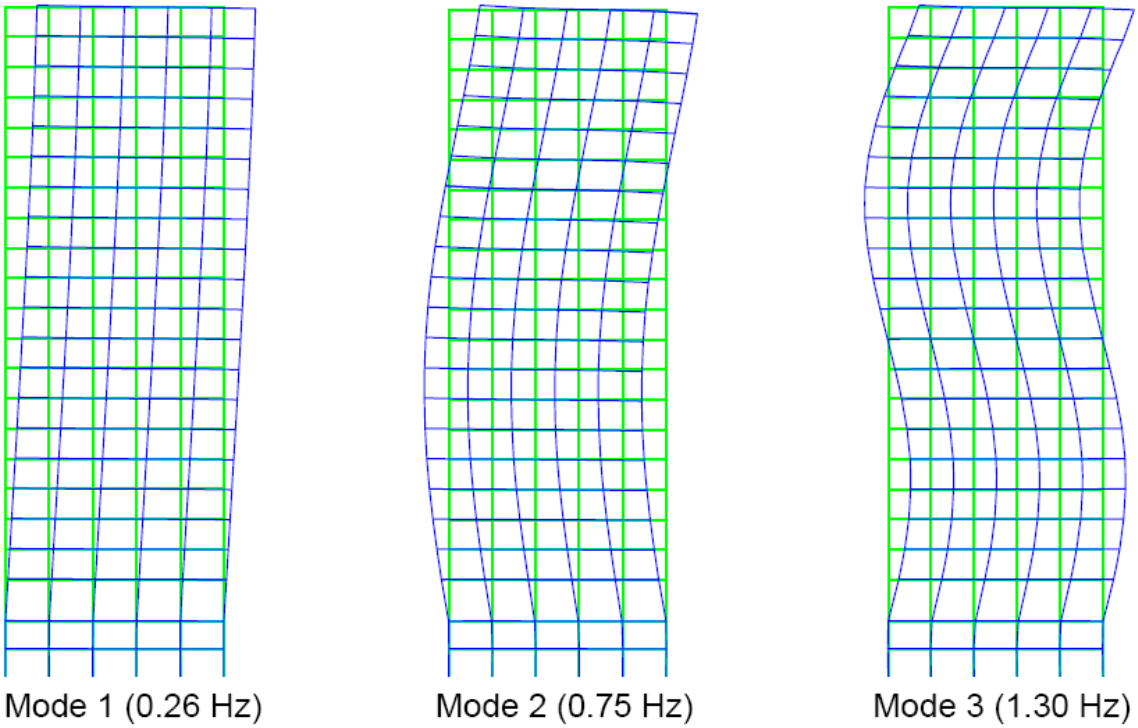

Fig. 7.3. First three mode shapes of the LA 20 story building structure (Spencer et al. 1999)

7.3 Evaluation Criteria

To evaluate the effectiveness of the proposed design methodology, four earthquake records are selected as disturbance signals: El Centro, Hachinohe, Northridge, and Kobe. In addition, several evaluation criteria, e.g., building responses such as displacement, acceleration, and drift, etc. are used.

A non-dimensional measure of the horizontal displacement relative to the ground level is given as the first evaluation factor

$$J_1 = \max_{\substack{\text{El Centro}\\ \text{Kobe}\\ \text{Hachinohe}\\ \text{Northridge}}} \left\{ \frac{\max\limits_{\substack{t\\ i\in\boldsymbol{\eta}}} \left| x_i(t) \right|}{x_{\mathrm{u}}^{\max}} \right\}, \tag{7.1}$$

where $\boldsymbol{\eta}$ represents the set of nodes that are associated with the horizontal displacements relative to the ground; $x_i(t)$ is the time history displacement of the i^{th} node; $x_{\mathrm{u}}^{\max}$ is the maximum value of the uncontrolled displacement responses; and $|\cdot|$ denotes absolute value.

The second evaluation factor is the drift ratio that represents a non-dimensional and normalized maximum drift with respect to the associated floor height

$$J_2 = \max_{\substack{\text{ElCentro}\\ \text{Kobe}\\ \text{Hachinohe}\\ \text{Northridge}}} \left\{ \frac{\max\limits_{t,i} \dfrac{\left|d_i(t)\right|}{h_i}}{d_{\mathrm{u}}^{\max}} \right\}, \tag{7.2}$$

where $d_i(t)$ is the interstory drift response; h_i is the height of the corresponding floors (h_1=5.49 m; h_i=3.96 m, i = 2,…,20); and $d_{\mathrm{u}}^{\max}$ is the maximum interstory drift ratio of the uncontrolled responses, i.e., $d_{\mathrm{u}}^{\max} = \max\limits_{i,t}\left\{d_i(t)/h_i\right\}$.

The third evaluation factor is the maximum acceleration

$$J_3 = \max_{\substack{\text{ElCentro}\\ \text{Kobe}\\ \text{Hachinohe}\\ \text{Northridge}}} \left\{ \frac{\max\limits_{\substack{t\\ i\in\boldsymbol{\eta}}} \left|\ddot{x}_i(t)\right|}{\ddot{x}_{\mathrm{u}}^{\max}} \right\}, \tag{7.3}$$

where $\ddot{x}_i(t)$ is the acceleration of the i^{th} node; $\ddot{x}_{\mathrm{u}}^{\max}$ is the maximum acceleration level of the uncontrolled response.

The fourth evaluation criterion is given by a non-dimensional base shear force

$$J_4 = \max_{\substack{\text{ElCentro}\\ \text{Kobe}\\ \text{Hachinohe}\\ \text{Northridge}}} \left\{ \frac{\max\limits_{t} \left|\sum\limits_{i=1}^{20} m_i \ddot{x}_i(t)\right|}{F_{\mathrm{b}}^{\max}} \right\}, \tag{7.4}$$

where m_i is the seismic mass of each floor of a single N-S MRF for the LA 20 story building structure: $m_1 = 2.83 \times 10^5$ kg; $m_i = 2.76 \times 10^5$ kg, $i = 2,\ldots,19$; and $m_{20} = 2.92 \times 10^5$ kg. For each earthquake record, $F_{\mathrm{b}}^{\max}$ is the maximum value of the uncontrolled base shear force.

In addition to the maximum norm, the L_2-norm measures are also considered. The associated fifth evaluation factor is the non-dimensional norm value of the maximum displacement of the building structure

$$J_5 = \max_{\substack{\text{ElCentro}\\ \text{Kobe}\\ \text{Hachinohe}\\ \text{Northridge}}} \left\{ \frac{\max_{i \in \boldsymbol{\eta}} \left\| x_i(t) \right\|}{\left\| x_{\mathrm{u}}^{\max} \right\|} \right\}, \tag{7.5}$$

where $\left\| x_i(t) \right\| \equiv \sqrt{\int_0^{t_{\mathrm{f}}} x_i^2(t) dt}$, t_{f} is a sufficiently large time, and $\left\| x^{\max} \right\| \equiv \max_{i \in \boldsymbol{\eta}} \left\| x_i(t) \right\|$.

The sixth evaluation factor is the non-dimensional norm of the maximum drift ratio

$$J_6 = \max_{\substack{\text{ElCentro}\\ \text{Kobe}\\ \text{Hachinohe}\\ \text{Northridge}}} \left\{ \frac{\max_{t,i} \dfrac{\left\| d_i(t) \right\|}{h_i}}{\left\| d_{\mathrm{u}}^{\max} \right\|} \right\}. \tag{7.6}$$

The seventh evaluation factor is the non-dimensional norm of the maximum acceleration response

$$J_7 = \max_{\substack{\text{ElCentro}\\ \text{Kobe}\\ \text{Hachinohe}\\ \text{Northridge}}} \left\{ \frac{\max\limits_{t} \left\| \ddot{x}_i(t) \right\|_{i\in\boldsymbol{\eta}}}{\left\| \ddot{x}_{\mathrm{u}}^{\max} \right\|} \right\}. \tag{7.7}$$

The eight evaluation factor is the non-dimensional norm of the base shear force

$$J_8 = \max_{\substack{\text{ElCentro}\\ \text{Kobe}\\ \text{Hachinohe}\\ \text{Northridge}}} \left\{ \frac{\left\| \sum_{i=1}^{20} m_i \ddot{x}_i(t) \right\|}{\left\| F_{\mathrm{b}}^{\max} \right\|} \right\}. \tag{7.8}$$

In addition to the control performances, the efficiency of the proposed control system is considered. Therefore, the ninth evaluation factor is a maximum value of control force

$$J_9 = \max_{\substack{\text{ElCentro}\\ \text{Kobe}\\ \text{Hachinohe}\\ \text{Northridge}}} \left\{ \frac{\max\limits_{t,i} \left| f_i^{\mathrm{MR}}(t) \right|}{W} \right\}, \tag{7.9}$$

where $f_i^{\mathrm{MR}}(t)$ is the MR damper force generated by the i^{th} MR damper and W is the seismic weight of the N-S MRF, excluding the mass of the 1st level, i.e., $W = 54,377\,\mathrm{kN}$ $(12,225\,\mathrm{kips})$.

The tenth evaluation factor is a measure of control device displacements

$$J_{10} = \max_{\substack{\mathrm{El\,Centro}\\ \mathrm{Kobe}\\ \mathrm{Hachinohe}\\ \mathrm{Northridge}}} \left\{ \frac{\max_{t,i} \left| y_i^{\mathrm{c}}(t) \right|}{x^{\max}} \right\}, \tag{7.10}$$

where $y_i^t(t)$ is the displacement of the i^{th} MR damper device.

The eleventh evaluation factor measures the maximum value of power resource required for vibration control

$$J_{11} = \max_{\substack{\mathrm{El\,Centro}\\ \mathrm{Kobe}\\ \mathrm{Hachinohe}\\ \mathrm{Northridge}}} \left\{ \frac{\max_{t} \left[\sum_i P_i(t) \right]}{\dot{x}^{\max} W} \right\}, \tag{7.11}$$

where $P_i(t)$ is the power that needs to operate the i^{th} MR damper device; $\dot{x}^{\max}$ is the maximum value of the uncontrolled relative velocity responses of the floor that the MR damper is installed.

The twelve evaluation factor is the total power to be used for vibration control.

$$J_{12} = \max_{\substack{\text{El Centro}\\ \text{Kobe}\\ \text{Hachinohe}\\ \text{Northridge}}} \left\{ \frac{\max_t \left\| \sum_i P_i(t) \right\|}{x^{\max} W} \right\}. \tag{7.12}$$

The thirteen evaluation factor is the number of control devices that are used

$$J_{13} = \text{number of control devices required.} \tag{7.13}$$

The fourteen evaluation factor is the number of sensors to implement the proposed control system

$$J_{14} = \text{number of sensors required.} \tag{7.14}$$

The final evaluation factor measures computational resources to implement the proposed control algorithm

$$J_{15} = \dim(\mathbf{x}_f), \tag{7.15}$$

where $\mathbf{x}_f$ is the state/output vector to be feedback to the proposed controller. In summary, these evaluation criteria are used for the performance evaluation of the

proposed SNFC system, following nonlinear system identification of the LA 20 story building structure equipped with MR dampers.

7.4 Nonlinear System Identification

In this section, a multiple ARX inputs model-based TS fuzzy model is applied to a set of input and output data that is generated from the 20 story building structure equipped with MR dampers. The multiple ARX model-based TS fuzzy model has two inputs and two outputs, i.e., two input signals, a disturbance and a control signal are applied to the LA 20 story building structure to generate two output data. Artificial earthquake (AEQ) ground accelerations, discussed in Section 3, are employed as the disturbance input signals. MR damper forces are used for control force signals. On the other hand, arbitrary output signals can be selected. In this research, the acceleration and drift at each floor are selected as output signals. Relative drift and acceleration responses at the 4^{th}, 8^{th}, 12^{th}, 16^{th}, and 20^{th} floors are identified to demonstrate the effectiveness of the proposed nonlinear multiple ARX-TS fuzzy model.

Fig. 7.4 depicts the comparison between the 4^{th} floor drift responses obtained by implementing the MR damper in the building structure and the response of the nonlinear identified model; Fig. 7.5 depicts the comparison between the 4^{th} acceleration responses obtained by implementing the MR damper in the building structure and the response of the nonlinear identified model. As can be seen, good agreement between the original values and the identified model is found in both drift and acceleration responses.

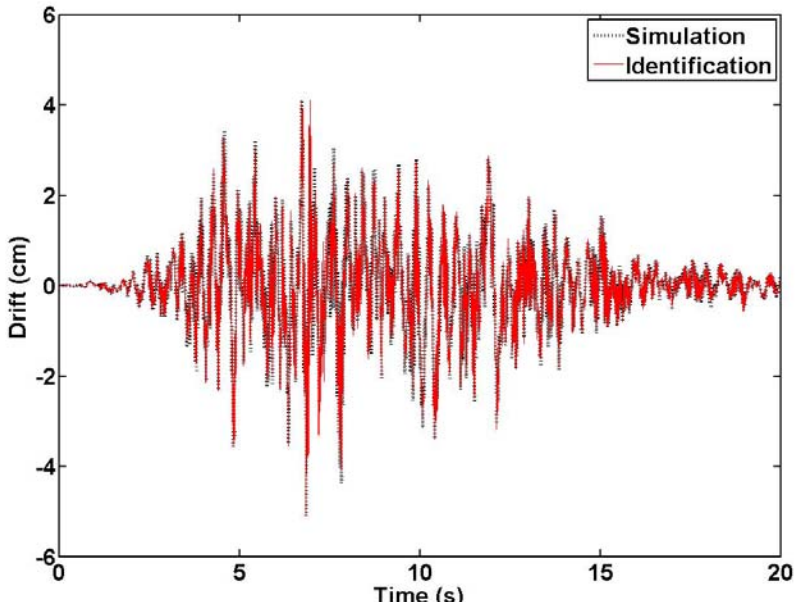

Fig. 7.4. Comparison of the 4th floor drift relative to the 3rd floor of the original responses with the responses using the nonlinear ARX-TS fuzzy model

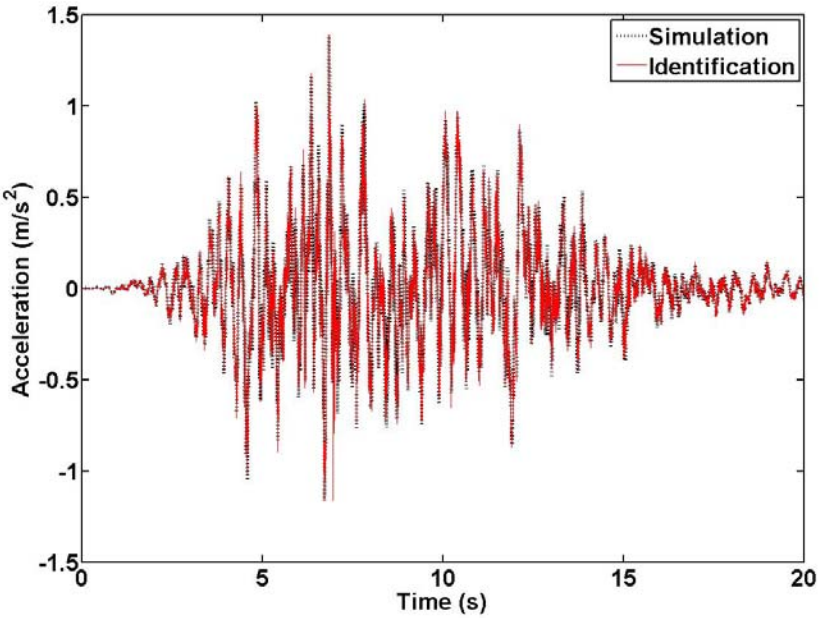

Fig. 7.5. Comparison of the 4th floor acceleration of the original responses with the responses using the nonlinear ARX-TS fuzzy model

Fig. 7.6 depicts the comparison between the 8th floor drift responses obtained by implementing the MR damper in the building structure and the response of the nonlinear identified model; Fig. 7.7 depicts the comparison between the 8th acceleration responses obtained by implementing the MR damper in the building structure and the response of the nonlinear identified model. As can be seen, good agreement between the original values and the identified model is found in both drift and acceleration responses.

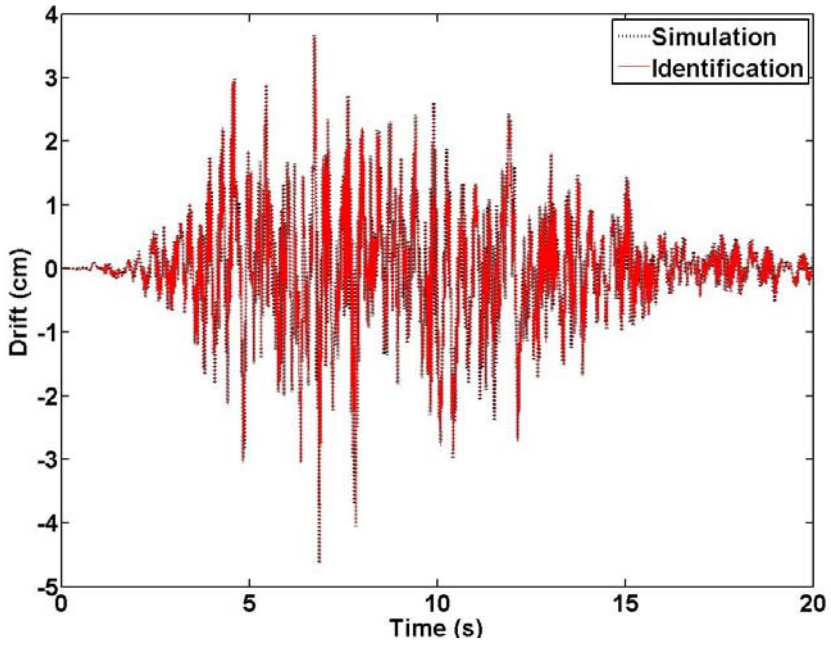

Fig. 7.6. Comparison of the 8th floor drift relative to the 7th floor of the original responses with the responses using the nonlinear ARX-TS fuzzy model

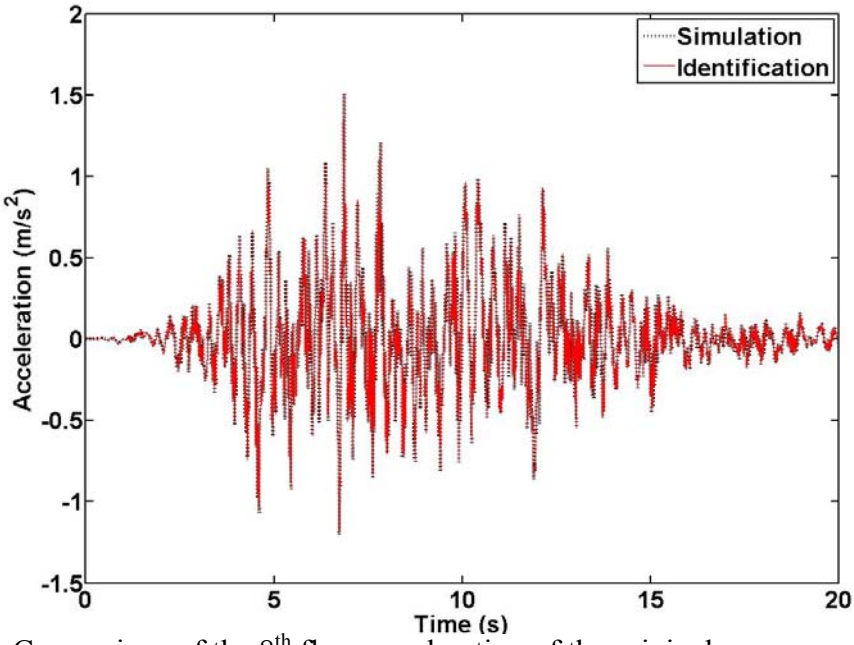

Fig. 7.7. Comparison of the 8th floor acceleration of the original responses with the responses using the nonlinear ARX-TS fuzzy model

Fig. 7.8 depicts the comparison between the 12th floor drift responses obtained by implementing the MR damper in the building structure and the response of the nonlinear identified model; Fig. 7.9 depicts the comparison between the 12th acceleration responses obtained by implementing the MR damper in the building structure and the response of the nonlinear identified model. As can be seen, good agreement between the original values and the identified model is found in both drift and acceleration responses.

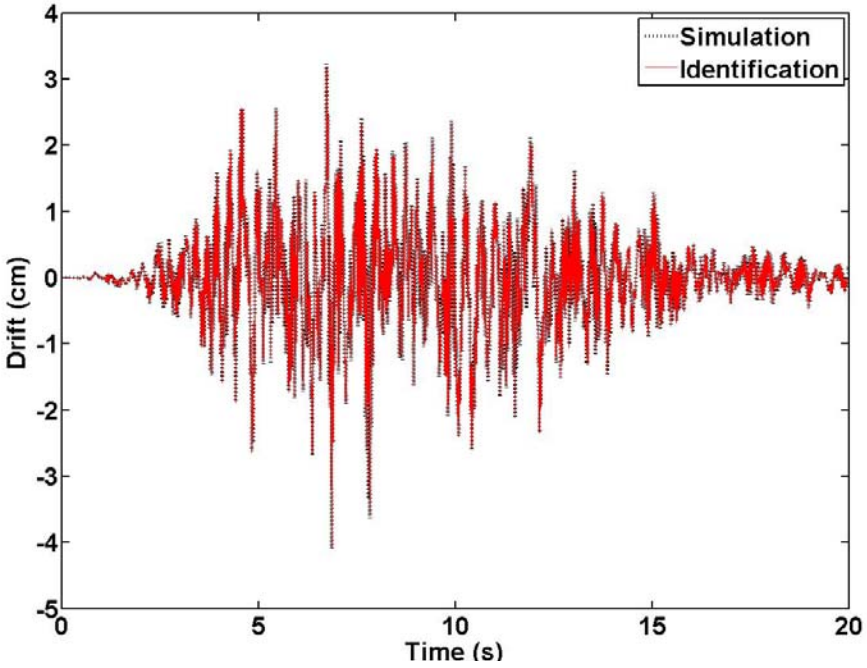

Fig. 7.8. Comparison of the 12th floor drift relative to the 11th floor of the original responses with the responses using the nonlinear ARX-TS fuzzy model

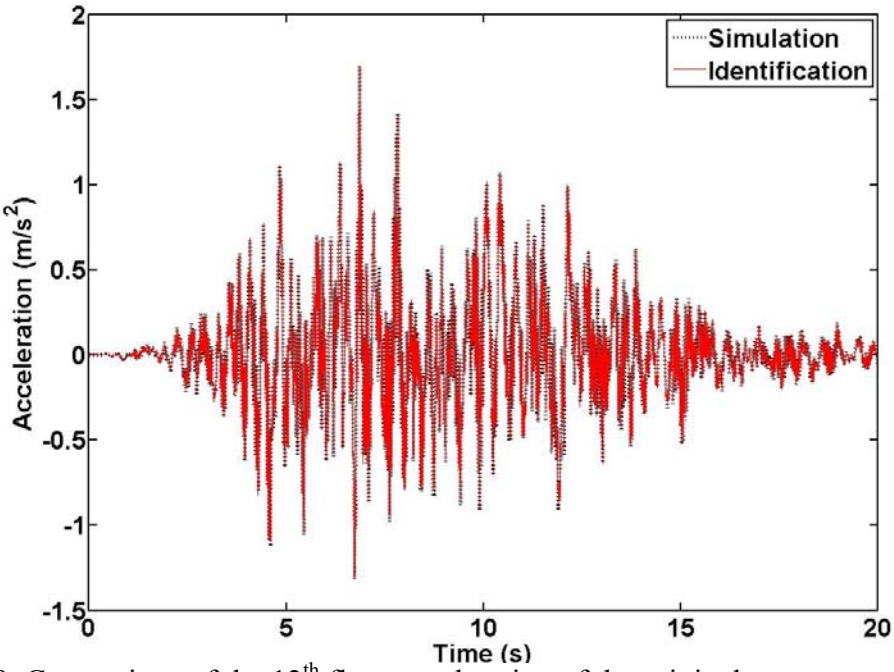

Fig. 7.9. Comparison of the 12th floor acceleration of the original responses with the responses using the nonlinear ARX-TS fuzzy model

Fig. 7.10 depicts the comparison between the 16th floor drift responses obtained by implementing the MR damper in the building structure and the response of the nonlinear identified model; Fig. 7.11 depicts the comparison between the 16th acceleration responses obtained by implementing the MR damper in the building structure and the response of the nonlinear identified model. As can be seen, good agreement between the original values and the identified model is found in both drift and acceleration responses.

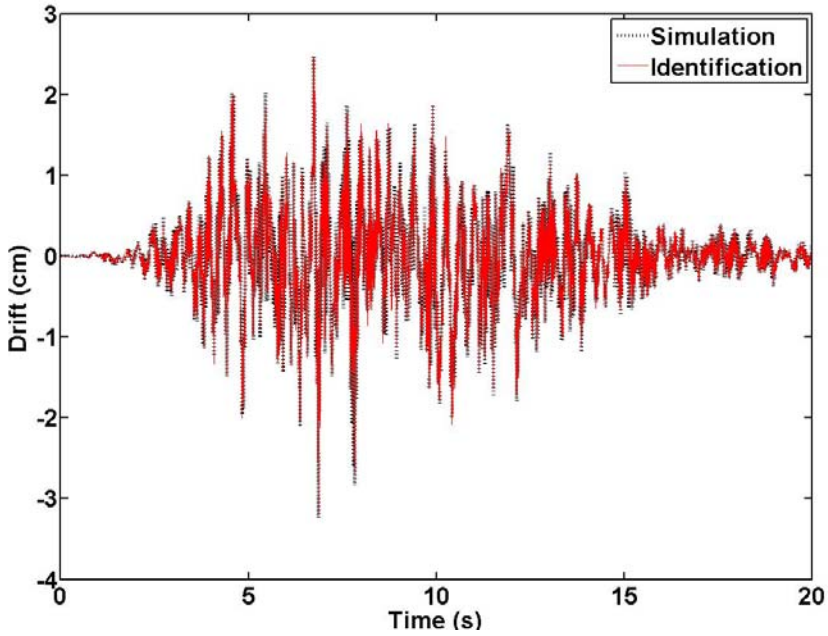

Fig. 7.10. Comparison of the 16th floor drift relative to the 15th floor of the original responses with the responses using the nonlinear ARX-TS fuzzy model

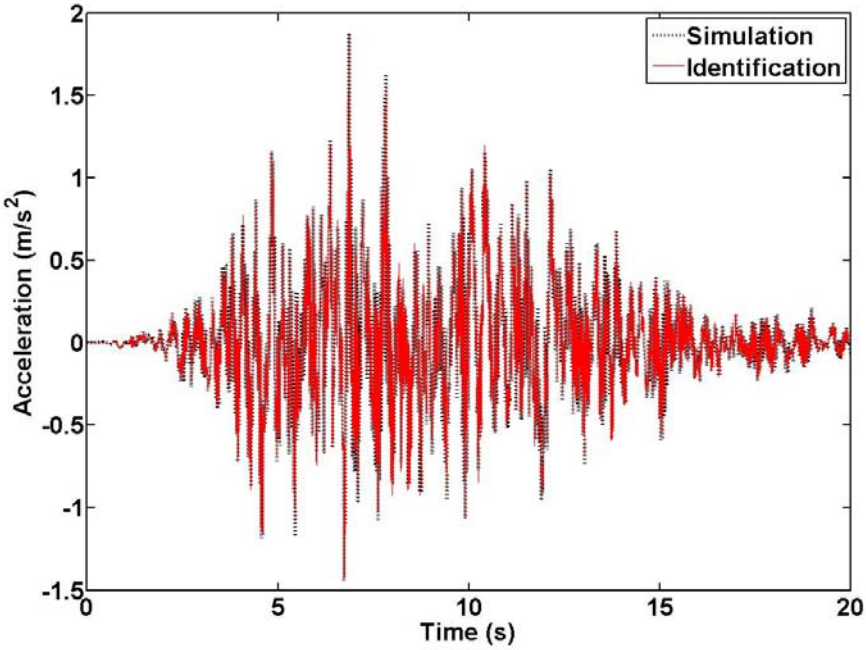

Fig. 7.11. Comparison of the 16th floor acceleration (bottom) of the original responses with the responses using the nonlinear ARX-TS fuzzy model

Fig. 7.12 depicts the comparison between the 20th floor drift responses obtained by implementing the MR damper in the building structure and the response of the nonlinear identified model; Fig. 7.13 depicts the comparison between the 20th acceleration responses obtained by implementing the MR damper in the building structure and the response of the nonlinear identified model. As can be seen, good agreement between the original values and the identified model is found in both drift and acceleration responses. The identified models are used for MIMO semiactive nonlinear fuzzy control system design via decentralized control concepts.

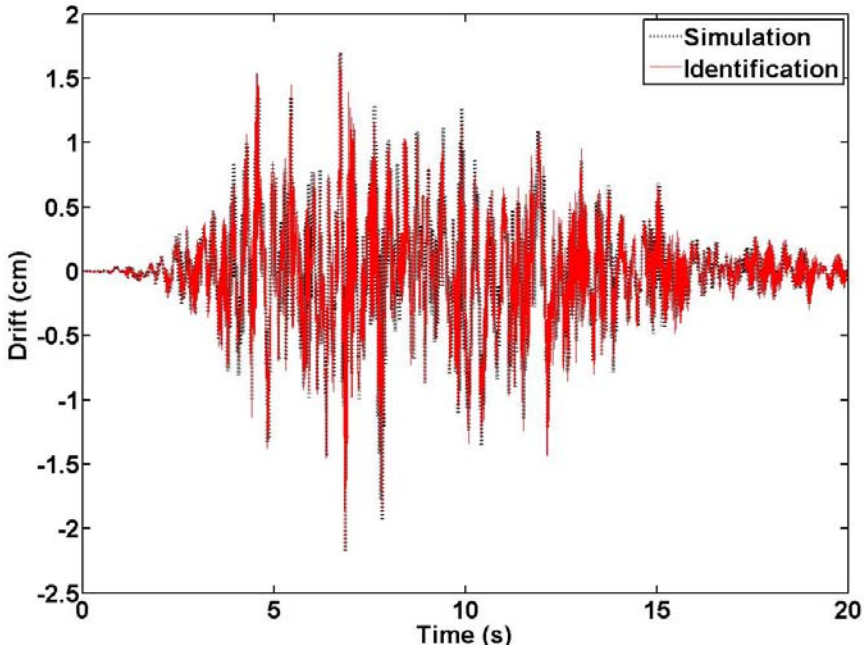

Fig. 7.12. Comparison of the 20th floor drift relative to the 19th floor of the original responses with the responses using the nonlinear ARX-TS fuzzy model

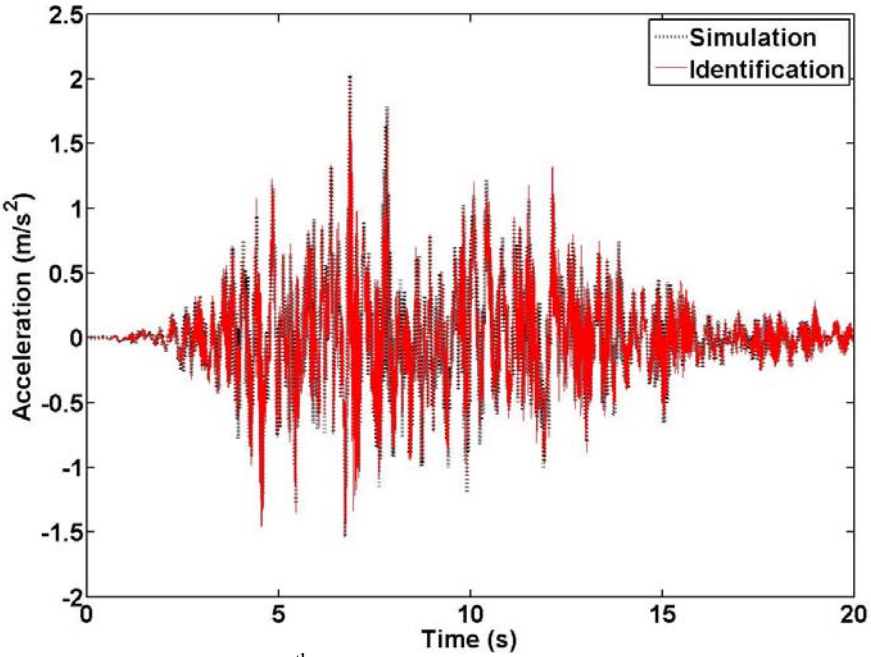

Fig. 7.13. Comparison of the 20th floor acceleration (bottom) of the original responses with the responses using the nonlinear ARX-TS fuzzy model

7.5 Semiactive Nonlinear Fuzzy Control System Design

In this section, a multi-input-multi-output semiactive nonlinear fuzzy controller is designed for vibration control of a seismically excited LA 20 story building structure equipped with MR dampers using the decentralized control concept. Fig. 7.14 is a schematic configuration of the LA 20 story building that MR dampers are installed. Three MR dampers are located on the first eight stories and two devices are installed on the next twelve stories. The total number of MR dampers is forty eight. The locations of MR dampers within the building structure are determined through many trial-and-error simulations. To convert active control systems into semiactive control ones, two different strategies are considered in this research. They include a modified clipped algorithm and a Bingham model-based inverse MR damper approach.

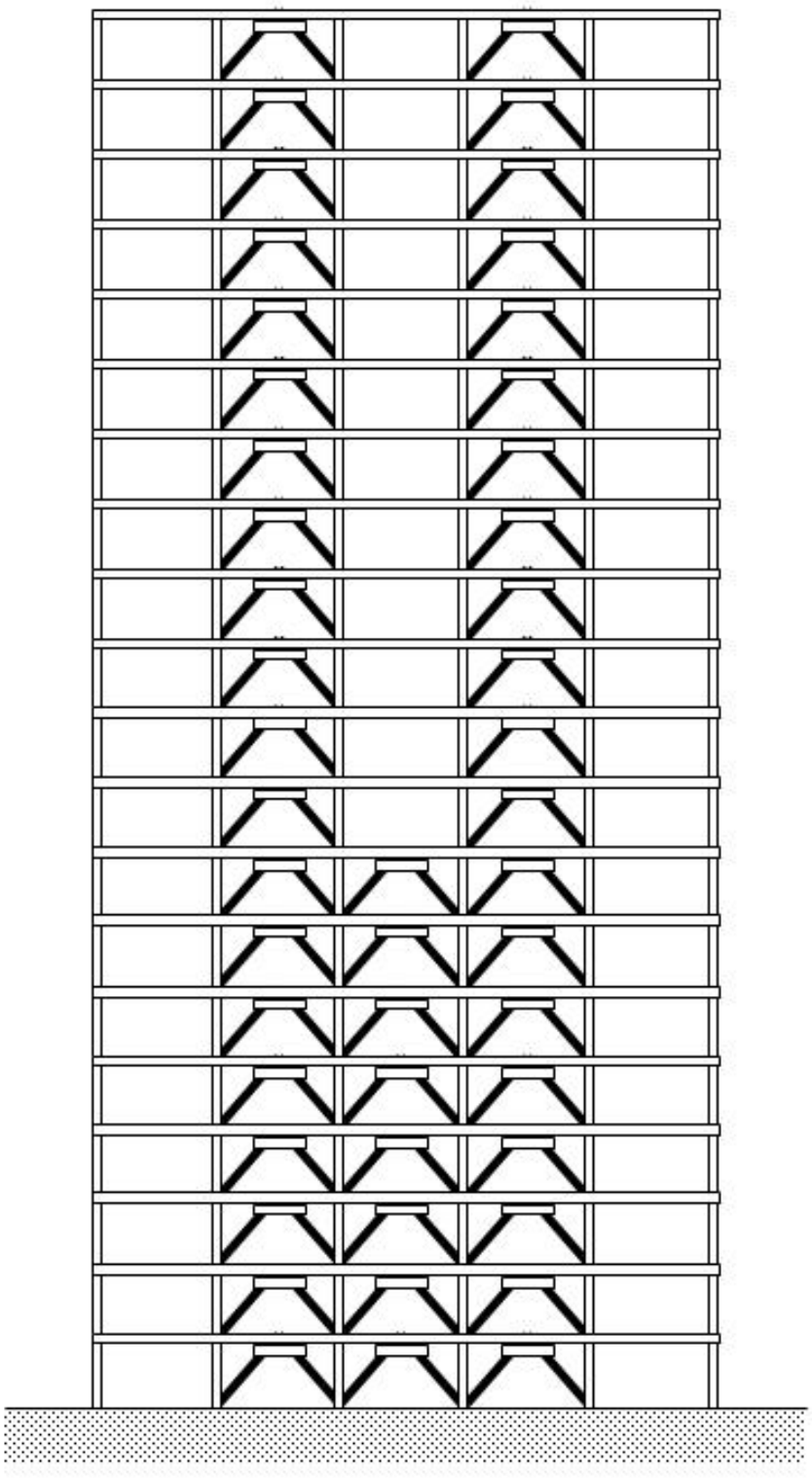

Fig. 7.14. Los Angeles 20 story building structure equipped with MR dampers

Fig. 7.15 and Fig. 7.16 compare the performance of the SNFC system employing the modified clipped algorithm with that of the SNFC system using the inverse Bingham MR damper model. Both near-and far-field earthquake records are considered, i.e., Kobe and El Centro earthquakes. The simulation results show that the inverse model approach is better than the modified clipped algorithm approach. Therefore, the inverse MR damper model approach is used to implement a SNFC system for the Los Angeles 20 story building structure.

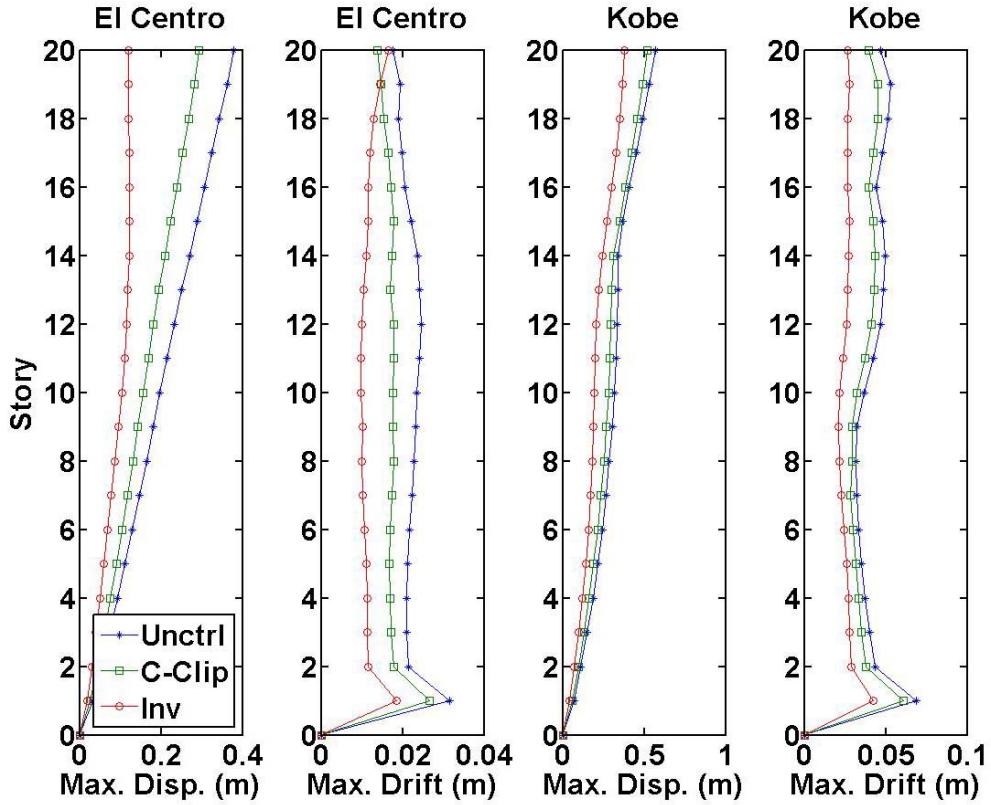

Fig. 7.15. Maximum interstory displacement responses of an uncontrolled, a SNFC systems using a modified clipped algorithm, and a SNFC system using an inverse MR damper model of a Los Angeles 20 story building excited by far- and near-field earthquakes

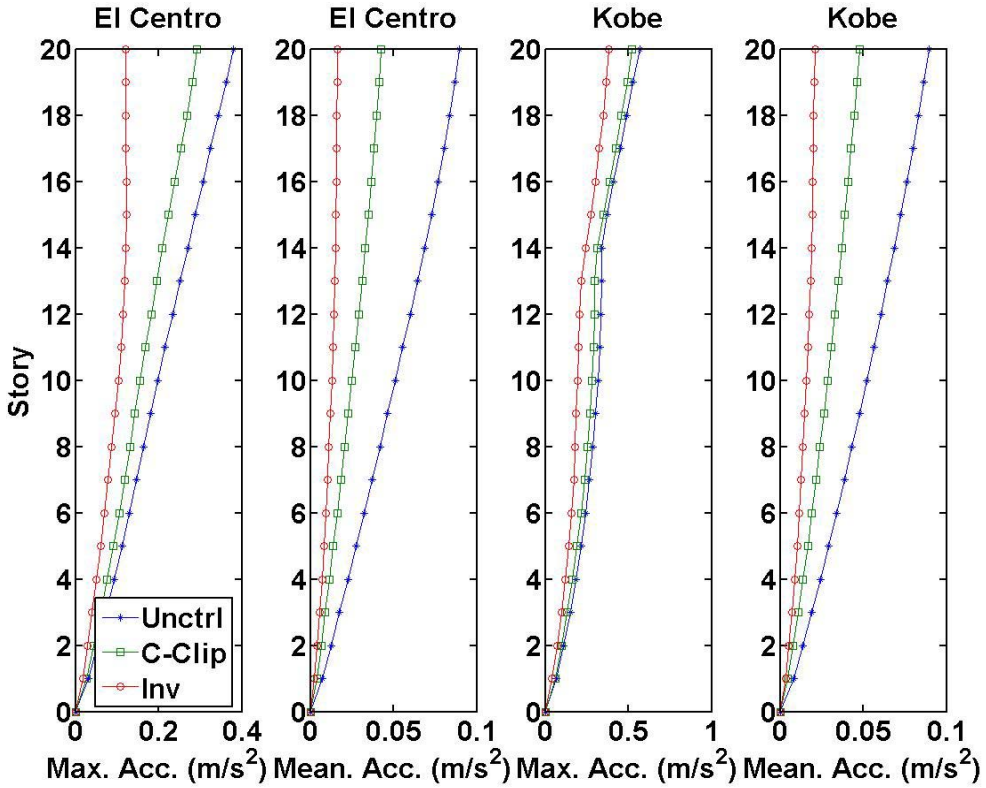

Fig. 7.16. Maximum Interstory acceleration responses of an uncontrolled, a SNFC systems using a modified clipped algorithm, and a SNFC system using an inverse MR damper model of a Los Angeles 20 story building excited by far- and near-field earthquakes

In addition, a traditional linear control, LQG-based controller is designed and the performance of the LQG controller is compared with the new proposed SNFC system. Four earthquake inputs are applied as a ground motion shown in Fig. 7.17. The time history responses that are controlled by the SNFC system at the 1st, 4th, 8th, 12th, 16th, and 20th floors are compared with the performance of the LQG controller, while the uncontrolled system response is used as the baseline. The parameters of the linear quadratic regulator (LQR) and the Kalman filter are adopted from Spencer et al. (1999): As R is a diagonal matrix, it has a 4 in the (1,1) position and ones in the remaining positions; Q is $3\times10^{-3}\left[\mathbf{I}\right]$; it is assumed that the measurement noises are identically distributed, statistically independent Gaussian white noise processes; and $S_{\ddot{x}_g\ddot{x}_g}/S_{v_iv_i}=25$.

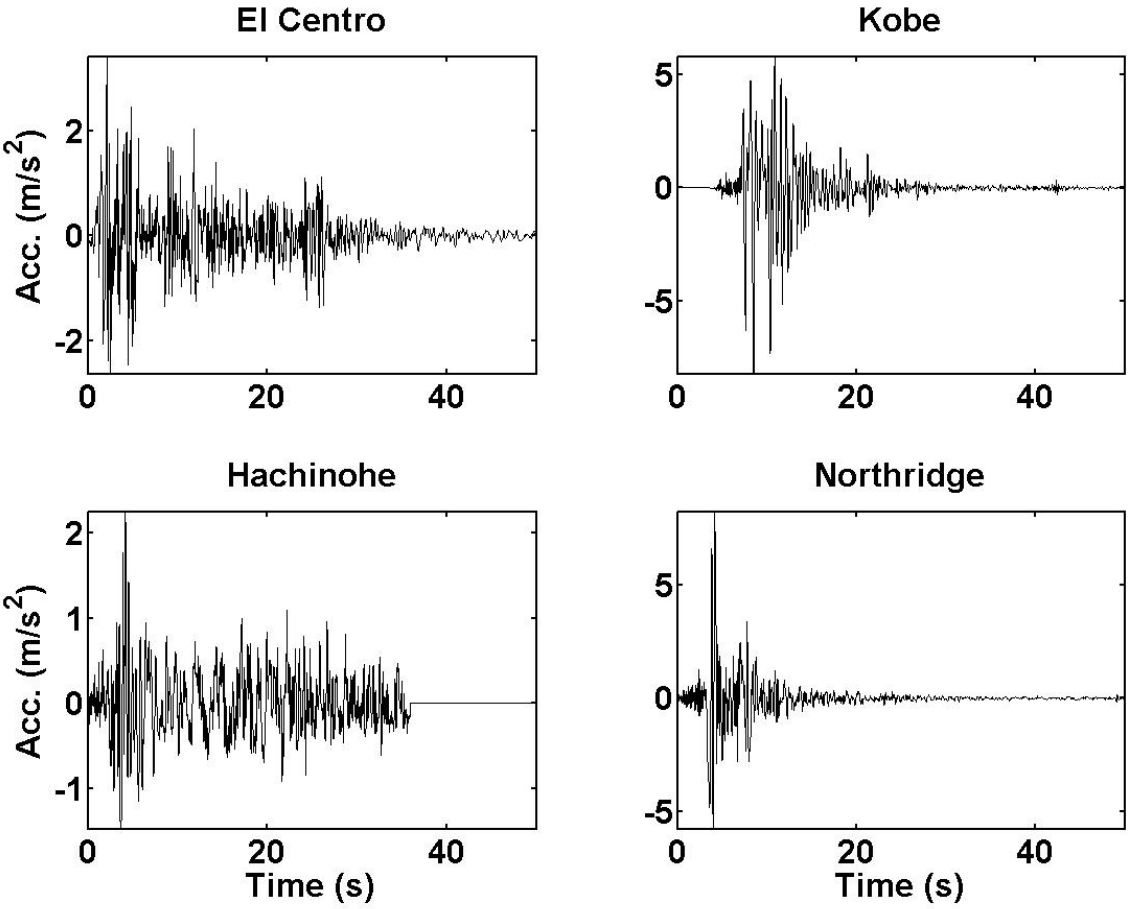

Fig. 7.17. Time histories of the far- and near-field earthquake signals

Fig. 7.18 compares uncontrolled, a LQG controlled, and a SNFC controlled time history displacement responses of the Los Angeles 20 story building subjected to El Centro earthquake. According to the time history responses, responses are dramatically reduced when either a LQG or a SNFC system is applied. In particular, the SNFC system has the better performance than the LQG control system in terms of time history displacement responses.

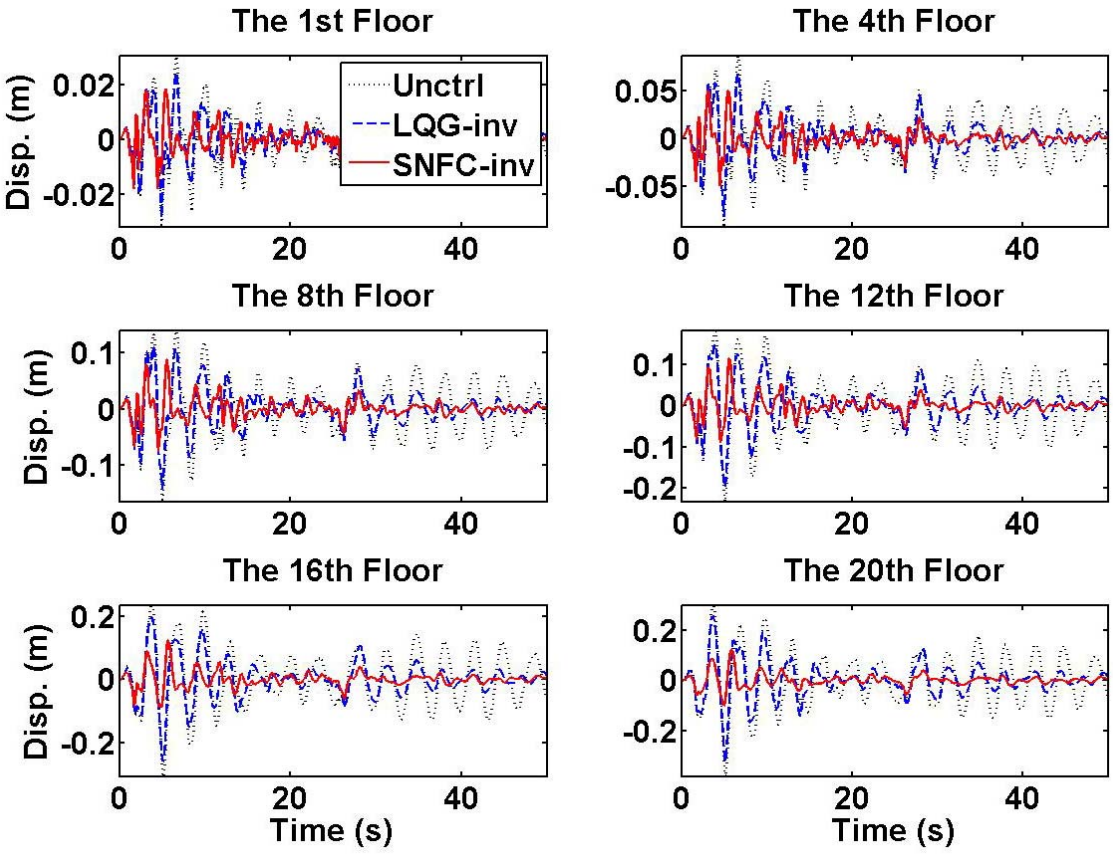

Fig. 7.18. Time history displacement responses of an uncontrolled, a LQG control, and a SNFC systems of a Los Angeles 20 story building excited by El Centro earthquake

Fig. 7.19 compares uncontrolled, a LQG controlled, and a SNFC controlled time history displacement responses of the Los Angeles 20 story building subjected to Kobe earthquake. According to the time history responses, responses are dramatically reduced when either a LQG or a SNFC system is applied. In particular, the SNFC system has the better performance than the LQG control system in terms of time history displacement responses.

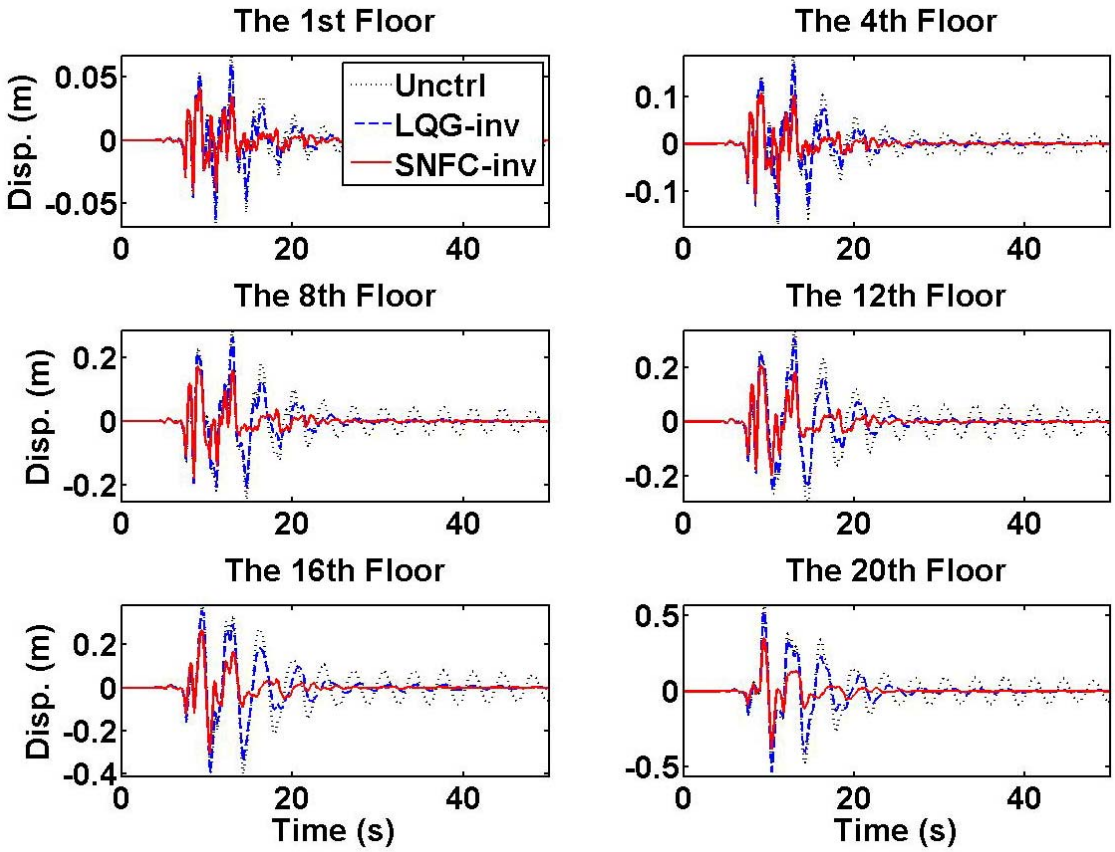

Fig. 7.19. Time history displacement responses of an uncontrolled, a LQG control, and a SNFC systems of a Los Angeles 20 story building excited by Kobe earthquake

Fig. 7.20 compares uncontrolled, a LQG controlled, and a SNFC controlled time history displacement responses of the Los Angeles 20 story building subjected to Hachinohe earthquake. According to the time history responses, responses are dramatically reduced when either a LQG or a SNFC system is applied. In particular, the SNFC system has the better performance than the LQG control system in terms of time history displacement responses.

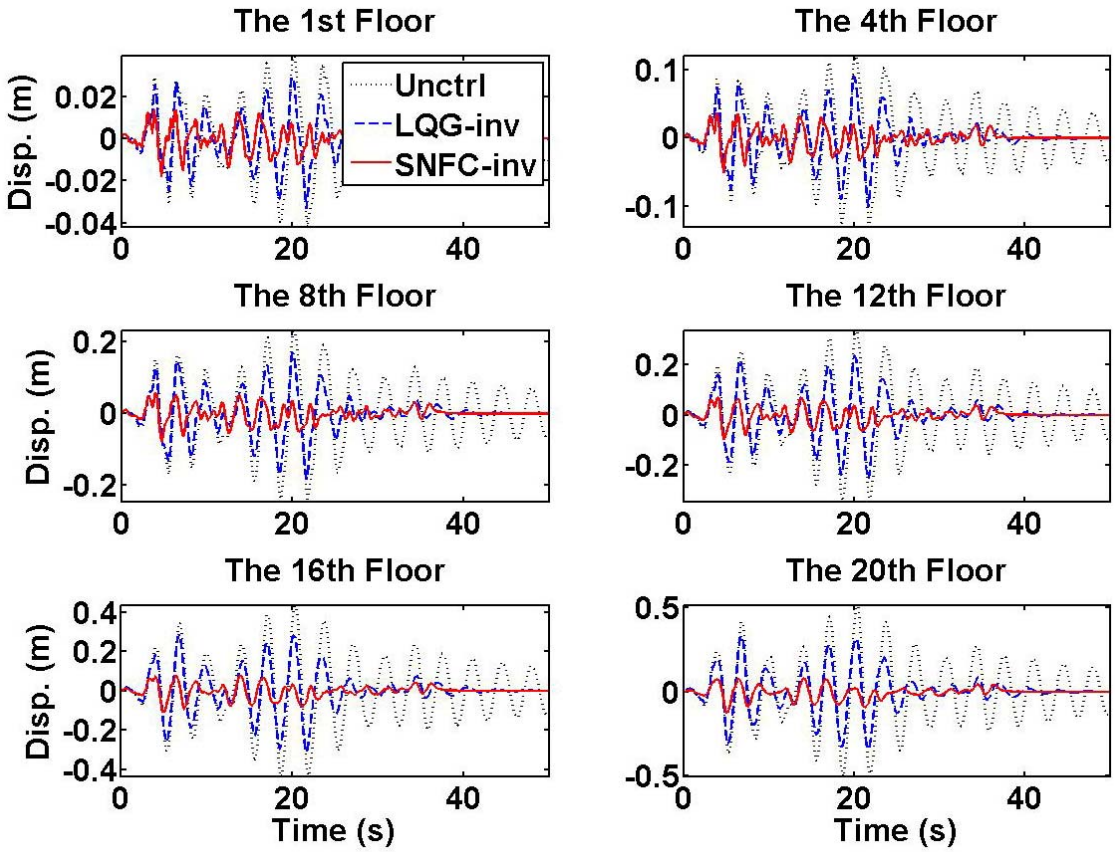

Fig. 7.20. Time history displacement responses of an uncontrolled, a LQG control, and a SNFC systems of a Los Angeles 20 story building excited by Hachinohe earthquake

Fig. 7.21 compares uncontrolled, a LQG controlled, and a SNFC controlled time history displacement responses of the Los Angeles 20 story building subjected to Northridge earthquake. According to the time history responses, responses are dramatically reduced when either a LQG or a SNFC system is applied. In particular, the SNFC system has the better performance than the LQG control system in terms of time history displacement responses.

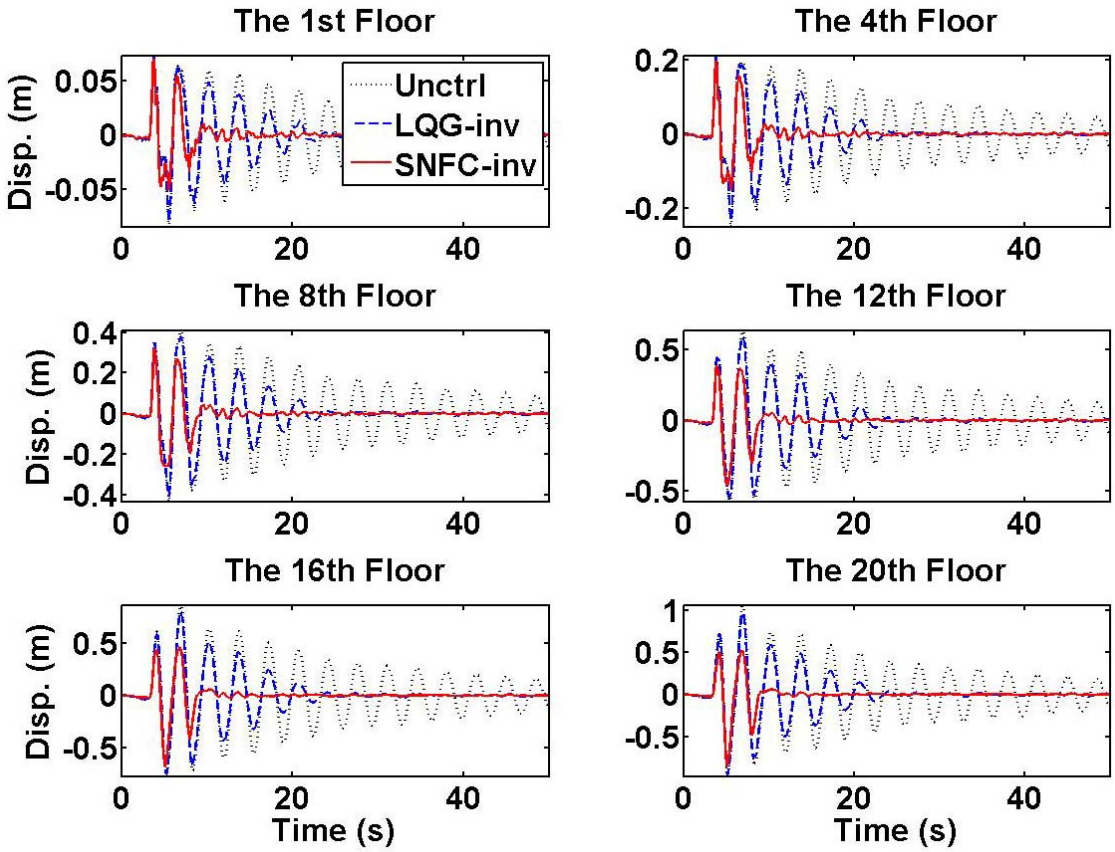

Fig. 7.21. Time history displacement responses of an uncontrolled, a LQG control, and a SNFC systems of a Los Angeles 20 story building excited by Northridge earthquake

Fig. 7.22 compares maximum interstory displacement responses of the uncontrolled, the LQG controlled and the SNFC controlled systems, respectively. In almost all the responses, the performance of the SNFC system is better than that of the LQG controller.

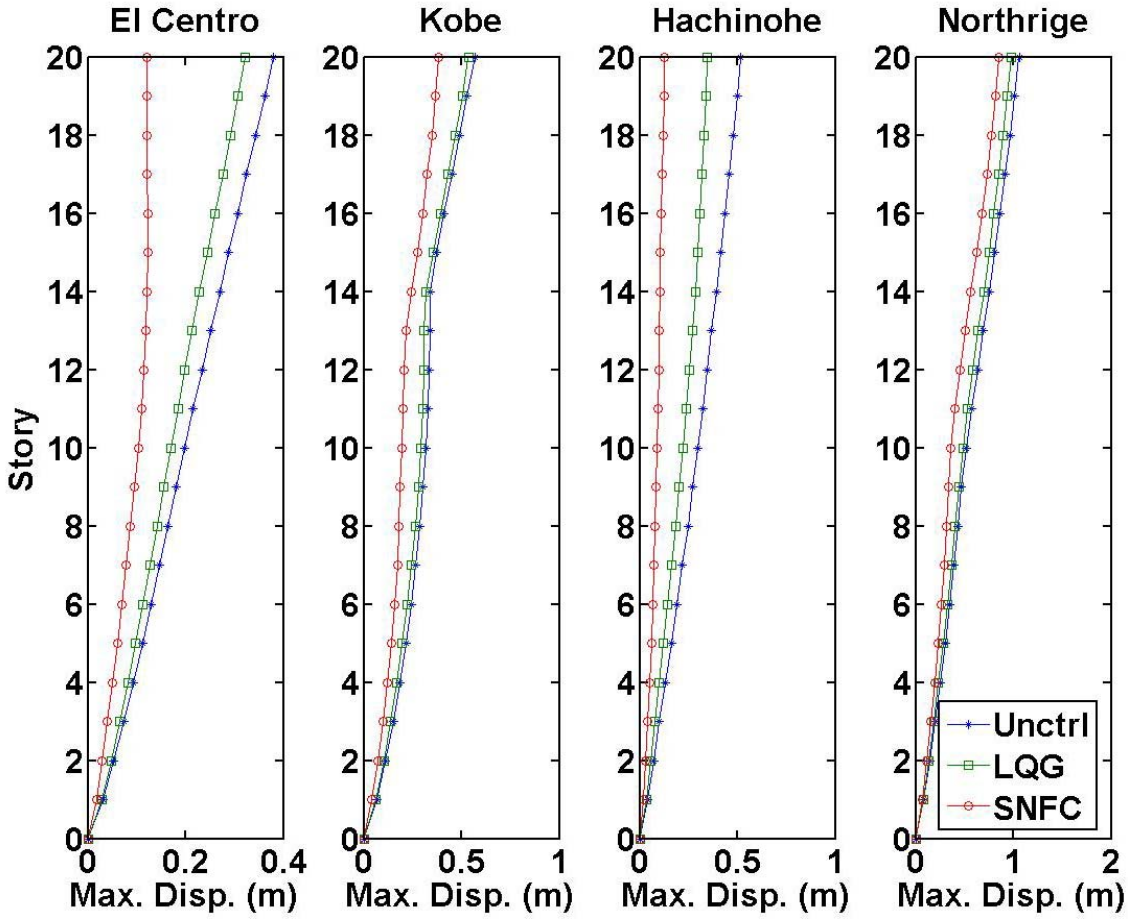

Fig. 7.22. Interstory displacement responses of an uncontrolled, a LQG control, and a SNFC systems

Fig. 7.23 compares maximum interstory drift responses of the uncontrolled, the LQG controlled and the SNFC controlled systems, respectively. In almost all the responses, the performance of the SNFC system is better than that of the LQG controller.

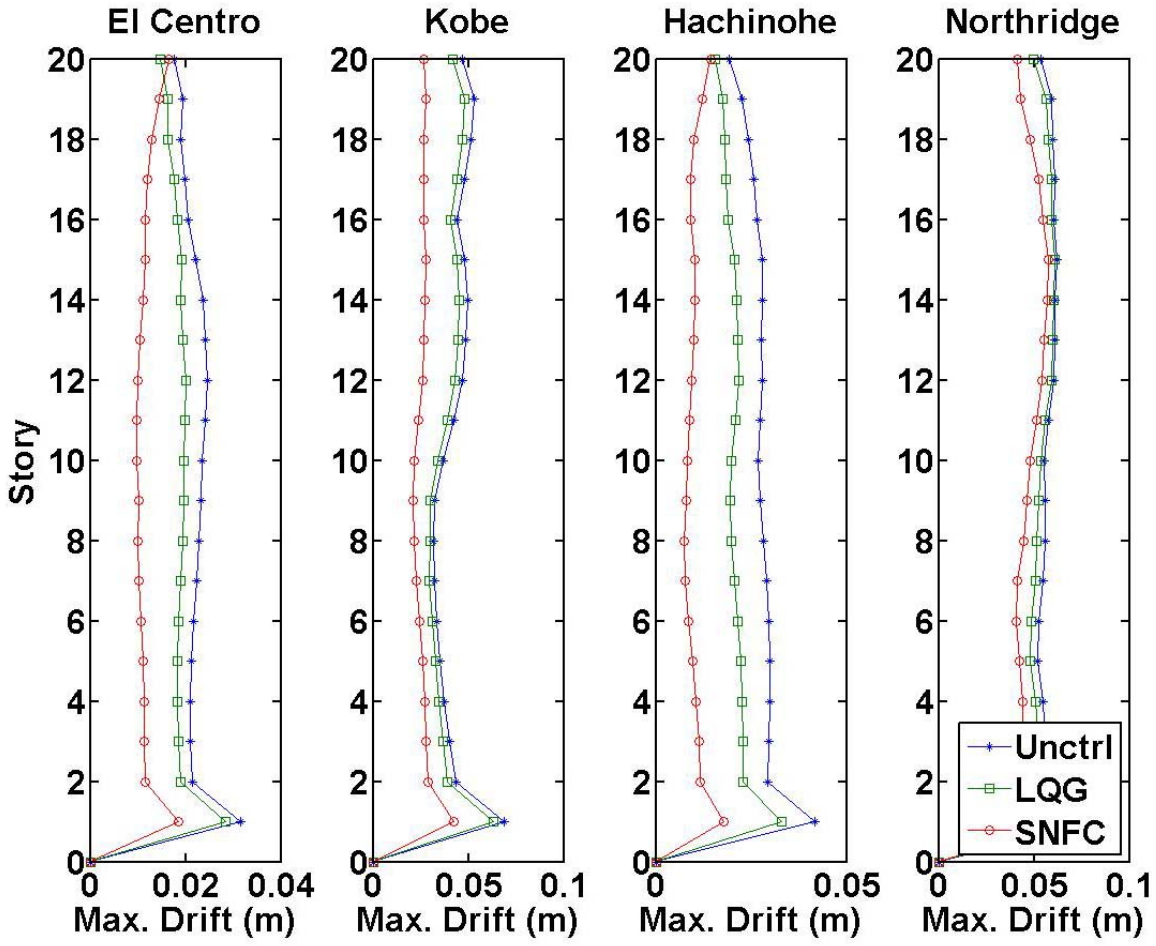

Fig. 7.23. Interstory drift responses of an uncontrolled, a LQG control, and a SNFC systems

Fig. 7.24 compares maximum interstory acceleration responses of the uncontrolled, the LQG controlled and the SNFC controlled systems, respectively. In almost all the responses, the performance of the SNFC system is better than that of the LQG controller, while the LQG controller shows better performance than the SNFC system in the acceleration responses due to Northridge and Hachinohe earthquakes.

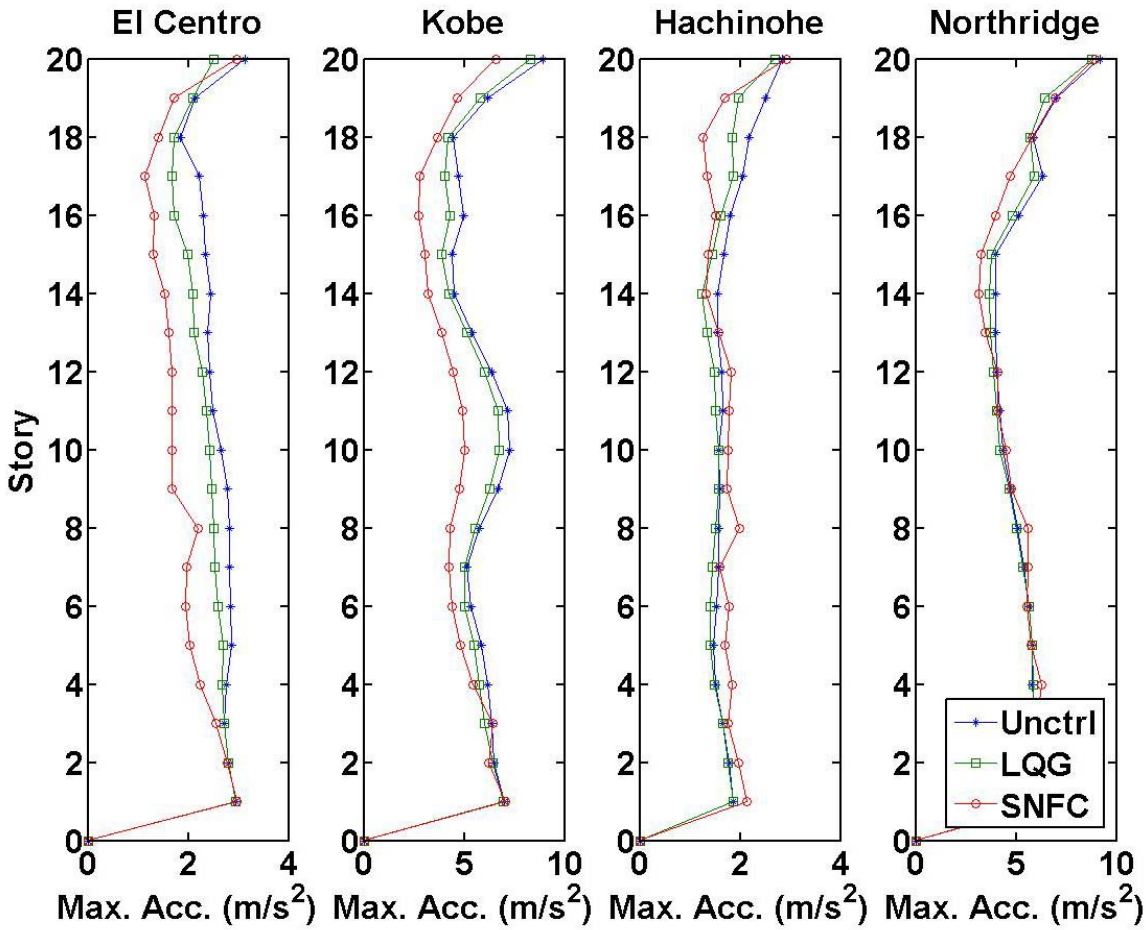

Fig. 7.24. Interstory acceleration responses of an uncontrolled, a LQG control, and a SNFC systems

The performance comparison between the LQG-based semiactive control and the SNFC system is given in Table 7.1. In this table, the evaluation criteria index is shown in the first column, the evaluation values are shown in the 2nd column to the 5th column, and the maximum value taken from the evaluation values is provided in the last column. According to the evaluation criteria J_1 to J_8 that represent the control performance of structures, the evaluation factor is less than one for almost all twenty nine cases, except three cases (J_3-Hachinohe, J_4-El Centro, and J_4-Northridge). This means that the controlled responses are lower than the uncontrolled responses in most of cases. Compared to the uncontrolled responses, the proposed SNFC system reduces the maximum displacement responses by 19.6-75.2 % and the maximum drift by 6.8-52.5 %. In addition, the control performance of the proposed SNFC system is better than the LQG-based semiactive control system for almost all twenty seven cases, except five cases (J_3-El Centro, J_3-Hachinohe, J_3-Northridge, J_4-El Centro, and J_4-Northridge).

Table 7.1. Performance evaluation of a SNFC and a LQG-based semiactive controls

	El Centro		Hachinohe		Northridge		Kobe		Max Value	
	SNFC	LQG	SNFC	LQG	SNFC	LQG	SNFC	LQG	SNFC	LQG
J_1	0.323	0.846	0.248	0.666	0.804	0.921	0.668	0.940	0.804	0.940
J_2	0.667	0.831	0.475	0.790	0.932	0.987	0.578	0.904	0.932	0.987
J_3	0.949	0.941	1.031	0.946	0.970	0.956	0.789	0.927	1.031	0.956
J_4	1.021	0.956	0.781	0.820	1.087	0.921	0.799	0.924	1.087	0.956
J_5	0.221	0.634	0.162	0.560	0.380	0.684	0.398	0.774	0.398	0.774
J_6	0.521	0.648	0.354	0.550	0.390	0.672	0.560	0.823	0.560	0.823
J_7	0.562	0.778	0.427	0.671	0.556	0.786	0.623	0.881	0.623	0.881
J_8	0.723	0.675	0.495	0.564	0.481	0.677	0.727	0.830	0.727	0.830
J_9	0.015	0.002	0.015	0.002	0.020	0.002	0.019	0.002	0.020	0.002
J_{10}	0.049	0.075	0.034	0.064	0.066	0.075	0.075	0.111	0.075	0.111
J_{11}	0.019	0.004	0.015	0.003	0.039	0.005	0.035	0.006	0.039	0.006
J_{12}	0.049	0.015	0.035	0.015	0.092	0.018	0.122	0.026	0.092	0.026
J_{13}	48									
J_{14}	40	5	40	5	40	5	40	5	40	5
J_{15}	6	62	6	62	6	62	6	62	6	62

7.6 Concluding Remarks

In this section, a Los Angeles 20 story building structure is investigated to demonstrate the effectiveness of the proposed nonlinear system identification method and the newly developed semiactive nonlinear fuzzy control (SNFC) system. In order to implement the SNFC system, a modified clipped algorithm and an inverse MR damper approach are considered. However, the inverse MR damper approach is selected to implement a semiactive control system into the LA 20 story building structure because it generates the better performance than the modified clipped algorithm. The simulation results show that the newly developed SNFC systems are effective to vibration control of the 20 story building structure equipped with MR dampers.

In addition, based on linear quadratic Gaussian (LQG) approach, a semiactive control system are designed. The performance of the LQG-based semiactive control systems is compared with newly developed SNFC system proposed in this research. It was demonstrated from the simulation that the proposed SNFC system has the better performance than the LQG-based control system.

8. CONCLUSIONS AND FUTURE STUDIES

8.1 Summary of Concluding Remarks

This dissertation proposes a multiple model approach for multi-input-multi-output (MIMO) nonlinear identification of seismically excited building-magnetorheological damper systems. The proposed framework is developed through integration of multiple autoregressive exogenous (ARX) inputs-based Takagi-Sugeno (TS) fuzzy model with weighted least squares and data clustering algorithms. This method does not require decoupling of identification procedures for subcomponents because it identifies a building structure and a MR damper as an integrated system. In other words, the MIMO nonlinear behavior of the building structure employing a MR damper are represented by a family of local linear ARX input models whose operating regions are integrated via a TS fuzzy interpolation method. The premise parts of the multiple ARX inputs-based TS fuzzy model are partitioned to subdivide the input space into several operating regions using clustering techniques. The consequent part is optimized by a set of linear weighted least squares algorithm. Comparison of the identified model with displacement and acceleration data obtained from a numerical simulation shows that the proposed MIMO nonlinear fuzzy identification algorithm is effective in estimating nonlinear behavior of a building structure equipped with a MR damper.

In addition to the novel system identification method, this dissertation also proposes linear matrix inequalities (LMIs)-based systematic design methodology for nonlinear control of building structures equipped with a magnetorheological damper. This approach considers the stability performance as well as transient characteristics in a unified framework. First, multiple Lyapunov-based controllers are formulated in terms of LMIs such that global asymptotical stability is guaranteed and the performance on transient response is also satisfied. Such Lyapunov-based state feedback controllers are converted into output feedback regulators with a Kalman estimator. Then, these Lyapunov-based controllers and a Kalman observer are integrated as an output feedback-based active nonlinear control system. Finally, the active nonlinear controller is integrated with a converting algorithm, e.g., either an inverse MR damper model or a clipped algorithm to convert the active system into a semiactive system. To demonstrate the effectiveness of the proposed semiactive nonlinear fuzzy control system, a three story building structure employing a MR damper is studied. The performance of the semiactive nonlinear control system is compared with that of a traditional optimal linear control, H2/LQG controller, while the uncontrolled system response is used as the baseline. It is demonstrated from comparison of the uncontrolled and semiactive controlled responses that the proposed semiactive nonlinear control system design framework is effective in controlling vibration of seismically excited building structure equipped with a MR damper. Furthermore, the newly developed controller is more robust with respect to sensor noise than the H2/LQG controller.

Third, this dissertation also proposes hierarchical semiactive nonlinear fuzzy control (SNFC) techniques for a building structure equipped with multiple magnetorheological (MR) dampers. Based on acceleration and drift information, a set of sub-controllers using the SNFC algorithm are designed for sub-structures at the specific floor levels within the building structure for the lower level control systems. At the higher level, a supervisor controller, a velocity feedback-based active nonlinear fuzzy controller is built up to supervise the performance of the sub-controllers at the lower level. Then, the nonlinear sub-controllers at the lower level are integrated with the supervisory nonlinear controller. Both higher and lower level nonlinear controllers are formulated in terms of linear matrix inequalities (LMIs) such that global asymptotical stability is guaranteed and the performance on transient responses is also satisfied. Then, multiple Kalman estimators that are associated with the coordinator controller and sub-controllers are designed to construct output feedback regulators. Finally, the output feedback-based active sub-controllers are converted into semiactive sub-controllers using converting algorithms. To demonstrate the effectiveness of the proposed hierarchical SNFC approach, an eight-story building structure employing MR dampers are studied. It is demonstrated from comparison of the uncontrolled and semiactive controlled responses that the proposed hierarchical SNFC design framework is effective in controlling vibration of seismically excited a building structure equipped with MR dampers.

Last, the effectiveness of the newly developed methods for identification and control is further studied for nonlinear control of seismically excited high-rise building

structures. A benchmark full-scale building structure is selected as a target model that meets seismic code for Los Angeles, California region designed by Brandow & Johnston Associates for the SAC Phase 2 Steel Project. To evaluate the effectiveness of the control system subjected to earthquake, four real-recorded earthquake signals, El Centro, Kobe, Northridge, and Hachinohe are used. To implement semiactive control systems, a modified clipped algorithm and a Bingham model-based inverse MR damper approach were considered here. In addition, the performance of the proposed SNFC system is compared with that of a linear quadratic Gaussian (LQG)-based semiactive control system. It is demonstrated from the simulation that the proposed SNFC has the better performance than the LQG-based semiactive control strategy for a seismically excited LA 20 story building structure.

8.2 Future Research

The nonlinear identification and semiactive nonlinear fuzzy control frameworks addressed in this dissertation have been demonstrated theoretically and numerically. Although useful for design guidelines, further research is recommended to do experimental studies to demonstrate the effectiveness of the proposed methodologies.

It is recommended that the proposed identification and control methods be applied to wind-excited high-rise building structures equipped with MR dampers. It is also recommended that the proposed methods be applied to large-scale bridge structures employing MR dampers.

Further research is recommended to apply for the proposed methods to structural systems equipped with a variety of semiactive devices such as an electrorheological damper and a piezoelectric friction damper.

REFERENCES

Abe, M. (1996). "Rule-Based Control Algorithm for Active Tuned Mass Dampers." *J. Eng. Mech*., 122(8), 705-713.

Abonyi, J. (2003). *Fuzzy Model Identification for Control*, Birkhauser, Boston.

Abonyi, J., Babuska, R., Verbruggen, H.B. and Szeifert, F. (2000). "Incorporating Prior Knowledge in Fuzzy Model Identification." *Int. J. of Sys. Science*, 31(5), 657-667.

Ahlawat, A.S and Ramaswamy, A. (2002a). "Multi-objective Optimal Design of FLC Driven Hybrid Mass Damper for Seismically Excited Structures." *Earth. Eng. Struct. Dyna*., 31(7), 1459-1479.

Ahlawat, A.S and Ramaswamy, A. (2002b). "Multiobjective Optimal FLC Driven Hybrid Mass Damper System for Torsionally Coupled, Seismically Excited Structures." *Earth. Eng. Struct. Dyna*., 31(12), 2121-2139.

Ahlawat, A.S and Ramaswamy, A. (2004). "Multiobjective Optimal Fuzzy Logic Control System for Response Control of Wind-Excited Tall Buildings." *J. Eng. Mech*., 130(4), 524-530.

Al-Dawod, M., Samali, B., Naghdy, F., and Kwok, K.C.S. (2001). "Active Control of Along Wind Response of Tall Building Using a Fuzzy Controller." *Eng. Struct.*, 23(11), 1512-1522.

Al-Dawod, M., Samali, B., Naghdy, F., Kwok, K.C.S. and Naghdy, F. (2004). "Fuzzy Controller for Seismically Excited Nonlinear Buildings." *J. Eng. Mech*., 130(4), 407-415.

Alli H. and Yakut, O. (2005). "Fuzzy Sliding-Mode Control of Structures." *Eng. Struct*., 27(2), 277-284.

Åström, K.J. and Eykhoff, P. (1971). "System Identification-A Survey." *Automatica*, 7(2), 123-162.

Battaini, M., Casciati, F. and Faravelli, L. (1998). "Fuzzy Control of Structural Vibration. An Active Mass System Driven by a Fuzzy Controller." *Earth. Eng. Struct. Dyna*., 27(11), 1267-1276.

Battaini, M., Casciati, F. and Faravelli, L. (2004). "Controlling Wind Response through a Fuzzy Controller." *J. Eng. Mech*. 130(4), 486-491.

Boyd, S., Ghaoui, L.E., Feron, E., and Balakrishnan, V. (1994). *Linear Matrix Inequalities in System and Control Theory*, SIAM, Philadelphia.

Casciati, F. (1997). "Checking the Stability of a Fuzzy Controller for Nonlinear Structures." *Microcomputers in Civil Eng*., 12(3), 205-215.

Chilali, M. and Gahinet, P. (1996). "H^{∞} Design with Pole Placement Constraints: An LMI Approach." *IEEE Trans. Automatic Control*." 41(3), 358-367.

Choi, K.M, Cho, S.W., Jung, H.J., and Lee, I.W. (2004). "Semi-active Fuzzy Control for

Seismic Response Reduction using Magnetorheological Dampers." *Earth. Eng. Struct. Dyna*., 33(6), 723-736.

Choi, S.B., Lee, S.K., and Park, Y.P. (2001). "A Hysteresis Model for the Field-dependent Damping Force of a Magnetorheological Damper." *J. Sound and Vibration*, 245(2), 375-383.

Chung, L.L., Lin, R.C., Soong, T.T., and Reinhorn, A.M. (1989). "Experiments on Active Control for MDOF Seismic Structures." *J. Eng. Mech*., 115(8), 1609-1627.

Craig, R.R. (1981). *Structural Dynamics: An Introduction to Computer Methods*, John Wiley & Sons, New York.

Crassidis, J.L. and Junkins, J.L. (2004). *Optimal Estimation of Dynamic Systems*, Chapman & Hall, Washington, DC.

Dyke, S.J., Spencer, B.F. Jr., Sain, M.K., and Carlson, J.D. (1996). "Modeling and Control of Magnetorheological Dampers for Seismic Response Reduction." *Smart Mater. and Struct.,* 5(5), 565-575.

Dyke, S.J., Spencer, B.F. Jr., Sain, M.K., and Carlson, J.D. (1998). "An Experimental Study of MR Dampers for Seismic Protection." *Smart Mater. and Struct.,* 7(5), 693-703.

Faravelli, L. and Rossi, R. (2002). "Adaptive Fuzzy Control: Theory versus Implementation." *J. Struct. Control,* 9(1), 59-73.

Faravelli, L. and Yao, T. (1996). "Use of Adaptive Networks in Fuzzy Control of Civil

Structures." *Microcomputers in Civil Eng*., 11(1), 67-76.

Farinwata, S.S, Filev, D., and Langari, R. (2000). *Fuzzy Control-Synthesis and Analysis*, John Wiley & Sons, New York.

Hart, G.C. and Wong, K. (2000). *Structural Dynamics for Structural Engineers*, John Wiley & Sons, New York.

Hashemian, H. and Ryaciotaki-Roussalis, H.A. (1995). "Decentralized Approach to Control Civil Structures." *Proc., the 1995 American Control Conf.,* Seattle, WA, USA, 4, 2936-2937.

Hong, S.K. and Langari, R. (2000). "An LMI-based H^{∞} Fuzzy Control System Design with TS Framework." *Information Sciences*, 123(3), 163-179.

Hurlebaus, S. and Gaul, L. (2006). "Smart Structure Dynamics", *Mechanical Systems and Signal Processing*, 20(2), 255-281.

Jang, J.S.R, Sun, C.T., and Mizutani, E. (1997). *Neuro-Fuzzy and Soft Computing-A Computational Approach to Learning and Machine Intelligence*, Prentice Hall, Upper Saddle River, NJ.

Jansen, L.M. and Dyke, S.J. (2000). "Semiactive Control Strategies for MR Dampers: Comparative Study." *J. Eng. Mech*., 126(8), 795-803.

Jiang, X. and Adeli, H. (2005). "Dynamic Wavelet Neural Network for Nonlinear Identification of Highrise Buildings." *Computer-Aided Civil and Infrastructure Eng.*, 20(5), 316-330.

Jin, G., Sain, M.K., and Spencer, B.F. Jr. (2005). "Nonlinear Blackbox Modeling of MR-Dampers for Civil Structural Control." *IEEE Trans. on Control Syst. Technology*, 13(3), 345-355.

Joh, J, Langari, R., Jeung, F.T., and Chung, W.J. (1997). "A New Design Method for Continuous Takagi-Sugeno Fuzzy Controller with Pole Placement Constraints: An LMI Approach." *Proc., 1997 IEEE Int. Conf. on Syst., Man, and Cybernetics*, Orlando, FL, 2969-2974.

Johansen, T.A. (1994). "Fuzzy Model Based Control: Stability, Robustness, and Performance Issues." *IEEE Trans. Fuzzy Sys*. 2(3), 221-234.

Jung, H.J, Spencer, B.F. Jr., and Lee, I.W. (2003). "Control of Seismically Excited Cable-Stayed Bridge Employing Magnetorheological Fluid Dampers." *J. Struct. Eng*., 129(7), 873-883.

Khalil, H. K. (2002). *Nonlinear Systems*, Prentice Hall, Upper Saddle River, NJ.

Kim, Y., Langari, R. & Hurlebaus, S. (2007), Nonlinear System Identification of a Building-MR Damper System, *Journal of Intelligent Material Systems and Structures*, (submitted).

Kim, Y., Langari, R. & Hurlebaus, S. (2007), Semiactive Nonlinear Control of a Building Structure equipped with a Magnetorheological Damper System, *Mechanical Systems and Signal Processing*, (submitted).

Kim, S.B, Yun, C.B., and Spencer, B.F. Jr. (2004). "Vibration Control of Wind-Excited Tall Buildings Using Sliding Mode Fuzzy Control." *J. Eng. Mech*. 130(4), 505-510.

Kim, Y. and Langari, R. (2007). "Nonlinear Identification and Control of a Building New York City, NY, CD-Rom.

Kim, Y., Langari, R., and Roschke, P.N. (2006). "Control of a Nonlinear Building Employing Magnetorheological Dampers." *Proc., 4th World Conf. on Struct. Control Monit.*, San Diego, CA.

Kim, H.S. and Roschke, P.N. (2006). "Design of Fuzzy Logic Controller for Smart Base Isolation System Using Genetic Algorithm." *Eng. Struct.*, 28(1), 84-96.

Kuehn, J.L. and Stalford, H.L. (2000). "Stability of a Lyapunov Controller for a Semi-active Structural Control System with Nonlinear Actuator Dynamics." *J. Mathematical Analysis and Applications*, 251(2), 940-957.

Langari, R. (1993). "Synthesis of Nonlinear Control Strategies via Fuzzy Logic." *Proc., the 1993 American Control Conf.,* San Francisco, CA, 1855-1859.

Langari, R. (1999). "Past, Present and Future of Fuzzy Control: A Case for Application of Fuzzy Logic in Hierarchical Control." *Proc., Annual Conf. of the North American Fuzzy Information Processing Society*, New York, NY, 760-765.

Lei, S. and Langari, R. (2000). "Hierarchical Fuzzy Logic Control of a Double Inverted Pendulum." *Proc., IEEE Int. Conf. on Fuzzy Syst.,* San Antonio, TX, 1074-1077.

Liu, W.Y., Xiao, C.J., Wang, B.W., Shi, Y., and Fang, S.F. (2003). "Study on Combining Subtractive Clustering with Fuzzy C-Means Clustering." *Proc., 2nd Int. Conf. on Machine Learning and Cybernetics*, Xi'an, China, 2659-2662.

Loh, C.H., Wu, L.Y., and Lin, P.Y. (2003). "Displacement Control of Isolated Structures with Semi-active Control Devices." *J. Struct. Control*, 10(2), 77-100.

Lynch, J.P. and Law, K.H. (2000). "A Market-based Control Solution for Semi-Active Structural Control." *Computing in Civil and Building Eng.*, 1, 588-595.

Lynch, J.P. and Law, K.H. (2002). "Decentralized Control Techniques for Large-scale Civil Structural Systems." *Proc., the 20th Int. Modal Analysis Conf.*, Los Angeles, CA, USA, 1074-1077.

Ohtori, Y., Christenson, R.E., Spencer, B.F. Jr., and Dyke, S.J. (2004). "Benchmark Control Problems for Seismically Excited Nonlinear Buildings." *J. Eng. Mech*., 130(4), 366-385.

Park, K.S., Koh, H.M., Ok, S.Y., and Seo, C.W. (2005). "Fuzzy Supervisory Control of Earthquake-excited Cable-stayed Bridges." *Eng. Struct*., 27(7), 1086-1100.

Ramallo, J.C., Johnson, E.A., and Spencer, B.F. Jr. (2002). "Smart Base Isolation Systems." *J. Eng. Mech*., 128(10), 1088-1099.

Ramallo, J.C., Yoshioka, H., and Spencer, B.F. Jr. (2004). "A Two-Step Identification Technique for Semiactive Control Systems." *Struct. Control Health Monit*., 11(4), 273-289.

Reigles, D. G. and Symans, M.D. (2006). "Supervisory Fuzzy Control of a Base-isolated Benchmark Building Utilizing a Neuro-fuzzy Model of Controllable Fluid Viscous Dampers." *Struct. Control Health Monit.*, 13(2-3), 724-747.

Rofooei, F.R. and Monajemi-nezhad, S. (2006). "Decentralized Control of Tall

Buildings." *The Struct. Design of Tall and Special Buildings*, 15(2), 153-170.

Samali, B., Al-Dawod, M., Kwok, K.C.S., and Naghdy, F. (2004). "Active Control of Cross Wind Response of 76-Story Tall Building Using a Fuzzy Controller." *J. Eng. Mech*., 130(4), 492-498.

Schurter, K.C and Roschke, P.N. (2001). "Neuro-Fuzzy Control of Structures Using Magnetorheological Dampers." *Proc., the 2001 American Control Conf*., Arlington, VA, 1097-1102.

Soong, T.T. (1990). *Active Structural Control: Theory and Practice*, Addison-Wesley Pub., New York.

Soong, T.T. and Grigoriu, M. (1993). *Random Vibration of Mechanical and Structural Systems*, Prentice Hall, Upper Saddle River, NJ.

Spencer, B.F. Jr. (1986). *Reliability of Randomly Excited Hysteretic Structures*, Springer, New York.

Spencer, B.F. Jr., Christenson, R.E., and Dyke, S.J. (1999). "Next Generation Benchmark Control Problem for Seismically Excited Buildings." *Proc., the Second World Conf. on Struct. Control*, Kyoto, Japan, 1351-1360.

Spencer, B.F. Jr., Dyke, S.J., Sain, M.K., and Carlson, J.D. (1997). "Phenomenological Model for Magnetorheological Dampers." *J. Eng. Mech*., 123(3), 230-238.

Spencer, B.F. Jr., Suhardjo, J., and Sain, M.K. (1994). "Frequency Domain Optimal Control Strategies for a Seismic Protection." *J. Eng. Mech*., 120(1), 135-158.

Stanway, R., Sproston, J.L., and Stevens, N.G. (1985). "Non-linear Identification of an Electro-rheological Vibration Damper." *IFAC Identification and System Parameter Estimation*, 7, 195-200.

Stanway, R., Sproston, J.L., and Stevens, N.G. (1987). "Non-linear Modeling of an Electro-rheological Vibration Damper." *J. Electrostatics*, 20(2), 167-184.

Subramaniam, R.S, Reinhorn, A.M., Riley, M.A., and Nagarajaiah, S. (1996). "Hybrid Control of Structures Using Fuzzy Logic." *Microcomputers in Civil Eng*. 11(1), 1-17.

Symans, M. and Kelly, S.W. (1999). "Fuzzy Logic Control of Bridge Structures using Intelligent Semi-active Seismic Isolation Systems." *Earth. Eng. Struct. Dyna*., 28(1), 37-60.

Takagi, T. and Sugeno, M. (1985). "Fuzzy Identification of Systems and Its Applications to Modeling and Control." *IEEE Transactions on Syst., Man, and Cybernetics*, 15(1), 116-132.

Tanaka, K. and Sano, M. (1994). "A Robust Stabilization Problem of Fuzzy Control Systems and its Application to Backing up Control of a Truck-trailer." *IEEE Trans. Fuzzy Syst*., 2(2), 119-134.

Tanaka, K. and Sugeno, M. (1992). "Stability Analysis and Design of Fuzzy Control Systems." *Fuzzy Sets and Syst.*, 45(2), 135-156.

Tani, A., Kawamura, H., and Ryu, S. (1998). "Intelligent Fuzzy Optimal Control of Building Structures." *Eng. Struct.* 20(3), 184-192.

Tsang, H.H., Su, R.K.L., and Chandler, A.M. (2006). "Simplified Inverse Dynamics Models for MR Fluid Dampers." *Eng. Struct*. 28(3), 327-341.

Tse, T. and Chang, C.C. (2004). "Shear-Mode Rotary Magnetorheological Damper for Small-Scale Structural Control Experiments." *J. Struct. Eng*., 130(6), 904-911.

Wang, A.P and Lee, C.D. (2002). "Fuzzy Sliding Mode Control for a Building Structure based on Genetic Algorithms." *Earth. Eng. Struct. Dyna*., 31(4), 881-895.

Wang, H.O., Tanaka, K., and Griffin, M. (1995). "An Analytical Framework of Fuzzy Modeling and Control of Nonlinear Systems: Stability and Design Issues." *Proc., the 1995 American Control Conf*., Seattle, WA, Proc., 2272-2276.

Wang, L. and Langari, R. (1996). "Complex Systems Modeling via Fuzzy Logic." *IEEE Trans. Syst. Man. Cybernetics-Part B: Cybernetics*, 26(1), 100-106.

Wen, Y.K (1976). "Method for Random Vibration of Hysteretic Systems." *J. Eng. Mech*., 102(2), 249-263.

Xu, B., Wu, Z.S., and Yokoyama, K. (2003). "Neural Networks for Decentralized Control of Cable-stayed Bridge." *J. Bridge Eng.*, 8(4), 229-236.

Yan, G. and Zhou, L.L. (2006). "Integrated Fuzzy Logic and Genetic Algorithms for Multi-Objective Control of Structures Using MR Dampers." *J. Sound and Vibration*, 296(1-2), 368-382.

Yang, G., Spencer, B.F. Jr., Carlson, J.D., and Sain, M.K. (2002). "Large-scale MR Fluid Dampers: Modeling and Dynamic Performance Considerations." *Eng. Struct*., 24(3), 309-323.

Yang, J.N. (1982). "Control of Tall Building under Earthquake Excitation." *J. Eng. Mech. Div.*, 108(EM5), 833-849.

Yang, J.N., Akbrapour, A., and Ghaemmaghami, P. (1987). "New Optimal Control Algorithms for Structural Control." *J. Eng. Mech*., 113(9), 1369-1386.

Yen, J. and Langari, R. (1999). *Fuzzy Logic-Intelligence, Control, and Information*, Prentice Hall, Upper Saddle River, NJ.

Yoshida, O. and Dyke, S.J. (2004). "Seismic Control of a Nonlinear Benchmark Building Using Smart Dampers." *J. Eng. Mech*., 130(4), 386-392.

Zadeh, L.A. (1965). "Fuzzy Sets." *Information and Control*, 8(3), 338 – 353.

Zhou, L., Chang, C.C., and Wang, L.X. (2003). "Adaptive Fuzzy Control for Nonlinear Building-Magnetorheological Damper System." *J. of Struct. Eng.*, 129(7), 905-913.

APPENDIX A

Table A.1. Parameters of a Bouc-Wen model for SD-1000 MR damper (Spencer et al. 1997)

Parameter	Value
c_0	50 Nscm^{-1}
k_0	25 Ncm^{-1}
x_0	3.8 cm
N	2
α	880 Ncm^{-1}
β	100 cm^{-2}
γ	100 cm^{-2}
A	120

APPENDIX B

Table A.2. Optimum coefficients of the polynomial model for MRF 132-LD damper (Choi et al. 2001)

Parameters	Value
b_0^{Upper}	-371.8
b_1^{Upper}	6.205
b_2^{Upper}	0.03728
b_3^{Upper}	-3.487e-4
b_4^{Upper}	-2.767e-6
b_5^{Upper}	6.924e-9
b_6^{Upper}	5.604e-11
c_0^{Upper}	-659.4
c_1^{Upper}	8.955
c_2^{Upper}	0.1062
c_3^{Upper}	-1.584e-4
c_4^{Upper}	-5.908e-6
c_5^{Upper}	1.137e-9
c_6^{Upper}	1.087e-10
b_0^{Lower}	-235.8
b_1^{Lower}	5.391
b_2^{Lower}	-0.02774
b_3^{Lower}	-3.788e-4
b_4^{Lower}	2.449e-4
b_5^{Lower}	8.804e-9
b_6^{Lower}	-5.374e-11
c_0^{Lower}	693.7
c_1^{Lower}	7.034
c_2^{Lower}	-0.1020
c_3^{Lower}	6.729e-5
c_4^{Lower}	4.967e-6
c_5^{Lower}	-4.924e-9
c_6^{Lower}	-8.196e11

APPENDIX C

Table A.3. Parameters of a modified Bouc-Wen model for SD-1000 MR damper model (Spencer et al. 1997)

Parameter	Value
c_{0a}	21.0 Nscm^{-1}
c_{0b}	3.50 Nscm^{-1}V^{-1}
k_0	46.9 Ncm^{-1}
c_{1a}	283 Nscm^{-1}
c_{1b}	2.95 Nscm^{-1}V^{-1}
k_1	5.00 Ncm^{-1}
x_0	14.3 cm
α_a	140 Ncm^{-1}
α_b	695 Ncm^{-1}V^{-1}
γ	363 cm^{-2}
β	363 cm^{-2}
A	301
N	2
η	190 s^{-1}

APPENDIX D

Table A.4. Parameters for 1000 kN MR damper model (Jung et al. 2003)

Parameter	Value
c_{0a}	110.0 Nscm^{-1}
c_{0b}	114.3 Nscm^{-1}V^{-1}
k_0	0.002 Ncm^{-1}
c_{1a}	8359.2 Nscm^{-1}
c_{1b}	7482.9 Nscm^{-1}V^{-1}
k_1	0.0097 Ncm^{-1}
x_0	0 cm
α_a	46.2 Ncm^{-1}
α_b	41.2 N cm^{-1}V^{-1}
γ	164.0 cm^{-2}
β	164.0 cm^{-2}
A	1107.2
N	2
η	100 s^{-1}

VITA

Yeesock Kim received a B.E. diploma, summa cum laude, in the Department of Architectural Engineering with an emphasis in structural engineering from Kwandong University in February 2000. From the spring of 2000 to the fall of 2001, he pursued his Master of Science degree for structural engineering in the Department of Architectural Engineering at Yonsei University. His research was to formulate structural vibration control issues as constrained optimization problems. Later he received his Doctor of Philosophy degree in Civil Engineering at Texas A&M University in December 2007.

Zachry Department of Civil Engineering

Texas A&M University, M.S. 3136

College Station, TX 77843

USA